Document made available under the Patent Cooperation Treaty (PCT)

International application number: PCT/US04/043408

International filing date: 22 December 2004 (22.12.2004)

Document type: Certified copy of priority document

Document details: Country/Office: US
Number: 60/533,384
Filing date: 30 December 2003 (30.12.2003)

Date of receipt at the International Bureau: 31 January 2005 (31.01.2005)

Remark: Priority document submitted or transmitted to the International Bureau in compliance with Rule 17.1(a) or (b)

1275641

THE UNITED STATES OF AMERICA

TO ALL TO WHOM THESE PRESENTS SHALL COME:

UNITED STATES DEPARTMENT OF COMMERCE

United States Patent and Trademark Office

January 19, 2005

THIS IS TO CERTIFY THAT ANNEXED HERETO IS A TRUE COPY FROM THE RECORDS OF THE UNITED STATES PATENT AND TRADEMARK OFFICE OF THOSE PAPERS OF THE BELOW IDENTIFIED PATENT APPLICATION THAT MET THE REQUIREMENTS TO BE GRANTED A FILING DATE.

APPLICATION NUMBER: *60/533,384*
FILING DATE: *December 30, 2003*
RELATED PCT APPLICATION NUMBER: *PCT/US04/43408*

Certified by

Jon W. Dudas

Under Secretary of Commerce
for Intellectual Property
and Director of the United States
Patent and Trademark Office

PTO/SB/16 (08-03)
Approved for use through 07/31/2006. OMB 0651-0032
U.S. Patent and Trademark Office; U.S. DEPARTMENT OF COMMERCE

PROVISIONAL APPLICATION FOR PATENT COVER SHEET

This is a request for filing a PROVISIONAL APPLICATION FOR PATENT under 37 CFR 1.53(c).

Express Mail Label No. EV 301746874 US

INVENTOR(S)

Given Name (first and middle [if any])	Family Name or Surname	Residence (City and either State or Foreign Country)
Rainer	**Martini**	**Hoboken, NJ**

☒ *Additional inventors are being named on the* 1 *separately numbered sheets attached hereto*

TITLE OF THE INVENTION (500 characters max)

3D IMAGE SCANNER USING ULTRA SHORT PULSES

Direct all correspondence to: **CORRESPONDENCE ADDRESS**

☒ Customer Number **27614**

OR

☐ Firm *or* Individual Name	**McCarter & English, LLP**				
Address	**Four Gateway Center**				
Address	**100 Mulberry St.**				
City	**Newark**	State	**NJ**	ZIP	**07102**
Country	**USA**	Telephone	**973-622-4444**	Fax	**973-6224-7070**

ENCLOSED APPLICATION PARTS *(check all that apply)*

☒ Specification *Number of Pages* **50**
☒ Drawing(s) *Number of Sheets* **4**
☐ Application Data Sheet. See 37 CFR 1.76
☐ CD(s), Number
☐ Other (specify)

METHOD OF PAYMENT OF FILING FEES FOR THIS PROVISIONAL APPLICATION FOR PATENT

☒ Applicant claims small entity status. See 37 CFR 1.27.
☐ A check or money order is enclosed to cover the filing fees
☒ The Director is hereby authorized to charge filing fees or credit any overpayment to Deposit Account Number **501402**
☐ Payment by credit card. Form PTO-2038 is attached.

FILING FEE AMOUNT ($) **$80.00**

The invention was made by an agency of the United States Government or under a contract with an agency of the United States Government.

☒ No.
☐ Yes, the name of the U.S. Government agency and the Government contract number are: _____

Respectfully submitted,

SIGNATURE Allen N. Friedman

Date 12/30/03

TYPED or PRINTED NAME **Allen N. Friedman, Esq.**

TELEPHONE **973-639-6946**

REGISTRATION NO. *(if appropriate)* **25,973**

Docket Number: **97084/00047**

USE ONLY FOR FILING A PROVISIONAL APPLICATION FOR PATENT

PROVISIONAL APPLICATION COVER SHEET
Additional Page

PTO/SB/16 (08-03)
Approved for use through 07/31/2006. OMB 0651-0032
U.S. Patent and Trademark Office; U.S. DEPARTMENT OF COMMERCE

Docket Number	97084/00047

INVENTOR(S)/APPLICANT(S)

Given Name (first and middle [if any])	Family or Surname	Residence (City and either State or Foreign Country)
John J.	**Keating III**	**Hoboken, NJ**

Number 2 of 2

WARNING: Information on this form may become public. Credit card information should not be included on this form. Provide credit card information and authorization on PTO-2038.

97084-00047

IN THE UNITED STATES PATENT AND TRADEMARK OFFICE

In re patent application of
RAINER MARTINI, ET AL.

Serial No.: TO BE ASSIGNED

Filed: FILED HEREWITH

For: 3D IMAGE SCANNER USING ULTRA SHORT PULSES

Mail Stop Prov. Patent Application
Commissioner for Patents
P.O. Box 1450
Alexandria, VA 22313-1450

CERTIFICATE OF MAILING BY "EXPRESS MAIL"

Sir:

"Express Mail" Mailing Label Number: EV 301746874 US

Date of Deposit: December 30, 2003

I hereby certify that this paper and/or fee is being deposited with the United States Postal Service "Express Mail Post Office to Addressee" service under 37 C.F.R. 1.10 on the date indicated above and is addressed to the Commissioner for Patents, Mail Stop Prov. Patent Application, P.O. Box 1450, Alexandria, VA 22313-1450.

Stephanie B. Drabyk

Docket: 97084/00047

IN THE UNITED STATES PATENT AND TRADEMARK OFFICE

PROVISIONAL APPLICATION

Inventors Rainer Martini, John J. Keating III

Both residing at 613 Hudson Street, Hoboken NJ 07030

Title: 3D Image Scanner Using Ultra Short Pulses

1. **Summary of the Invention:** This invention takes a three dimensional (3D) picture of an object. By capturing multiple images from additional viewpoints, a complete 3D representation of the object may be captured and provide data to construct a 3D model of the object. This invention captures three dimensional information from still or moving objects, for example, by use of infrared light without disturbance or the danger of hurting or destroying the object.
2. **Description**: The target object is illuminated by ultra short optical pulse. The depth profile of the target is translated thereby into a time profile of the reflected light. Detecting the reflected light with high temporal resolution will therefore reveal the depth profile of the target. In this approach, time gating prior to the 2D imaging system, is achieved by non linear optical effect [for example, up-conversion]. This non-linear effect utilizes a second ultra short gating pulse, which has a controlled time delay with respect to the first pulse. When temporal overlap of the two pulses occurs, a signal (i.e. light with higher frequency) from the interaction of the two ultra short pulses is transmitted to the 2 dimensional imaging system. By varying the time delay between the two (reflected and gating) ultra short pulses, reflections with selected ranges (i.e., distance from the optical source) are gated into the 2D imaging system.

   In this approach, time gating prior to the 2D imaging system, is achieved by a non linear optical effect [optical up/down conversion]. This non-linear effect utilizes a second ultra short

optical pulse as a gating pulse, which is differentially time delayed from the first (reflected) pulse by traveling a path to a mirror that is moveable in the z dimension, as illustrated in Figure 1, or is differentially delayed, as illustrated in Figure 2, by use of a digital control system. When a temporal overlap of the two pulses occurs in the optical mixer [a,b,c,d], the optical output from the mixer is the sum and difference frequencies of the pulse source F1 and gating pulse source F2. The output of the optical mixer is a light pulse generated from the non-linear interaction of the reflected and gating optical pulses is then transmitted to the 2 dimensional imaging system. By varying the time delay between the two (reflected F1 and gating F2) ultra short optical pulses, pulses with selected ranges, generated in the non-linear mixer, are gated into the 2D imaging device (e.g. camera).

The optical frequencies of the ultra short pulse generators F1 and F2 can be chosen such that only the desired sum and/or difference frequencies generated in the optical mixer are within the range that are processed by the 2D imaging device. For example, F1 and F2 can be chosen to be optical frequencies below the frequency processed by the 2D imaging device while the sum of these frequencies is within the processing range of the 2D imaging device.

A three dimension image of the object is obtained by generating ranges for a succession of two dimensional images that encompass all external views of the three dimension object. This is accomplished by either rotating the target object, or moving the 2D apparatus around the target object.

3. Compared to other depth information systems this concept can have enhanced sensitivity, as the time resolution is given strictly by the length of the optical pulses and the optical non-linear process. The detection technique can be comparatively slow and, therefore, can have a high spatial resolution. The use of IR ultra short pulse sources allows the creation of visible light in the optical non-linear process, thereby permitting use of standard imaging systems for the acquisition of the 2D image. The depth sensitivity and range can easily be adjusted to

needed specifications by the selection of optical pulse length and the precision of the control in the time delay of the second "gating" light pulse. Additionally, depth information can be obtained even from very low reflecting objects, since in the non-linear mixing process the signal strength can be enhanced by use of an intense "gating" pulse.

4. This invention is another application of the concepts, methods and systems described in a companion Provisional Application by the same inventors entitled "Three Dimensional Display Using Ultrashort Optical Pulses." That application is included as part of this application as an Appendix.

Docket: 97084/00048

IN THE UNITED STATES PATENT AND TRADEMARK OFFICE

APPENDIX TO PROVISIONAL APPLICATION

Inventors: John J. Keating III and Rainer Martini,

Both residing at 613 Hudson Street, Hoboken NJ 07030

Title: Three Dimensional Display Using Ultra Short Optical Pulses

1. **Purposes and advantages of invention:** This invention describes equipment to render for viewing, a three dimensional spatial representations of three dimensional objects. This invention provides three dimensional displays of objects in a single optical frequency or multiple optical frequencies including the visible colors.
2. **Description:** Three or more optical light sources, up to k sources, producing ultra short optical pulses (i.e., in the femtosecond to picosecond range) are spatially positioned on one or both sides of the optical mixer shown at [abcd] in Figure 1. These sources are separated from one another by a minimum distances from the other k-1 optical sources such that pulses emanating from the optical sources with appropriate timing arrive at a desired point in three dimensional space together with the optical mixer, furthermore, the optical sources are sufficiently close to the optical mixer, such that a pulses from the k sources arriving at point P1 at the same point in time minimize the spatial spread of the overlapping pulses. The relative timing of the ultra short optical pulses determines the location on the optical mixer [abcd], e.g. P1, where the ultra short pulses overlap. At all other points on the optical mixer, the pulses arrive at different times, thus do not overlap. The pulse timing is controlled by electronics in the optical sources and this timing information is determined by the computers and software controlling the display.

   The optical mixer is constructed from an optically non-linear material, for example, a nearly transparent composition containing lithium niobate, within which the optical pulses mix

(interact optically) and generate the sum and difference combinations of the k optical frequencies impinging on the optical mixer at that time. Figure 1 shows one possible physical arrangement of 4 ultra short optical sources, whose pulse timing is such that these 4 optical pulses interact at point P1 on the optical mixer. For this case of k=4 optical sources of optical source frequencies F1, F2, F3 and F4, which interact in the non-linear mixer, all sum and difference frequencies of the combinations of F1, F2, F3 and F4, are produced including the highest frequency output of the non-linear optical mixer which is F1 + F2 + F3 + F4. Therefore, any person or equipment observing the output of the optical mixer which is simultaneously illuminated at point P1 by the pulses from F1, F2, F3 and F4 will observe a

pulse of frequency F1 + F2 + F3 + F4 . If they view the output of the optical mixer through a filter with passes only F1 + F2 + F3 + F4, then only optical frequency F1 + F2 + F3 + F4 will be observed at point P1 in the mixer plane [a,b,c,d] and not any other sum or difference frequency.

Selectively choosing F1, F2, F3 and F4 and selectively choosing the upper and lower cutoff frequencies of the viewing filter to be within a selected range of the optical spectrum allows this equipment to generate a specific range optical of frequencies, for example, the visible colors. In the case where F1 is a frequency tunable ultra short optical pulse source, a judicious selection of the frequencies for F1, F2, F3 and F4 produces an output pulse from the optical mixer of a specified optical frequency (color). Alternatively, source F1 may contain three ultra short pulse sources of frequencies F1a, F1b and F1c, which are electronically selectable by the electronics, which also controls the pulse timing, and whose frequencies are so chosen such that mixer produces optical frequencies corresponding to one of the three colors (such as the primary colors) when F1a, F1b and F1c are respectively selected.

Moving the optical mixer periodically back and forth along the z axis of Figure 1, under the control of the electronics that also controls the pulse timing of the ultra short optical pulses

provides a mechanism to generate an optical mixer output, of the desired optical wavelength (color) at any point in the volume of space that is traversed by the optical mixer. The optical mixer and one possible way to move the mixer, shown in Figure 2, is operable over both increased and reduced atmospheric pressures, including placed the equipment in a vacuum to minimize the air resistance when moving the optical mixer at high speeds.

3. **Sketches:** Physical Arrangement:

In Figure 1, pulses of light are generated in the ultra short optical sources and these pulses are timed such they will overlap only at desired points, such as P1, in the plane of the optical mixer. In the optical mixer, these pulses optically interact and produce optical pulses frequencies at all the sum and difference frequencies of the interacting pulses. Only the desired combinations of frequencies pass thru the optical filter to the viewer or viewing equipment.

Figure 1 shows one possible arrangement of the ultra short optical sources, in which four sources, F1, F2, F3 and F4 are placed on the same side of the optical mixer [abcd]. This apparatus is operable with as few as three ultra short optical sources. The apparatus is also operable with additional sources to minimize distortion or to facilitate the simplified generation of optical frequencies (colors) from the optical mixer. For example, one or more of the ultra short optical sources may contain multiple sources capable of generating alternative frequencies. Objects or their representations are displayed by creating the desired optical frequencies in the optical mixer at points in the optical mixer, such as P1, as the mixer moves periodically back forth, in parallel to the XY plane along the Z axis in Figure 1. This apparatus creates pulses of light in the optical mixer at desired points, such as P1, that then travels thru the optical filter to the viewer or viewing equipment. The light pulses are generated as required in the volume of space swept out by the optical mixer as it moves back and forth. The optical mixer moves back and forth at sufficient speed that persistence of vision makes it appear that a three dimension rendering (representation) of the object

appears in the space traversed by the optical mixer [abcd] as the optical mixer moves between z1 and z3. Brightness of the display may be enhanced by use of an intense "gating" pulse F4.

Figure 2 shows a simple mechanism to move the optical mixer back and forth. The optical mixer has each corner supported by tracks which maintain a constant position relative to the x,y plane. A rotational source, synchronized to the ultra short pulse generation turns the idler drive gear which in turn is connected to the top and bottom gear drive. As the top gear drive turns, linear motion is transferred to the top of the optical mixer by the top gear arm. As the bottom gear drive turns, linear motion is transferred to the bottom of the optical mixer by the bottom gear arm.

Moving the optical mixer periodically back and forth along the z axis under the control of the electronics that also controls the pulse timing of the ultra short optical pulses provides a mechanism to generate an optical mixer output, of the desired optical wavelength (color) at any point in the volume of space that is traversed by the optical mixer. The optical mixer, shown in Figure 2, is operable over both increased and reduced atmospheric pressures, including placed the equipment in a vacuum to minimize the air resistance when moving the optical mixer at high speeds.

Figure 3 shows one form of moving the optical mixer rotationally, in which four sources, F1, F2, F3 and F4 are not placed on the same side of the optical mixer [abcd]. This apparatus is operable with as few as three ultra short optical sources. The apparatus is also operable with additional sources to minimize distortion or to facilitate the simplified generation of optical frequencies (colors) from the optical mixer. For example, one or more of the ultra short optical sources may contain multiple sources capable of generating alternative frequencies.

Figure 4 shows a top view of the rotational display apparatus of Figure 3, with one optical source placed on the other side of the mixer from the other k-1 sources, which shows that the concept of this apparatus is not dependent upon sources to be on one side of the plane. This production of an optical signal from the mixer in this configuration is enhanced by coating one side of the optical mixer with a partially transparent and partially reflective surface, similar to a half silvered mirror and/or constructing the optical mixer of a thin material that will diffuse light. The other side of the optical mixer may also include an optical filter to selectively transmit only the desired sum and difference products of this optical mixer.

This top view of the apparatus shows both that the rotating optical mixer is parallel to the x,y plane and that the ultra short optical source F4 generates a pulse that arrives at the plane of the optical mixer at the same time as axis of the source is aligned with the perpendicular to the optical mixer. At the same time the pulse from F4 arrives at the optical mixer, pulses from the Sources F1 to F3 also arrive at their intended convergent points at the optical mixer.

Figure 5 shows an arrangement of multiple sources, beginning with F4, then F5 and continuing to F_k that are successively utilized as the optical mixer rotates clockwise around the z axis. This sequential use of optical sources, starting with F4 and proceeding to F_k, maintains the alignment of the axis of F4 then F5 up to F_k with the normal to the plane of the optical mixer and thus helps insure that the pulses from F4 to F_k from these sources impinges on the optical mixer at approximately the same time. Maintaining this alignment simplifies the design of the electronics which generate overlapping optical pulses at desired points in the three dimensional display space. In a similar fashion, F1, F2 and F3 can be replicated, positioned in space to maintain the alignment of their axis with the normal to the optical mixer at it rotates.

For apparatus designs in which the pulse width of F4 to F_k is shorter than other sources such as F1, F2 and F3, this physical arrangement of successively timed sources F4 to F_k will

reduce the spatial dispersion of the overlapping optical pulses at the desired point in three dimensional display space. This apparatus arrangement also simplifies the design of the electronics that control the pulse timing of the optical pulse sources F1 to F_k

Figure 6 shows a variation of the apparatus in which the optical mixer moves rotationally, and is shaped somewhat like a screw, a polygon of which [a,b,c,d], is used to create a three dimensional display in a region of display space as the apparatus rotates. The optical mixer and the equipment to rotate the optical mixer, is operable over both increased and reduced atmospheric pressures including placement of the equipment in a vacuum to minimize the air resistance when moving the optical mixer at high speeds. In this example, in which the optical mixer is constructed as a spiral like shape, the four sources, F1, F2, F3 and F4 are placed on the same side of the optical mixer [abcd], however, they could be positioned on either side of the optical mixer.

Improved Nonlinear Optical Mixer

The optical mixer shown in Figures 1, 2, 3, 4, 5 and 6 is show as a single contiguous sheet of a material, that when impinged upon by two or more light pulses of different frequencies, produces sum and difference frequencies in the optical mixer. Three problems arise from using a single contiguous substance to implement the optical mixer. First, due to variations in the timing of pulses relative to each other, the spatial area where pulses spatially overlap is not as spatially focused as may be desired. Second, the conversion efficiency (ratio of energy conversion from multiple optical input pulses to the desired frequency output pulse) varies as a function of input optical frequencies. A single, homogeneous optical mixer cannot vary the conversion efficiency by desired output frequency as it is fixed across a homogeneous optical mixer. Finally, larger sizes of the nonlinear optical conversion material are more expense to fabricate per unit of surface area than are the smaller sizes.

A novel solution to these problems is to arrange smaller elements of the optical mixer in a regular array across the surfaces indicated by the optical mixer in Figures 1, 2, 3, 4, 5 and 6. Consider the simplest implementation, Figure 7, in which the optical mixer is the planar structure shown in Figure 1. Discrete Optical Mixers are placed the intersections of the curves in P1in Figure 7. Thus the intersections of the curves (shown as lines on P1 to simplify the illustration) of P1 define the regular array of the discrete elements of the Optical Mixer. For example, the intersection of Curve Xi and Yj defines the location of the nonlinear mixer regular arrangement. Nonlinear elements which are arranged as a discrete element implementation of an optical mixer moderate the spatial spreading of the desired output frequencies as the spatial area in which the impinging (input) optical pulses interact is limited to the those discrete locations in the regular array which form the nonlinear conversion elements of the Optical Mixer.

Figure 8 shows the details of a subsection the improved Optical Mixer. Discrete elements within the Optical Mixers are placed at the intersection of the curves which delineate the regular arrangement of the discrete Optical Mixer. In Figure 8, Optical Mixer F5 is at the intersection of Curve Xi and Curve Yj. While Figure 8 shows these curves as straight lines for the simplicity of the drawing, in general they are of a shape which enhances desired properties of the Optical Mixer.

In order to compensate for differences in optical conversion efficiencies at different optical frequencies or to compensate for different intensity levels of the impinging pulse sources, the nonlinear mixing elements in the regular arrangement are of different shapes and sizes. That is, the shape or size of the elements in the nonlinear mixing regular arrangement is chosen, as illustrated in Fig.9, to compensate for conversion efficiency variations by frequency, power output variations of pulse sources by frequency or other attenuation and losses in the system and thus equalize the display characteristics so as to calibrate the color response of the display system.

Consider Optical Mixer composed of discreet elements composed of an optically nonlinear material such as lithium niobate crystal. Consider the cylindrical nonlinear mixing element shown in Figure 8. Two optical frequencies (colors) F1 and F2 impinge upon the mixing element and one of the frequencies produced in the Optical Mixer Element is the sum of these Frequencies F1 + F2. Conversion efficiency improves as the diameter of the cylindrical element is increased as a greater amount of light enters the mixing element. Conversion efficiency also improves as the length of the cylinder increases. The novel aspect of the Optical Mixer in Figure 8 is that the shapes of the individual elements are chosen to achieve an equalization of the display characteristics. This novel aspect extends to elements of other shapes that allow optical pulses of two or more frequencies to enter one side of the mixer element and the pulses generated by nonlinear interactions to exit the other side of the mixer element. Similarly, one end of the mixer element may be coated with a reflective substance to give it a mirrored surface and the input optical pulses and the nonlinear frequencies exit from the same end of the mixer element as the input optical pulses entered. Traveling through the mixer element twice further increases the conversion efficiency.

4. For this three dimensional display apparatus, the spatial (time) resolution is given strictly by the length of the optical pulses and the optical non-linear process. The use of newly available IR ultra short pulse sources allows the creation of visible light in the optical non-linear process and thereby generates three dimensional images in the visible range and optical images discernable by commercially practical equipment. The spatial accuracy of the displayed image is adjustable by the selection of optical pulse duration and timing of the pulses by digital processing equipment. The brightness of the display may be enhanced by use of an intense "gating" pulse.

Exemplary methods and devices for generating and controlling ultra short optical pulses are disclosed in the following U. S. patents, which are incorporated by reference in this application:

#6,603,778, #5,898,714, #5,852,700, and #5,177,752.

Copies of these patents are attached as part of this application.

Further disclosure of such matter is included in the following technical journal articled, copies of which are appended hereto:

John D. Simon, Reviews of Scientific Instruments 60 (12), December 1989

G. Steinmeyer, Science Vol. 286, November 19, 1999

Roberto Paiella, Science Vol. 290, December 1,2000.

NWK2: 1114472.03
97084-00048

Ultrashort light pulses

John D. Simon[a)]

Department of Chemistry, Institute of Nonlinear Studies, University of California at San Diego, La Jolla, California 92093

(Received 9 June 1989; accepted for publication 26 August 1989)

This article reviews the generation and amplification of ultrashort laser light pulses, $\tau_p \leqslant 10^{-12}$ s. Current methods for generating optical pulses in the ultraviolet, visible, and infrared regions of the spectrum are described. Devices based on mode-locking techniques, as well as various novel sources for ultrashort light pulses, are examined. In addition, recent advances in using fiber optics to shape and compress optical pulses are presented. Optical amplifiers that have been developed to generate kilowatt and higher peak powers at a variety of repetition rates are described and compared. In the last section of the paper, various nonlinear optical techniques that have been developed to extend the tuning range of ultrashort laser pulses are briefly discussed.

INTRODUCTION

Recent advances in laser technology now enable the generation of ultrashort laser pulses throughout the ultraviolet, visible, and infrared regions of the spectrum. Reviews on several aspects of the developments and applications of short-pulsed lasers have been the topic of recent books,[1-3] special issues of various journals,[4,5] and conference proceedings.[6-13]

The objective of this paper is to examine current techniques for the generation and amplification of ultrashort laser pulses, $\tau_p \leqslant 10^{-12}$ ps. Advances in laser designs, nonlinear optical materials, and optical fibers have resulted in a variety of approaches for generating short light pulses. The advent of these technologies now enable one to study dynamics processes in real time with femtosecond time resolution. With the development of devices that can deliver a wide variety of pulse widths, tunability, and average and peak power at various repetition rates, a large variety of scientific applications have arisen.[1-13] Before examining experimental devices, some of the general technical features of ultrashort light sources are reviewed.

I. GENERAL CONSIDERATIONS

A. Active and passive mode locking

The majority of devices used to generate ultrashort laser pulses rely on the technique of mode locking.[14-16] In principle, mode locking entails modulation of the loss (or gain) in a laser at a frequency equal to the inverse of the time required for a pulse to travel one round trip inside the cavity. In order to effectively generate short pulses using mode locking, the laser resonator must support a large number (10^4–10^5) of longitudinal modes. Under these conditions, modulation results in the locking together of the phases of the oscillating longitudinal modes, generating a series of discrete laser pulses that are separated by the cavity round-trip time. In this section, we examine the basic experimental approaches used to achieve mode-locked behavior.

Experimentally, both passive and active approaches for mode-locking continuous-wave and pulsed lasers are commonly used to generate short light pulses. Passive mode locking involves placing a saturable absorber in the laser cavity. This passive device (usually a dye solution) is characterized by a transmission that increases nonlinearly with increasing light intensity. The saturable absorber thus causes the laser to operate in a pulsed mode. Passive mode locking has been used in a variety of optical configurations. For example, addition of a passive dye cell to a flash-lamp-pumped Nd:glass laser produces a train of pulses, each of which are <5 ps as measured by the full width at half maximum (FWHM).[17] Addition of a saturable absorber into a continuously pumped ring dye laser has been used to generate pulses as short as 27 fs.[18] We will examine such systems in detail in Sec. II.

On the other hand, active mode locking involves modulating loss in a cavity using an acousto-optic device.[14,15,19] The loss is created by Bragg diffraction in a quartz prism, which is inserted into the laser resonator. This approach to mode locking is commonly used to generate short pulses from continuous-wave argon-ion,[20] krypton-ion,[21] and various Nd^{+3} doped solid-state lasers.[22-36] These mode-locked laser systems can generate pulse widths from 30 to 150 ps. In the past few years, there have been significant advances in the development of continuous-wave mode-locked neodymium (III) solid-state lasers. Various configurations, continuous-wave mode-locked,[25-27] mode-locked and Q-switched,[28-31] and mode-locked, Q-switched, and cavity-dumped,[32,36,37] have been explored. The characteristics of these lasers have recently been reviewed.[38] The combination of active and passive mode locking has also been used to generate short pulses from flash-lamp-pumped Nd:glass (2.5 ps, Ref.39), Nd:$LiYF_4$ (YLF) (10 ps, Ref. 40), and Nd:YAG (25 ps, Ref. 41) lasers. Furthermore, Alcock and Ferguson have reported the mode locking of a miniature diode pumped YAG laser that can produce 240-ps 138-pJ pulses at a repetition rate of 245.7 MHz.[42]

In addition to generating short pulses by themselves, actively mode-locked lasers are commonly used to synchronously pump dye-laser systems. By matching the cavity length of the dye laser to the interpulse separation of the mode-locked pump laser, the gain in the dye laser is modulated at the round-trip frequency, resulting in efficient mode

 0034-6748/89/123597-28$01.30

locking. Synchronous pumping of dye lasers offers two significant advantages in generating ultrashort laser pulses. First of all, the dye-laser pulses are generally shorter than the pump pulses. Second, unlike most actively mode-locked lasers, the dye lasers can be tuned over a large frequency range. With recent advances in dye-laser design, discussed in Sec. II B, this technique can be used to generate ultrafast pulses throughout the visible and near-infrared regions of the spectrum.

B. Group-velocity dispersion and self-phase-modulation

The generation and amplification of femtosecond laser pulses require that one compensate for pulse-broadening effects that result from the propagation of light through dispersive media.[43] Dispersive media include dye streams, lenses, and other optical elements that are used inside the laser resonators and amplifiers. In addition, significant pulse distortions have been observed for high-intensity short light pulses traveling through air.[44] In the past decade, two major broadening mechanisms have received considerable attention. These are group-velocity dispersion[18] (GVD) and self-phase-modulation (SPM).[45] While the effects of GVD can be compensated by passing the light through a grating pair[46] prism pair (Sec. II D) or a Gires–Tournois interferometer,[48–50] SPM can lead to irreversible temporal broadening. In considering the origin of these effects, one can treat the optical pulse as a wave packet with central frequency ω_0 propagating through a dispersive medium. Expansion of the propagation wave vector k with respect to frequency gives rise to the following equation:

$$k(\omega) \simeq k(\omega_0) + \left(\frac{\partial k}{\partial \omega}\right)_{\omega_0} \delta\omega + \tfrac{1}{2}\left(\frac{\partial^2 k}{\partial \omega^2}\right)_{\omega_0} \delta\omega^2 + \cdots . \tag{1}$$

The first term in this Taylor-series expansion represents the propagation of the central frequency of the pulse. The linear term in $\delta\omega$ is related to the inverse of the group velocity of the pulse. The quadratic term measures the change in shape of the pulse as it propagates through the medium. This term gives rise to the effect commonly referred to as GVD. Mathematically, the GVD can be related to the second derivative of the change in index of refraction with wavelength as shown below:

$$\mathrm{GVD} = \frac{\partial^2 k}{\partial \omega^2} = \frac{\lambda^3}{2\pi c^2} \frac{\partial^2 n}{\partial \lambda^2}. \tag{2}$$

Thus, GVD induced by propagation through a dispersive medium results in a time-dependent frequency spread or "chirp" in the laser pulse. In most materials, the lower-frequency components travel faster than the higher-frequency components, resulting in an increase in pulse length. For Fourier-transform laser pulses, the broadening due to GVD depends upon the initial laser pulse width. For example, if a 75-fs pulse is passed through a 25-cm cell of water, the output pulse is broadened to 410 fs.[51] However, a 1-ps pulse would exhibit essentially no distortion passing through this cell. Since the temporal dispersion introduced results in an approximately linear frequency "chirp," this effect can be reversed by means of an additional negative dispersive delay using either a pair of prisms or gratings.

Nonlinear broadening mechanisms, i.e., SPM, can also occur in dye solutions and yield irreversible temporal broadening of the laser pulse. This phenomenon results in the generation of new frequencies in the laser pulse, which combined with GVD can lead to significant changes in the spectral and temporal shape of the laser pulses. The broadening mechanism is a function of the nonlinear index of refraction n_2 and can be expressed as[52,53]

$$\frac{\delta\omega}{\omega} = \frac{-n_2 l}{c} \frac{\delta\langle E^2\rangle}{\delta t}. \tag{3}$$

In the above expression, c is the speed of light, $\langle E^2\rangle$ is the square of the instantaneous electric field, and δt is the laser pulse width. This expression demonstrates that the broadening increases with the inverse pulse width. Thus effects of SPM are far greater for femtosecond than picosecond pulses. Experiments and theoretical calculations suggest that the output characteristics of femtosecond laser pulses produced in mode-locked dye lasers can be strongly influenced by SPM effects that occur in the dye jet streams.[52] Thus, in designing both dye-laser cavities and dye amplifiers, effects of SPM need to be minimized in order to prevent irreversible broadening of the laser pulse. Recent technologies have been developed that take advantage of SPM to generate shorter pulses than those available from mode-locked lasers. As discussed Sec. II D, SPM arising from the propagation of short pulses through optical fibers is now commonly used to generate new frequencies into the spectrum of the laser pulse, allowing for compression techniques to be applied to generate even short optical pulses.

C. Optical components

Finally, one needs to consider the components used in constructing ultrafast dye lasers and amplifiers. In particular, the choice of mirrors can have a large effect on the characteristics of the laser pulse. Early studies on the output pulses from colliding-pulse mode-locked (CPM) dye lasers (Sec. III A) revealed that the laser pulse width and shape were very sensitive to the selection of cavity mirrors.[54–58] These results were consistent with theoretical calculations which predicted that dispersive effects due to resonator mirrors would become important for pulse widths under 100 fs.[55] At that point, the majority of mirrors used in dye laser systems were broadband multilayered dielectric reflectors. For multilayer dielectric mirrors, the reflected wave is produced by the interference of the multiple reflections that take place within the structure. This produces a phase shift of the reflected wave that depends on laser frequency. This distribution of phase shifts can result in significant pulse distortion, as partial reflections originating at different points in the mirror structure will tend to broaden the laser pulses and in some cases result in satellite pulses. Systematic studies showed that multilayer substrates broadened the output from CPM lasers.[54–58] On the other hand, single-stack dielectric coatings used near the center of their reflective bandwidth showed essentially no effect on the reflected laser pulse shape. Thus current ultrafast dye lasers predominantly

use narrow-band single-stack dielectric mirrors. Because of the narrow bandwidth of single-stack coatings, different mirrors are needed to cover the entire optical range accessible by tunable dye laser. Outside the laser resonator, metallic coated mirrors are commonly used; negligible broadening effects are observed.

Many of the devices that are used to generate ultrashort light pulses are based on flowing the gain medium in a high-pressure jet. Fluctuations in the flow of a dye jet can influence cavity length in synchronously pumped dye lasers (Sec. II B), the stability of mode locking in CPM lasers (Sec. II A), and the mode quality of the output beam. Nonuniformity in the flow can arise from pulsations in the pumping source and the smoothness of the material used in manufacturing the dye nozzle. The most common nozzles are made from stainless steel. Detailed studies of steel nozzles revealed surface grooves on the 10-μm scale. For many applications, this surface roughness can result in transient effects on the dye flow, effecting the laser output. In 1982, Harri, Leutwyler, and Schumacher reported a design for a dye nozzle constructed from sapphire plates.[59] This approach generated interferometrically flat flows over a region of 9 mm^2, far superior to that observed with metal nozzles. These devices have been used in many ultrafast laser systems and are currently used in several commercially available high-resolution and ultrafast dye lasers.

The above discussion surveys some of the major important considerations in constructing ultrafast laser systems. Additional features are discussed in the following sections in conjunction with the devices that have been developed. The remainder of this review will focus on experimental techniques which are used to generate, amplify, and extend the tuning range of ultrashort laser pulses. Many of these topics have been treated extensively by theoretical models. Although we will not examine the theoretical aspects in detail, references are provided.

II. SHORT-PULSE GENERATION USING MODE-LOCKED LASERS

In this section we examine several techniques for the generation of picosecond and subpicosecond laser pulses. Four general topics will be examined. In Secs. II A and II B, the generation of tunable ultrafast light pulses using continuous-wave mode-locked dye lasers is examined. Section II A focuses on passively mode-locking dye laser systems. In recent years, several different dye combinations have been used in these devices to generate stable pulses with durations less than 100 fs. This is followed by a survey of laser systems that are synchronously pumped by an actively mode-locked solid-state or gas laser. Several different dye-laser configurations that are currently used are examined and compared. Synchronously pumped F-center lasers are examined in Sec. II C. Section II D examines recent advances in fiber-optic compression techniques. Unlike the other topics discussed in this section, this approach for the generation of femtosecond pulses involves manipulating the output of a longer pulse dye laser, taking advantage of the SPM and GVD caused by the propagation of intense short pulses in optical fibers. As a result, some of the limitations associated with direct generation of subpicosecond laser pulses by complicated dye-laser designs are overcome. This is followed by a discussion of pulse-shaping techniques and recent advances in the development of tunable mode-locked solid-state lasers.

A. Passively mode-locked dye lasers

Passive mode locking of cw dye lasers is currently a very powerful technique for the generation of subpicosecond optical pulses. In this approach, the gain medium of the dye laser is pumped by a continuous-wave laser, and a second saturable absorber dye jet is inserted in the dye cavity. In the mid-1970s, several different passively mode-locked cavity configurations were explored. Devices with single-wavelength outputs[60,61] as well as those operated at dual frequencies[62] were reported. In Fig. 1, the standing-wave passively mode-locked cavity design of Shank and Ippen is shown.[61] The gain medium, a dye jet of Rhodamine-6G (R6G) in ethylene glycol, was excited by a continuous-wave argon-ion laser. In this design the saturable absorber 3,3'-diethyloxadicarbocyanine iodide (DODCI) was mixed with the gain medium. In more recent designs, separate jets are used for the gain and absorber media. The various combinations of dyes and absorbers that have been used in standing-wave passively mode-locked dye lasers are tabulated in Table I. In addition, flash-lamp-pumped passively mode-locked dye lasers can also be used to produce short pulses. For a tabulation of the various dyes that have been used in this arrangement, the reader is referred to the book by Fleming.[1] These lasers have proven difficult to use; complications arising from relaxation oscillations and associated instabilities hindered their applications and prompted research for superior cavity configurations.

In 1981, Fork, Greene, and Shank introduced the colliding-pulse mode-locked (CPM) dye laser.[63] The improved mode locking in these devices resulted in easy and reliable generation of < 100-fs optical pulses. The central idea in the laser design is to use the collision of two pulses that are counterpropagating in the laser cavity to enhance the effective-

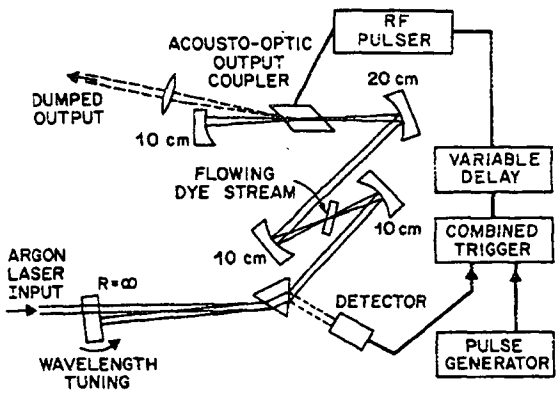

FIG. 1. Passively mode-locked linear dye-laser design of Shank and Ippen. The output from this resonator was cavity dumped at a repetition rate of 100 kHz. The gain and absorber mediums were R6G and a mixture of DODCI and MG in ethylene glycol jets, respectively. The pump laser was a continuous-wave argon-ion laser. Reprinted from Ref. 61 with permission.

TABLE I. Output pulses from passively mode-locked dye laser systems. Pump laser abbreviations: Ar, continuous-wave argon-ion laser; Ar-UV continuous-wave ultraviolet argon-ion laser; ML-Ar, actively mode-locked argon-ion laser; Kr, continuous-wave krypton-ion laser; Xe, pulsed xenon laser; Continuum, white-light continuum generated from an amplified CPM system.

Pump	Gain[d]	Saturable absorber[d]	λ (nm)	τ_p (fs)	GVD compensated	Reference
			Linear cavity			
Ar-UV	Coum. 102	DODCI	487–508	508	no	87
Ar	R110	DASBTI	553–570	210	no	88
Ar	R110	HICI		152	no	88
Ar	R6G	DASBTI	570–600	520	no	89
Ar	R110	HICI	579	120	yes	72
Ar	R6G	DODCI-MG	608–614	340	no	90
Ar	R6G	DODCI	612–630	130	no[a]	81,91,213
Ar	R6G	DODCI	620	500	no	61
Ar	R6G	DODCI	620	60	yes[a]	92
Ar	DCM	DQTCI	655–673	680	no	93
Ar	RB	DQTCI	616–658	220	no	94
Ar	R6G-SR101	DCCI	652–694	240	no	95
Ar	R6G-SR101	DQTCI	652–681	120	no	95
Kr	R700	DOTCI	727–740	1 ps	no	96
Kr	R700	DCI-DOTCI	740	350	no	96
Kr	R700	HITCI	762–778	850	no	96
			Colliding-pulse mode-locked cavity			
Ar	R6G	DODCI	310[b]	40	yes	83
Ar	R6G	DODCI	314[b]	120	yes	84
Ar	R6G	DODCI	315[c]	43	yes	85
Ar	Coum. 102	DOCI	487–510	>93	yes	97
Ar	Coum. 102	D9MOCI	488–511	>140	yes	97
Ar	Coum. 102	DQTI	492–512	>140	yes	97
Ar	Coum. 6h	DOCI	492–507	>110	yes	98
Ar	Coum. 103	DOCI	493–502	<100	yes	73
Ar	Coum. 102	DPQI	494–511	>150	yes	97
Ar	Coum. 1	DOCI	501–508	>130	yes	97
Ar	Coum. 6	DI	518–554	>95	yes	75
Ar	R110	HICI	581	80	yes	72
Ar	R6G	TCVEBI	617	60	yes	79
Ar	R590	DODCI	618	47	no	70
ML-Ar	R6G	DODCI	620	<100	no	71
Ar	R6G-KRed	DODCI	620	30	yes	77
Xe	R6G	DODCI	620	340	no	99
Ar	R6G	DODCI	620	90	no	63
Ar	R6G	DODCI	625	50	yes	68
Ar	R6G	DODCI	634	27	yes	18
Ar	R6G-SR101	DQTCI	685	58	yes	78
Continuum	Styry 19	IR140	840–880	65	yes	76
Kr	LiF:F_2^-	IR140	850	180	yes	100

[a] Antiresonant ring systems.
[b] Intracavity doubling using KDP.
[c] Intracavity doubling using β-BBO.
[d] Dye abbreviations: Coum = Coumarin; R = Rhodamine; SR = Sulphorhodamine; Kred = Kiton Red; DASBTI = 2-(*p*-dimethylaminostyryl)-benthiazolyl ethyl iodide; HICI = 1,1,3,3,3',3'-hexamethylindocarbocyanine iodide; MG = malechite green; DQTCI = 1,3'-diethyl-4,2'-quinolythiacarbocyanine iodide; DCCI = 1,1'-diethyl-2,4'-carbocyanine iodide; DOTCI = 3,3'-diethyloxatricarbocyanine iodide; DCI = 1,1'-diethyl-4,4'-carbocyanine iodide; HITCI = 1,1',3,3,3',3'-hexamethylindocarbocyanine iodide; DOCI = 3,3'-diethyloxacarbocyanine iodide; D9MOCI = 3',3'-diethyl-9-methyloxacarbocyanine iodide; DQTI = 1,3'-diethyl-2,2'-quinolylthiacyanine iodide; DPQI = 1,1'-diethyl-2,2'-pyridyl-quinolylcyanine iodide; DI = 1,1'-diethyl-2,2'-cyanine iodide; TCVEBI = 2-[2-(2,3,6,7-tetrahydro-1H,5H-benzo[*i*, *j*]chinolizin-9-yl)vinyl]-3-ethylbenzothyazolium iodide.

ness of the saturable absorber. In the past few years, several theoretical models for describing the details of mode locking in CPM lasers have appeared.[45,64 66] In order to accomplish colliding-pulse mode-locked behavior, Fork, Greene, and Shank designed the ring resonator shown in Fig. 2. In this configuration, excitation of the gain medium by a continuous-wave argon-ion laser generates two counterpropagating pulse trains. The optimal design involves separating the gain and saturable jets by 1/4 of the round-trip distance in the ring. To minimize energy loss in the resonator, counterpropagating pulses meet and collide at the saturable absorber; thus, this optical arrangement results in the two pulses arriving at the gain medium separated by exactly ½ the cavity round-trip time. In this way, both pulse trains see the same gain. It is also necessary that the saturable absorber be sufficiently thin that the optical path in the medium is less than the desired pulse width. Using the dye combination of R6G and DODCI, these lasers have produced pulses as short as 27 fs.[18]

Construction of a CPM dye laser involves serious consideration of the effects of GVD, SPM and mirror dispersion.[51] As stated in Sec. I C, single-stack dielectric mirrors

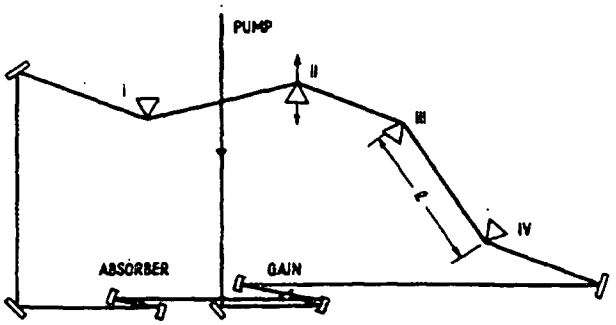

FIG. 2. Colliding-pulse mode-locked ring dye laser developed by Valdmanis, Fork, and Gordon. The prism sequence enables one to control the GVD inside the resonator (see text). The various gain and absorber dyes that have been used in this configuration are given in Table I. Output pulses as short as 27 fs have been reported from these devices. Reprinted from Ref. 18 with permission.

are currently the optimal choice for the cavity optics. In order to prevent pulse broadening or the creating of pulse structure in steering the laser output to experiments, aluminum mirrors are generally used. The effects of SPM in the gain and absorber jets have received significant attention.[67] In addition, GVD effects arising from the propagation of the pulses in the laser resonator can lead to significant broadening.[68]

The effects of GVD can be compensated by adding negatively dispersing elements into the cavity.[68] It is important that components added to the laser cavity have low loss as not to dramatically affect the threshold and operating conditions of the laser. Fork and co-workers demonstrated that the addition of a four-prism sequence into the CPM laser could be used to compensate for the GVD inherent in the laser cavity as well as that cause by the additional glass.[47,69] In addition, the prism sequence allows for control over the spectral properties of the pulse by placing a slit between the pairs of prisms. The basic design of this optical filter is shown in the optical resonator of the CPM depicted in Fig. 2. Each prism pair (I and II, III and IV) serves to disperse and collimate the laser light. In the region between prisms II and III, the laser light is spatially dispersed with respect to frequency; thus, in principle, addition of a slit between prisms II and III enables one to either tune the frequency of the cavity or limit the spectral shape of the pulse. Since each pair of prisms reverses the action of the other pair, no net spatial displacement of the wavelength components of the laser beam is caused by the prism sequence. Translation of one of the prisms normal to its base provides a tunable amount of negative dispersion. Addition of the prism sequence into CPM lasers results in pulse widths as short as 27 fs.[18] Several reports using R6G and DODCI have appeared.[18,63,70,71] In addition, various other dye combinations have been reported that enable generation of pulses with duration of < 100 fs at several frequencies.[72–79] French and Taylor have reported < 150-fs generation in the spectral range from 488 to 554 nm using Coumarin dyes as the gain medium.[80] The various combinations of gain and saturable absorbers dyes used in a CPM laser and the resulting pulse widths are given in Table I (see Refs. 83–100). Recently, high-energy femtosecond UV light has been generated using intracavity doubling in a CPM laser.[83–85] Reports using potassium dihydrogen phosphate (KDP) (Refs 83 and 84) and β-BaB_2O_4(β-BBO) (Ref. 85) have appeared. UV pulses as short as 40 fs are observed. The theory or intracavity doubling in a CPM laser has been addressed by Zhang *et al.*[86]

B. Synchronously pumped dye lasers

Synchronous pumping techniques are commonly used to generate ultrafast pulses throughout the visible and near-infrared regions of the optical spectrum. Synchronously pumped dye lasers are designed such that the cavity length is equal to (or a submultiple of) the interpulse spacing of the mode-locked pump laser. As discussed above, this results in a modulation in the gain of the laser at the round-trip frequency. The first such dye laser was reported by Soffer and Lin[101] in 1968 in which a R6G and Rhodamine B dye laser was synchronously pumped by a high-power pulsed mode-locked Nd:glass laser. Following this report, efficient tunable picosecond pulse dye lasers were developed using mode-locked ruby[102–104] and Nd:YAG (Refs. 105 and 106) lasers.

Today, the majority of the mode-locked systems used to generate ultrashort dye-laser pulses are based on continuous-wave dye lasers. These systems usually provide optical pulses with a repetition rate of 70–100 MHz, with an average power of 10–200 mW. The first report of mode locking a continuous-wave dye laser using synchronous pumping was reported by Dienes, Ippen, and Shank in 1971.[107] In this approach, a R6G cell was inserted directly inside a mode-locked argon-ion laser. In 1974, Chan and Sari described a simple dye-laser cavity that could be pumped by the output of a mode-locked argon-ion laser.[108] This device contained a dye stream of R6G in ethylene glycol at the focus of a conventional compensated folded cavity. A high reflector on a translation stage was used at one end of the cavity. This allowed for the adjustment of the dye-laser cavity length to match that of the argon-ion pump laser. Output pulses as short as 2.8 ps were reported from 560 to 610 nm. The design of this device forms the basis for virtually all synchronously pumped mode-locked dye lasers that are currently used. With advances in both controlling the GVD in laser cavities and acousto-optic mode-locking techniques, synchronously pumped dye lasers have generated tunable subpicosecond laser pulses (see Table II) throughout the visible and near-infrared regions of the spectrum. The theory of mode locking by synchronous pumping has been extensively studied.[109–111] A qualitative picture of the gain and pulse shaping in a synchronously pumped dye-laser system is shown in Fig. 3.

In the past few years, advances in mode-locked solid-state neodymium lasers have resulted in useful light sources for synchronously pumping dye lasers and color-center lasers. In order to pump dye lasers with mode-locked Nd:YAG lasers, the second-harmonic output at 532 nm is used. With the development of $KTiOPO_4$ (KTP) nonlinear optical crystals, efficient conversion of the mode-locked output to 532 nm was achieved. These solid-state lasers have advantages over the ion laser as shorter pulses can be genera-

TABLE II. Output pulses from a hybrid mode-locked dye laser pumped by a frequency-doubled continuous-wave mode-locked Nd:YAG laser.

Gain[c]	Saturable absorber[c]	λ (nm)	τ_p (fs)	GVD compensated	Reference
R110	DASBTI	560	280	yes	133
R6G	DODCI-DQOCI	583	69	yes	132
R6G	DQOCI	585	114	yes	132
RB	DQTCI-DDBCI	604–632	430[a]	yes	127
Kiton Red S	DODCI-DQOCI	615	29	yes	135
R6G	DODCI	615	90[b]	no	137
R6G	DQOCI	615	70[a]	no	126
R6G	DODCI	619	64[b]	yes	158
R6G	DODCI	622	<150	yes	132
RB	DTDCI	650	190	yes	134
SR101	DQTCI	675	55	yes	134
Pyr. 1	DDI	695	103	yes	133
Pyr. 2	DDI-DOTCI	733	263	yes	133
Pyr. 2	DDCI	745	420	no	162
Pyr. 2	DCI	745	455	no	162
Pyr. 2	DOTCI	745	845	no	162
Pyr. 2	HITCI	745	780	no	162
Pyr. 3	DNTTCI	745	650	no	162
R700-R640	DDCI	745	423	no	162
Pyr. 2	DDCI	745	210	yes	162
Pyr. 2	DDCI	751	163	yes	162
Styryl 8	HITCI	800	70	yes	133
Styryl 9	IR140	840	65	yes	133
Styryl 14	DQTrCI	897–905	265	yes	163
Styryl 13	IR143	926	830	yes	164
Styryl 14	DaQTeC	974	228	yes	163

[a] Gain and absorber dyes mixed in a single dye stream.
[b] Antiresonant ring containing the saturable absorber jet is at one end of the dye laser cavity.
[c] Dye abbreviations: Pyr = pyridine; RB = Rhodamine B; DQOCI = 1,3'-diethyl-4,2'-quinolyoxacarbocyanine iodide; DDBCI = 3,3'-diethyl-9-methyl-4,5,4',5'-dibenz-thiacarbcyanine iodide; DTDCI = 3,3'-diethylthiadicarbocyanine iodide; DDCI = 1,1'-diethyl-2,2'-dicabocyanine iodide; DNTTCI = 3,3'-diethyl-9,11-neopenylenthiatricarbocyanine iodide; DQTrCI = 1,1' = diethyl-4,4'-quinotricarbocyanine iodide; DaQTeC = 1,1'-diethyl-13-acetoxy-2,2'-quinotetracarbocyanine iodide.

ted. Synchronously pumped dye lasers have generated picosecond pulses continuously tunable from 560 to 1000 nm using mode-locked argon-ion-pumped dye lasers,[76,112–114] mode-locked krypton-ion-pumped dye lasers,[114,115] and mode-locked cw Nd:YAG pumped dye lasers as pump lasers.[116–123] Femtosecond output pulses from such a dye-laser design have also been reported using the frequency-doubled output of a fiber-optically compressed Nd:YAG laser (Sec. I D) as the pump source.[56,124,125] Current designs of picosecond Nd:YAG lasers were recently reviewed by Sizer and Duling[38] and therefore will not be covered in detail in the present review.

Modifications of the basic dye-laser design of Chan and Sari[108] now enable easy and reliable generation of tunable-

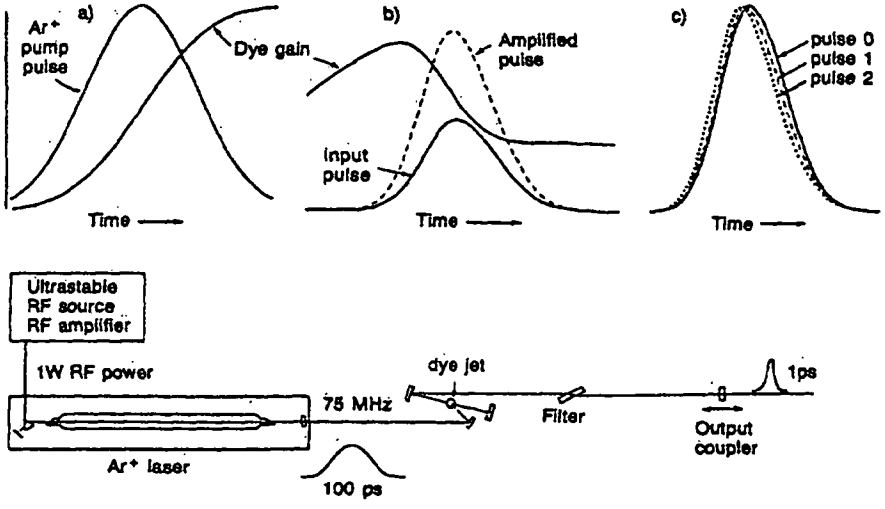

FIG. 3. The optical arrangement and pulse shortening mechanism in synchronously pumped dye lasers are shown. The top sequence of drawings depicts the pulse generation by synchronous pumping. (a) The argon-ion laser pulse and dye gain curve are superimposed as a function of time. (b) Qualitative representation of the dye gain and pulse shape of the input (solid line) and output (dashed line) pulses. (c) Normalized input (solid line) and output pulses after one round trip (dashed line) and two round trips (dotted line) are shown. Reprinted from Ref. 1 with permission.

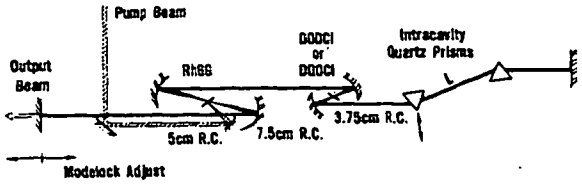

FIG. 4. The hybrid mode-locked dye laser design of Dawson, Boggess, and Garvey is shown. The intracavity prisms are used to compensate for GVD. The various gain and absorber dyes that have been used in this design are given in Table II. Subpicosecond pulses from 560 to 974 nm have been generated by synchronously pumping this device with a frequency-doubled continuous-wave mode-locked Nd:YAG laser. Reprinted from Ref. 132 with permission.

subpicosecond pulses. Output characteristics similar to those observed for CPM lasers have been observed. In order to generate the desired short pulses, passive mode locking is achieved by introducing saturable absorbers into the dye-laser cavity. These lasers are commonly referred to as hybrid mode-locked dye lasers, as both active and passive mode-locking techniques are used. Tuning of the laser can still be accomplished using a birefringent filter; however, this generally results in output pulses longer than a few hundred femtoseconds. Along a related line, Mourou and Sizer investigated the effects of mixing the gain and saturable absorber medium in a single dye jet.[126] Using a combination of R6G and the saturable absorber DQOCI, pulses as short as 70 fs were observed. A related study in which Rhodamine B and DQTCI-DDBCI were mixed in a single jet resulted in tunable <500-fs pulses from 604 to 632 nm.[127] Several theoretical discussions of hybrid mode locking have also appeared.[128-131]

In order to generate optical pulses under 200 fs, the tunability of the dye laser is generally sacrificed. Two basic optical designs are currently used. In Fig. 4, a schematic of the hybrid mode-locked dye laser reported by Dawson and coworkers is shown.[132-134] In this device, a linear dye cavity is synchronously pumped at 82 MHz by 650-mW 70-ps pulses from a frequency-doubled mode-locked cw Nd:YAG laser. The resonator incorporates both a gain and saturable absorber jet; in this particular case, the focusing mirrors around the gain and absorber have a radius of curvature of 7.5 and 3.75 cm, respectively. The pump beam is coupled into the resonator by a 5-cm radius of curvature focusing mirror. Output couplers ranging from 80% to 95% are used, depending on the specific dye combination. The end opposite to the output coupler is terminated by a pair of Brewster-angle prisms. As described in Sec. II A, the intracavity prisms enable one to compensate for GVD in the laser cavity. In a linear cavity, the pair of prisms in conjunction with the high reflector results in the same effect as the four-prism sequence in the ring lasers. Designs incorporating a four-prism sequence on the output coupler side of the cavity have also been reported.[135] Several research groups have characterized the output of this general laser design for a variety of dye combinations; the output powers, pulse widths, and references for various dye combinations are tabulated in Table II.

A second approach involves the addition of an antiresonant ring to one end of the linear dye laser; see Fig. 5.[136,137] This approach was first proposed by Siegman[138] and was successfully used to passively mode lock a Nd:YAG laser.[139,140] This approach combines the advantages of the CPM laser with synchronous pumping. The laser consists of a four-mirror linear cavity; one end is a 5% output coupler mounted on a translation stage and the other end is an antiresonant ring. The saturable absorber jet is positioned in the center of the antiresonant ring opposite a 50% beam splitter. Thus pulses propagating in the laser cavity are divided in half by the 50% reflector, reach the saturable absorber jet at the same time, and then recombine at the partial reflector. This behavior is similar to that encountered in a CPM laser. In addition, the critical position of the saturable absorber jet in the CPM configuration is not affected by adjustment of the cavity length. In the initial report of this laser design, Norris, Sizer, and Mourou found output pulses of 85 fs with an average power of 60 mW at 615 nm without using the intracavity prisms shown in Fig. 5.[137] Pump powers on the order of 1.5W at 532 nm (70-ps FWHM) were used. Pulses as short as 50 fs have been observed using intracavity prisms to control the GVD.[135,141]

Recently, cw mode-locked Nd:YAG lasers have been developed that can produce outputs in excess to 20 W. These devices, coupled with the development of new efficient nonlinear optical materials (e.g., β-BBO), enable the generation of high-intensity picosecond pulse trains at 355 nm. This

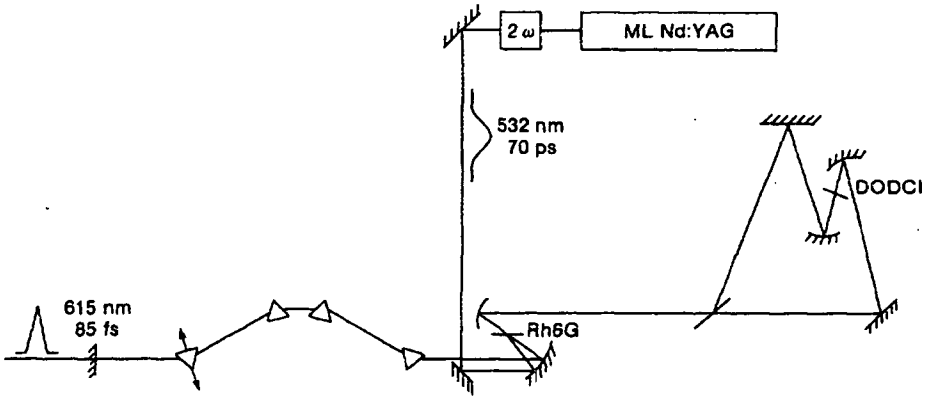

FIG. 5. The linear antiresonant ring dye laser developed by Norris, Sizer, and Mourou. The position of the saturable absorber in the antiresonant ring enables one to take advantage of the pulse shortening of a CPM arrangement in a linear cavity. The pump laser was a frequency-doubled continuous-wave mode-locked Nd:YAG laser. Addition of intracavity prisms on the output coupler side of the cavity has resulted in the generation of optical pulses which are <50 fs. Reprinted from Ref. 137 with permission.

light can be used to synchronously pump blue dye lasers. Using such a device Negus, Couillaud, and Brady[142] synchronously pumped a hybrid mode-locked dye laser using Stilbene 3 as the gain and Coumarin 535 as the saturable absorber. With a pump energy of 1.0 W at 355 nm, subpicosecond pulses were reported over the entire gain profile, the shortest pulse being 220 fs at 435 nm.

One complication that arises in synchronously pumped systems is that the spectral and temporal shape of the laser pulse is a sensitive function of detuning effects between the cavity lengths of the pump and dye lasers. This effect has been extensively studied both theoretically and experimentally.[143–151] For picosecond pulses, changes in cavity length on the micrometer scale can seriously effect the pulse. Changes on smaller distance scales become important with decreasing pulse width. Phase jitter in the pump laser, or changes in the cavity length of the pump or dye laser resulting from thermal fluctuations, can also have a large effect on the pulse width observed. As a result, various approaches for stabilizing the output pulses from mode-locked laser systems have been reported.[136,152–156] In general, these devices either monitor the intensity or spectral characteristic of the output pulse and adjust either the mode-locking frequency of the pump laser or the cavity length of the dye laser to maintain a constant temporal output. Without cavity stabilization, maintaining the short femtosecond output is extremely difficult.

In addition to synchronously pumped dye lasers, ultrashort pulses have been generated by pumping short-cavity dye lasers.[157–161] In general, these lasers are pumped by active-passive mode-locked Nd^{3+} lasers. Pulses as short as 460 fs have been reported using a short-cavity R6G-DODCI dye laser.[158] Picosecond pulses produced using a nitrogen laser as the pump source has also been reported.[161]

Other dye combination output characteristics for this general laser design are given in Table II.[162–164]

C. Synchronously pumped *F* center lasers

The above discussion examined ultrashort light pulses generated by the synchronous pumping of dye lasers. Picosecond pulses in the infrared region have been produced by synchronous pumping *F*-center lasers.[165–172] *F*-centers arise from defects in alkali halide crystals in which halide ion vacancy is occupied by an electron. The trapped electron gives rise to broad optical absorption and emission bands. The mode locking of color-center lasers involves challenges not faced in dye lasers. First of all, the crystals must be maintained at cryogenic temperatures.This places various constraints on the design of the optical cavity. Second, unlike organic dyes, the upper-state lifetime of an *F* center is longer than the cavity round-trip time. This means that the gain seen between successive pulses does not change significantly. As a result, when pumping an *F* center by a mode-locked laser, two thresholds for lasing are observed. At low pump powers, continuous lasing is observed. At higher pump power, mode locking is observed. In order to achieve stable mode locking, the intracavity power must be able to deplete the gain by stimulated emission. The first such system reported involved the pumping of a LiF:F_2^+ color center by an actively mode-locked krypton-ion laser.[172] This system provided tunable output between 0.82 and 1.07 μm with pulse widths as short as 5 ps. Since this report, a number of *F*-center lasers have been explored using both mode-locked ion lasers and Nd:YAG lasers as the excitation source. Picosecond pulses have been generated from 0.8 to 4 μm using these devices.

Recently, passive mode locking of a continuous-wave LiF:F_2^+ laser in a ring resonator was examined.[100] The optical configuration was analogous to a CPM laser. In this case, a cw krypton-ion laser was used as the pump source, the LiF:F_2^+ crystal was the gain medium, and the saturable absorber was the laser dye IR140. With four intracavity prisms to control GVD, 180-fs pulses at $\approx$850 nm with an average power of 16 mW were reported.

In 1984, Mollenauer and Stolen demonstrated a new concept in ultrashort light pulse generation with their design of the soliton laser.[173] This device, shown in Fig. 6, involves coupling a mode-locked color-center laser with an external cavity containing a single-mode optical fiber which has negative group-velocity dispersion. The gain medium was the Tl^0 (1) center in KCl. Generally, when a pulse is launched into an optical fiber, the temporal and wavelength profile distorts due to the combination of GVD and SPM. These phenomena are the basis of the fiber-optic compressor discussed in Sec. II D. However, if the pulse is a soliton,[174–178] the SPM and negative dispersion of the fiber cancel the effects of pulse distortion. Thus, in the case of an $N = 2$ soliton, the transmitted pulse is compressed and restored to its original shape as a function of distance traveled in the fiber. The fiber length of the external cavity is selected to be 1/2 the distance required for an $N = 2$ soliton to recover its pulse shape. Thus, one round trip in the external cavity produces a pulse whose shape is identical to the input pulse. The return-

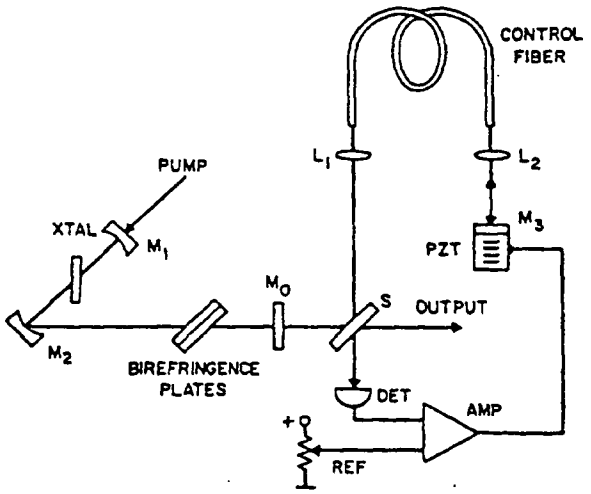

FIG. 6. The optical arrangement of the soliton laser developed by Mollenauer and co-workers (Refs. 176–179). The gain medium in an *F*-center crystal. See the text for a description of the role of the optical fiber in controlling the characteristics of the output pulses. The piezoelectric transducer (PZT) is used to adjust the length of the external cavity to match that of the color-center laser. The birefringence plates are used to tune the frequency of the main cavity. Reprinted from Ref. 179 with permission.

ing pulse is then injected back into the laser. The shortening of the laser pulse can be controlled by varying the length of the optical fiber. Mitschke and Mollenauer have reported outputs from a fiber-stabilized soliton laser as short as 60 fs at a wavelength of 1.5 μm.[179] External fiber-optic pulse compression (Sec. II D) resulted in light pulses as short as 19 fs. At the operating wavelength, 1.5 μm, this corresponds to four optical cycles.

In the last year, reports using NaCl as the gain medium for soliton lasers have been given.[166] The NaCl laser has a higher gain cross section and therefore is more easily saturated. This crystal has over five times the output power and three times the tuning range as the $Tl^0(1)$ center used by Mollenauer and Stolen. Pulses as short as 200 fs with output powers greater than 300 mW at 1.56 μm were observed.

The soliton laser has the complication that feedback stabilization is required to keep the two cavities interferometrically matched. Not only must cavity length be matched but the optical phase of the fiber output must be matched to the phase of the light in the *F*-center cavity.

Raman pumping processes in optical fibers seeded with the output of mode-locked color-center lasers have also been used to generate infrared light that is shifted from the color-center output.[180–189] Pulses as short as 240 fs have been reported using this technique. This approach has the advantage over the above-described soliton laser in that feedback stabilization is no longer needed.

In addition, in 1988, several research groups reported ultrashort light pulses using a positive dispersion fibers in the coupled cavity.[190–192] These fibers cannot support solitons; as such, a different mechanism must be involved in the generation of the ultrashort pulse. Mark *et al.*[193] have proposed a model that is based on the interference between the injected and circulated pulses. Pollock, Pinto, and Georgiou[166] have used this technique with both $Tl^0(1)$ and NaCl gain crystals. The NaCl produces more than 300 mW output power. Using a 60-cm single-mode optical fiber (Corning No. 1521), 150-fs pulses were produced when 70 mW is coupled to the fiber cavity.

D. Fiber-optic compressi n techniques

In 1981, Nakatsuka and Grischkowsky[194] introduced a method for optical pulse compression that took advantage of the SPM and GVD that arise from the propagation of intense light pulses in single-mode optical fibers. The basic arrangement of the optical device is shown in Fig. 7. This passive device simply consists of a fiber-optic and a dispersive delay line.

The basic principles of the device are as follows. The propagation of the pulse through the optical fiber broadens and chirps the laser pulse as a result of the combined effects of GVD and SPM. Thus, the output pulse is longer in time and is characterized by a broader frequency spectrum than the input pulse. Since the GVD results in a linear frequency sweep over the pulse duration, the output pulse can be recompressed by passing through a region of negative dispersion, such as a prism or grating pair. The increased spectral bandwidth of the output pulse enables one to generate a compressed pulse that is shorter in time than the input pulse.

In the past few years, fiber-optic pulse compressors have been used with picosecond and femtosecond dye lasers,[195–204] krypton-ion lasers,[205] continuous-wave mode-locked Nd:YAG lasers,[206–211] high-energy pulses generated from mode-locked and *Q*-switched Nd:YAG lasers,[212–215] pulsed amplified dye lasers,[216–220] and chirped amplification schemes.[221–225] In addition, the application of multiple stages of compression have been reported.[196–198,206,209] In Table III, the results of the use of fiber-optic compression with various laser configurations are given. Tomlinson, Stolen, and Shank[226] have discussed the conditions for optimal

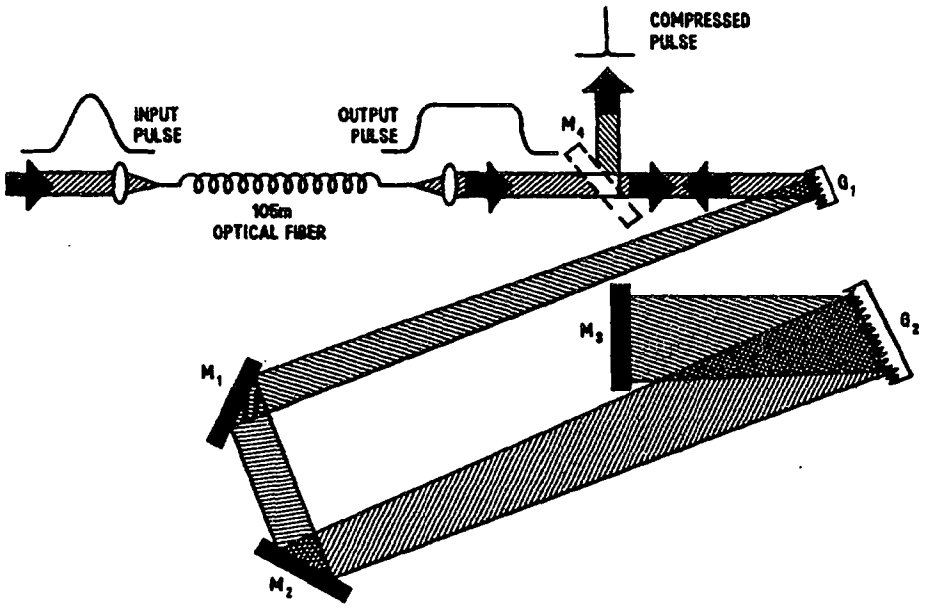

FIG. 7. Schematic of an optical pulse compressor. The seed pulse is chirped in an optical fiber. The output pulse is then recompressed by a delay line containing two gratings. The outputs of several different laser sources have been compressed using fiber-optic techniques; see Table III. Reprinted from Ref. 232 with permission.

TABLE III. Ultrashort pulse generation using fiber-optic compressors. The pulse width of the compressed pulse after one stage (τ_1) and two stages (τ_2, when applicable) are given. The compression factor is the ratio of the input to output pulse width for the total number of stages used in the device. Abbreviations used: CA, chirped amplification; He-Ne, mode-locked helium-neon laser; ML, mode-locked; QS, Q switched; Amp-CPM, amplified output of a colliding-pulse mode-locked dye laser; YAG-dye, dye laser synchronously pumped by a mode-locked Nd:YAG laser; Ar-dye, dye laser synchronously pumped by a mode-locked argon-ion laser; cw, continuous wave; Kr, krypton-ion laser; Regen., regenerative amplifier.

Source	λ(nm)	τ_m(ps)	Number of Stages	τ_1(ps)	τ_2(ps)	Compression factor	Peak power	References
He-Ne	632.8	500	1	250	···	2		231
cw ML-Nd:YAG	1060	90	2	4.2	0.2	450	8 kW	206
		70	1	0.54	···	130		207
		100	1	2.1	···	46	1 kW	208
		100	1	5	···	20	600 W	125
		80	1	1.6	···	45	3.8 kW	210
		85	2	2.8	0.75	113	400 W	209
		70	1	3.5	···	20	10 kW	211
	532	33	1	0.41	···	80	3.4 kW	232
	1319	100	2	2	0.090	1100	830 W	233,234
cw ML-Nd:YLF	1053	44	1-CA	8	···	5.5	63 MW	221
		55	1-CA	1	···	55	1 TW	222,235
cw ML, QS-Nd:YAG	1064	130	1	3.7	···	37	2 MW	24
		50	1	1.7	···	30	1 MW	213
		85	1	3.0	···	28	25 kW	212
		85	1	3.0	···	28	199 kW	215
Nd:glass	1050	5	1-CA	0.7	···	7	714 MW	224
ML-Kr	647	100	1	3	···	33	180 W	205
Amp-CPM	620	0.05	1	0.006	···	8.3		216
		0.04	1	0.008	···	5		217
		0.09	1	0.03	···	3		218
		0.11	1	0.012	···	9.2	0.5 MW	219
		0.05	1	0.016	···	3	37 MW	220
YAG-dye	615	0.24	1	0.056	···	4.3	188 kW	202
	596	0.3	1	0.06	···	5	32 kW	200
	745	1.5	1	0.15	···	10	5.2 kW	204
Ar-dye	616	6	1	0.6	···	10	1.3 kW	203
	570–600	5.4	1	0.45	···	12	3 kW	201
	580–610	5.9	2	0.2	0.09	65	10 kW	197
	585–605	5.4	2	0.180	0.016	337	80 kW	198
	597–615	1.5	1	<0.1	···	15		199
	590	6	1	0.038	···	157	720 W	195
	600	0.8	2	0.163	0.117	6.8	90 kW	196
Nd:YAG-Regen.	1064	80	1-CA	12	···	6.7	16 MW	225

pulse compression for a variety of input powers and pulse widths.

However, the dispersion properties of the optical components in this device impose a limitation on the maximum compression attainable. This can be best understood from the following considerations. Chirping the optical pulse can be viewed in terms of phase distortion. Mathematically this effect be expressed in terms of a Taylor-series expansion of the phase of the light pulse with respect to frequency:

$$\phi(\omega) = \phi(\omega_0) + \left(\frac{d\phi}{d\omega}\right)_{\omega_0} (\omega - \omega_0) + \frac{1}{2}\left(\frac{d^2\phi}{d\omega^2}\right)_{\omega_0} (\omega - \omega_0)^2 + \frac{1}{6}\left(\frac{d^3\phi}{d\omega^3}\right)_{\omega_0} (\omega - \omega_0)^3 + \cdots. \quad (4)$$

A simple device that compensates for the quadratic phase distortion, $(d^2\phi/d\omega^2)_{\omega_0}$, of a frequency-broadened pulse is a grating pair; this approach was originally proposed by Treacy.[46] In this work, he also pointed out that limitations in the pulse compression of large-bandwidth pulses due to cubic phase distortions; in particular grating pairs introduce positive cubic distortions. In the block diagram in Fig. 7, a pair of gratings is used. Variations on this approach using a prism have also been reported.[196] The diffraction efficiency of gratings are generally less than 80 and overall throughput of optical compressors of this design are on the order or 25%. Replacement of the grating with a highly dispersive prism also results in recompression of the optical pulse. However, the loss using prisms is negligible and higher throughputs are observed.[196] In addition, the characteristics of the output pulse is sensitive to the intensity fluctuations of the seed pulse.[227,228]

Correction of the phase distortion using grating pairs has been successfully used to compress optical pulses to du-

rations on the order of 10 fs. However, below 10 fs, serious limitations arise from the increase in importance of higher-order terms in Eq. (4). In particular, the cubic phase distortions increase in importance with decreasing pulse width (and increasing spectral width) and as stated above, a simple grating pair cannot be used to compensate for the total dispersion. Fork and co-workers have demonstrated that these phase distortions can be overcome by using a combination of prism and grating pairs.[229,47] This prism and grating combination avoids the generation of the long tailing edge of the pulse that is commonly observed in compressed pulses using a single grating pair for recompression. The principle feature of the prism pair that enables the improved phase compensation is that the cubic contribution to Eq. (4) is negative, opposite in sign to the contribution from the grating pair. Translation of the prisms in the beam enable one to tune the quadratic and cubic phase corrections. Using this approach, pulses as short as 6 fs,[216] the shortest pulses reported to date, have been reported. Cubic compensation using thin-film Gires-Tournois interferometers has also been addressed.[230]

Other ultrashort pulse data for fiber-optic compressors are given in Table III.[231-235] Recently, there has also been a great deal of interest in the development of efficient pulse-compression techniques for high-energy laser pulses.[212-215] In general, the limitation in the energy of the pulse that can be compressed arises from the threshold of stimulated Raman scattering (SRS) in the optical fibers.[207] In order to minimize SRS for high-energy pulses, fiber lengths significantly shorter than the optimal length[226] for pulse compression must be used. A detailed study of the compression of high-energy infrared pulses in optical fibers was recently reported by Dianov *et al.*[213] In this study, the 7.5-μJ 50-ps output pulses from a mode-locked Q-switched Nd:YAG laser operating at repetition rates up to 1 kHz were efficiently compressed to 1.7 ps. These results compare favorably to theoretical calculations. Jahn, Kasinski, and Miller[214] have also examined the compression of output pulses from a mode-locked Q-switched Nd:YAG laser. Various fiber materials and core diameters were compared. Compressed-pulse stability was found to depend on the core diameter of the fiber. An optimal compressor exhibiting compression ratios of 35 (generating 3.7-ps pulses) with output peak powers in excess of 2 MW was reported.

E. Shaping ultrashort light pulses

For many experimental applications, different optical pulse shapes are desired. Thus, in addition to the generation of short laser pulses, there has been recent interest in developing techniques for shaping the optical pulse. Research efforts lead by Heritage, and co-workers[236,237] and Warren and co-worker[238,239] have developed devices that allow one to shape optical pulses. For many experimental applications, different optical pulse shapes are desired. The two different approaches that have been developed take advantage of the chirped pulse that exits an optical fiber in a fiber-optic compressor. Warren developed a method based on intensity modulation of the chirped pulse. Programmable, arbitrary laser pulses with roughly 100-fs resolution have been reported. Optical pulses with $(\sin x)/x$ and square envelopes have been synthesized using this technique. Alternatively, Heritage and co-workers have used custom-made phase and amplitude masks between the gratings in the compressor. This approach effectively shapes the Fourier transform of the pulse, and thus upon recompression determines the laser pulse width and shape.

F. Tunable mode-locked solid-state lasers

In the above discussion, the pump lasers that are commonly used are either mode-locked Nd:YAG or ion lasers. These lasers have narrow gain curves and as a result are not tunable. Currently, there is interest in developing tunable mode-locked solid-state lasers. One such device receiving considerable attention is the titanium sapphire laser.[240] Titanium sapphire, unlike the other solid-state lasers discussed above, has a large gain bandwidth, covering the region from 770 to 860 nm. This solid-state device can be pumped by a continuous-wave argon-ion laser and has been successfully acousto-optically mode locked.[241-244] Several groups have reported outputs of 100 ps with powers of a few tens of mW. Recently Kafka, Alfrey, and Baer[241] generated 6-ps pulses, 750 mW at 790 nm using such a device. In addition, using a three-plate birefringent filter as a tuning element, pulses with duration under 10 ps were observed over the entire gain bandwidth. With advances in cavity design and the use of saturable absorbers, tunable femtosecond pulses may become possible.

In addition, infrared light generation from mode-locked Co:MgF_2 (Refs. 245 and 98) and Ni:MgF_2 (Ref. 98) lasers has been reported. In a study by Johnson, Moulton, and Mooradian,[98] 1.2-cm-long crystals of Co:MgF_2 and Ni:MgF_2 were longitudinally pumped with the 25-W TEM_{00} mode output from a continuous-wave Nd:YAG laser operating at 1.32 μm. The crystals were housed in a cryogenically cooled liquid N_2 Dewar, and the wavelengths of the laser were tuned using a quartz birefringent filter. The Co:MgF_2 system generated stable pulses from 1.65 to 2.01 μm; the shortest pulse observed over this range was 34 ps. The Ni:MgF_2 laser operated from 1.61 to 1.74 μm with pulses as short as 23 ps. Q-switched mode-locked operation of a Co:MgF_2 laser has also been developed; pulses as short as 200 ps with average powers of 400 mW have been observed.[245]

III. OTHER DEVICES FOR THE GENERATION OF ULTRASHORT PULSES

Although the majority of devices that have been used to generate ultrashort laser pulses rely on the technique of mode locking, other useful approaches have been developed. In this section we will briefly examine four different approaches: traveling-wave excitation (TWE), distributed feedback lasers (DFL), free-electron lasers, and semiconductor lasers. The major distinction between both TWE and DFLs and the conventional dye lasers described in Sec. II is that these devices do not use any cavity mirrors. A complete review of these devices is beyond the scope of the article. The

following discussion serves to introduce some of these novel approaches and provide references to the relevant literature.

A. Traveling-wav excitati ns

One method that has received attention involves pumping a dye laser with a traveling-wave excitation.[246-249] This technique uses spatially modulated light to transversely pump a dye cell; in this manner, the pumping beam can be synchronized with the amplified spontaneous emission in the dye cell. The optical arrangement for transverse excitation is shown in Fig. 8. Bor and co-workers have shown that pumping such a device with a 12-ps pulse produced a 6-ps amplified spontaneous emission (ASE) pulse.[246,248] The spectrum of the output pulse was strongly structured, with individual components having widths of 0.1–1.0 Å. Selection of narrow frequency regions from this broadband short pulse allows for the generation of narrow-band tunable picosecond pulses. Subsequent amplification using a second traveling-wave pumped cell is also discussed.

This technique has proven useful for pumping dyes with low quantum efficiencies. Scherer, Seilmeir, and Kaiser[250] and Kaiser and co-workers[251,252] have used traveling-wave excitation to generate picosecond optical pulses over the region from 1.2 to 1.8 μm. Rate-equation models for the laser action of infrared dye pumped by traveling-wave excitation have been developed.[253] Calculations of the spectrum and temporal characteristics of the output light compare favorably with the experimental data.

B. Distributed feedback lasers

DFLs are simple sources of transform-limited short light pulses. Using nanosecond pulses to pump the dye laser, output pulses that are 2 orders of magnitude shorter in time can be generated. This significant shortening in the output laser pulse results from self-Q-switching in the dye cell. The self-Q-switching is the direct result of feedback caused by the spatial modulation of the gain induced by pumping with two interfering beams.

Several reports describing the operation of DFLs have appeared.[245-271] The coherence properties of the pump laser, the length of the DFL, and the need for wavelength tunability are among the factors that must be considered in designing the optical device. Along these lines, a variety of pump arrangements have been examined. Shank, Bjorkholm, and Kogelnik[260] and Bakos and co-workers[261,262] used a beam splitter and two mirrors to produce the pumping interference pattern. Such devices require that the pump laser has a high spatial and temporal coherence. Prism-based DFLs were reported by Chandra, Takeuchi, and Hartman[263] and Efendiev, Bor, and co-workers[264-268]; however, similar coherence requirements of the pump laser were still needed. By spatially inverting one of the two interfering beams, Vashchuk, Zabello, and Tikhonov[269] and Katarkevich, Rubinov, and Efendiev[270] decreased the requirements of the spatial coherence of the pump laser. By using diffraction gratings to create the interfering pump beams, Ketskemety *et al.*[267] decreased the temporal coherence needed to pump a DFL. Bor[271] showed that using a holographic grating as the beam splitter decreased the need for both spatial and temporal coherence. These advances now allow for the generation of femtosecond pulses from DFLs pumped by excimer lasers. Using a cascading arrangement of three dye lasers, Szabo and Bor[259] reported the generation of 198-fs pulses at 497 nm.

Szabo and Bor[258] combined the above two approaches, pumping a DFL by traveling-wave excitation. Using R6G as the gain medium, pulse durations less than 1 ps were reported.

C. Free-electron lasers

In the past five years, there has been a substantial effort in developing broadband tunable free-electron lasers (FELs).[272,273] Although a detailed discussion of these devices is beyond the scope of this review, it is important to mention that ultrashort light pulses have been generated using FELs. In particular, Cutolo *et al.*[274] have recently reported the generation of picosecond and femtosecond pulses from the Mark III FEL. The output micropulse at 3 μm is composed of a series of micropulses, each micropulse being separated by $\approx$250 ps. Autocorrelation and spectral studies of the micropulses indicate approximately Fourier-transform-limited (linewidth 250 Å at 3 μm) 0.5–1.2-ps pulses. Near-infrared (4.3% efficiency in $LiNbO_4$) and visible (0.5% efficiency in β-BBO) subpicosecond light has also

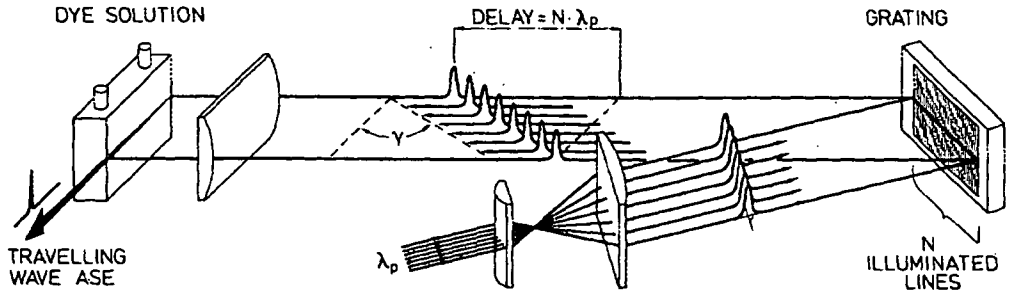

FIG. 8. A schematic of dye-laser pulse generation using traveling-wave excitation. The pump pulse is reflected by a diffraction grating, giving rise to spatially modulated light. This results in a time-dependent excitation of the dye solution, giving rise to a traveling-wave amplified spontaneous emission pulse. Femtosecond pulses at several frequencies have been generated using this approach. Reprinted from Ref. 248 with permission.

been generated at 1.5 μm and 750 nm, respectively, using harmonic conversion techniques.

D. Semiconductor lasers

An exciting area that is receiving significant current effort is the generation of short optical pulses from semiconductor lasers. These devices are important for many applications such as optical switching, high-speed optical multiplexing, and optical logic circuits. Generation techniques involving mode locking,[275,276] Q-switching,[277] regenerative feedback,[278] optoelectronic feedback,[279] and gain switching[280–283] have been reported. Among these approaches, gain switching appears to be the most popular as no external mirrors or special cavity design are required.

Mode-locking techniques have been primarily used with two semiconductor materials, GaAlAs/GaAs (Refs. 284–288) and InGaAsP (Refs. 275, 276, 289, and 290) structures, producing short pulses at repetition rates up to several GHz. In the particular, pumping an InGaAsP DFL by gain switching using 1-GHz, 100-ps FWHM, 100-mA pulses resulted in output pulses as short as 25 ps around 1300 nm.[290] Other reports pumping thin-film InGaAsP lasers with the 1-ps output from a mode-locked dye laser produced 6-ps pulses at 1.16 μm. Similar reports have appeared on GaAlAs laser diodes.

A fundamental problem in the development of passively mode-locked semiconductor lasers has been the identification and characterization of saturable absorbers. In 1980, Ippen, Eilenberger, and Dixon[284] reported the passive mode locking of a modified strip buried heterostructure GaAlAs diode in an extended resonator. Pulses as short as 5 ps were generated at a repetition rate of 850 MHz, with an average power output of 5 mW. In 1984, Silberberg and Smith reported a different approach for passively mode-locking semiconductor devices.[285] This apparatus is shown in Fig. 9. The gain medium was a GaAs laser diode. The saturable absorber was a GaAs/GaAlAs multiple-quantum-well structure.[291] Using this device, output pulses as short as 1.6 ps were produced. The average output power was 1 mW and pulse repetition rates of 1 GHz were achieved. Using a grating pair, these pulses were compressed to 0.8 ps.[292] Vasil'ev[293] has recently generated 5-ps 10-W average power outputs with a repetition rate of 18.5 GHz from a AlGaAs/GaAs structure.

IV. AMPLIFICATION OF PICOSECOND AND FEMTOSECOND DYE-LASER PULSES

The output pulse energies of passively mode-locked and synchronously pumped dye-laser systems are generally on the order of a few nanojoules. For many experimental investigations, the peak power of these pulses is insufficient. As a result, there has been a tremendous effort in developing optical devices for amplifying ultrashort laser pulses. In designing amplifiers, there are tradeoffs between pulse energies and repetition rates. Different research applications have different requirements, and subsequently a wide variety of amplifiers have been developed. Despite the large number of configurations that have been reported to date, the principle of all these devices is similar. The low-energy pulse to be amplified is passed through an active medium in which a population inversion can be created by an additional pump laser. Through stimulated emission, the energy of the ultrashort pulse is increased. Dye cells, solid-state materials, and excimer cavities have all been used as potential gain mediums. These developments have resulted in a variety of amplification techniques for different spectral ranges. The theory of pulsed dye amplification has also received considerable attention and the reader is referred to Ref. 294 for more details.

There are several concerns that need to be considered in the design of an optical amplifier.[295] Group-velocity dispersion, self-phase-modulation, gain saturation,[296] thermal blooming, and ASE generated by the optical device can significantly distort the laser pulse. As mentioned above, GVD can be compensated for by prism or grating pairs. The nonlinear broadening effects, such as SPM, are more serious as they are not easily avoided. This can be seen by examining the requirements for producing the highest gain possible from an optical amplifier. To achieve gain saturation, energy densities of $h\nu/\sigma$ are required (h is Planck's constant, ν is the optical frequency, and σ is the gain cross section). Combined with the short duration of the laser pulse, this suggests that one needs pulse intensities of 10^{10} W/cm^2.[151] Unfortunately, this energy density is similar to thresholds for nonlinear frequency generation[297] (i.e., continuum generation). As a result, the tradeoff between gain saturation and various nonlinear processes is an important consideration in designing femtosecond pulse amplifiers. The details of these effects are not well understood at present; however, they result in a limitation on the maximum extractable gain from an optical

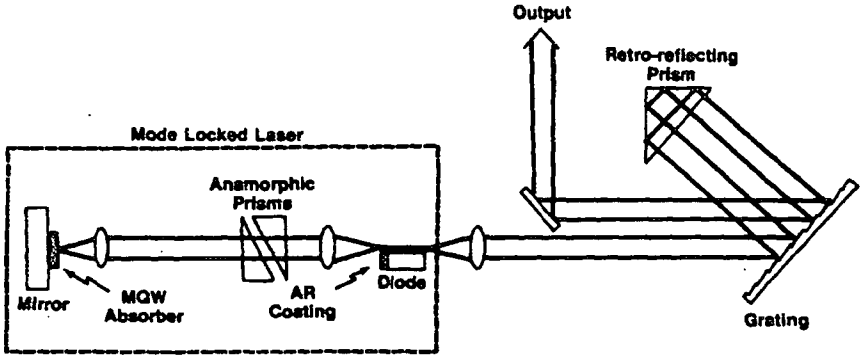

FIG. 9. The ultrafast semiconductor laser of Silberberg and Smith. The gain medium is the GaAs diode laser. This device is passively mode-locked using a GaAlAs/GaAs multiple-quantum-well structure as the saturable absorber. Reprinted from Ref. 285 with permission.

TABLE IV. Characteristics of the outputs from pulsed dye amplifiers. Abbreviations: CD, cavity dumped; SP-dye; synchronously pumped dye laser; DFL, distributed feedback dye laser; FC, fiber-optic compressed; ARR, antiresonant ring dye laser; HML, hybrid mode-locked dye laser; CPM, colliding-pulse mode-locked dye laser; CVL, copper-vapor laser; Mp, multipass; Dp, double pass; Ar, continuous-wave argon-ion laser; ML, mode-locked; 3×SP-dye, third harmonic of the output of a synchronously pumped dye laser. SP-FC-dye, fiber-optic compressed output of a synchronously pumped dye laser.

Pump laser	Repetition rate	Gain[a]	Number of stages	Source	λ(nm)	τ_p(ps)	E_p	References
CD-Ar	3 MHz	SR640	2 Mp	CPM-CD	625	0.1	10 nJ	354
CD-Ar	4 MHz	R590-R610	1 Dp	CD-SP-dye	610	12	17 nJ	353
CVL	5 kHz	Kiton red	1 Mp	CD-SP-dye	620	25	100 μJ	349
	5 kHz	R640	1 Mp	CPM	625	0.1	1.1 μJ	348
	6 kHz	LDS-821	1 Mp	HML	800	0.12	1 μJ	345
	8.2 kHz	Styryl 8	1 Mp	HML	790	0.07	6 μJ	351
	8.4 kHz	R110	1 Mp	CPM	625	0.06	50 μJ	346
	10 kHz	R610	1 Mp	CPM	610	0.045	5 μJ	350
cw ML, QS-Nd:YAG	1 kHz	R6G	3	SP-dye	560–620	150-300	< 50 μJ	211
	500 Hz	KR640	2	CPM	625	0.11	1 μJ	370
Nd:YAG regen.	1 kHz	Kiton red	2	ARR	625	0.17	1.5 μJ	321
Nd:YLF regen.	1 kHz	R6G	3	HML	600	< 0.2	10 μJ	371
Excimer	< 100 Hz	R640	4	CPM	625	0.07	0.55 mJ	312
	100 Hz	R640	3	CPM	620	0.2	> 30 μJ	313
QS-Nd:YAG	10 Hz	SR640	4	CPM	625	0.09	1 mJ	300
	10 Hz	Various	1 Dp	Continuum	400–1200	< 0.1	10 μJ	305
	10 Hz	SR101	1 Mp	CPM	620	0.1	1 μJ	302
	10 Hz	SR640	5	CPM	619	0.1	2.5 mJ	301
	10 Hz	R110-DCM	1 Mp	CPM	615	0.02	1 μJ	314
Flash-lamp regen.	10 Hz	Kiton red	3	SP-dye	570–620	1	5 mJ	310
Discharge	< 10 Hz	XeCl	1 Dp	DFL	308	0.22	5 mJ	359
		XeCl	2	2×CPM	308	0.16	12 mJ	360
		ArF	1 Dp	3×SP-dye	193	10	40 mJ	369
		XeF	1 Dp	DFL	351	0.56	1 mJ	372
		KrF	2 Dp	3×SP-dye	248	3.5	2.5 J	362
		KrF	2	2×SP-FC-dye	248	0.22	20 mJ	204
		KrF	1 Dp	DFL	248	0.08	15 mJ	365

[a] Dye abbreviations: KR = Kiton red; DCM = 4-(Dicyanomethylene)-2-methyl-6-(*p*-dimethylamino-styryl)-4H-pyran.

amplifier. In practice, the overall efficiency of energy extraction from an optical amplifier decreases with the decreasing pulse width of the input pulse. In addition, thermal blooming effects can arise from heat dissipation from the region excited by the pump beam. This can lead to the generation of thermal lenses in the amplifier cells, resulting in distortion and spatial displacement of the dye pulse being amplified.

In Table IV, the output characteristics of several different optical amplifiers are compared.[295] These devices are discussed in detail in the remainder of this section. For discussion purposes, the various approaches are grouped together by repetition rates.

A. Low repetition rate (<100-Hz) amplifiers

Several low repetition rate optical amplifiers use a *Q*-switched Nd:YAG laser as the excitation source.[294,298-302] These pump lasers can provide a 2–10-ns pulse with energies between 300 and 500 mJ/pulse at 532 nm with repetition rates up to 50 Hz. In Fig. 10, we show a block diagram of a four-stage optical amplifier developed by Fork, Shank, and Yen[300] for the amplification of femtosecond laser pulses. This device used dye cells as the amplification medium. The amplifier was pumped by a 10-Hz Nd:YAG laser (5 ns/pulse, 300 mJ/pulse at 532 nm). The ≈70-fs input pulse was generated by a CPM laser (Sec. II A). Each successive pair of gain cells is separated by a saturable absorber jet. These dye jets are used to suppress amplified spontaneous emission. Output pulse energies of ≈1 mJ are observed for an input pulse energy of 0.1 nJ. In this design, methanol

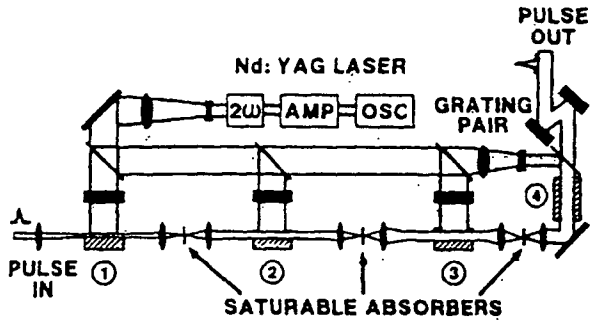

FIG. 10. Four-stage optical amplifier for ultrashort light pulses developed by Fork, Shank, and Yen. A grating pair is used on the output pulse to compensate for the GVD of the amplifier. This arrangement can be used to generate gigawatt peak powers at low repetition rates. Reprinted from Ref. 300 with permission.

solutions of Kiton Red and Sulphorhodamine 640 (SR640) are used in the first and remaining gain cells, respectively. Malechite green (MG) dissolved in ethylene glycol was used as the saturable absorber. The first three cells were transversely pumped while the final cell was pumped longitudinally. The output pulse has a temporal width on the order of 400 fs, indicating a broadening of a factor of 6–7 in the amplifier. The major cause of this broadening comes from GVD; using a grating pair following the amplifier enabled recompression of the output pulse to $\approx$80 fs. Several variations on this basic optical arrangement have appeared in recent years. The original design suffered from poor beam quality, resulting in part from the beam characteristics of the pump laser and the transverse pumping geometry. Designs that involve longitudinal pumping of the entire amplifier chain have been reported.[303,299] However, the beam quality of the amplified pulse still suffered from the poor mode quality of the nanosecond pump pulse. Improved beam quality was observed using Bethume cells,[304,305] but these cells are not ideally matched to the circular shape of the laser beam. In addition, using a final gain stage of conical axion geometry, Wood, Focht, and Downer[306] achieved near-diffraction-limited focusing of the output pulses without any spatial filtering. Recent advances using diode-injection techniques to produce single-mode output from high-powered Q-switched Nd:YAG lasers now enable one to produce high-quality Gaussian beam profiles from these devices. Pulsed dye amplification using diode-injection Nd:YAG lasers as the pump lasers should result in substantially improved output beam quality.

In order to obtain stable pulsed dye amplification, the timing jitter between the arrival times of the pump and dye laser pulses at the gain cells must be minimized. Various circuits have been developed, depending on the source of the ultrafast laser pulse.[307,308] Using Q-switched Nd:YAG lasers as the pump source, the timing is controlled by the following general approach. The nanosecond Nd:YAG laser pulse is obtained by switching an electro-optic Q-switch in the optical cavity at a fixed time delay following the firing of the flash lamps. In order to synchronize the pulsed output with an ultrafast pulse generated from a synchronously pumped mode-locked dye laser, the Q-switch trigger is generally intercepted and compared to the rf wave used to drive the acousto-optic mode locker. In this way, the opening of the Q-switch can be easily synchronized with respect to the mode-locked pulse train. This generally results in a temporal jitter of better than 0.1 ns.[308] Since CPM dye lasers are pumped by continuous-wave argon-ion lasers, a slightly different approach is required. A photodiode detecting the output pulse train from the CPM is generally used to provide the synchronizing pulse used to trigger the Q-switch in the nanosecond laser.

In recent years, a variety of dye saturable absorber combinations have been developed that enable pulsed dye amplification over a large range of wavelengths.[303,309,122] Limitations on the wavelengths that can be amplified by this approach generally depend on the availability of a saturable absorber. Because of the long pump pulse, the control of ASE in the amplifier chain is imperative. Without adequate suppression, this results in decreased gain and a large amount of background light. Effective saturable absorbers need to recover on the few-picosecond time scale. With the increasing availability of saturable absorbers in various spectral regions, the short pulses generated by hybrid mode-locked dye lasers can be efficiently amplified using this approach.

Despite the problems associated with this device, the output pulses have proven to be very useful for studying a large variety of scientific problems. The maximum repetition rate of these systems is limited by the pump laser. For Q-switched YAG lasers, this presently places a limit of $\approx$50 Hz. Advances in solid-state laser design indicate that flash-lamp-pumped Nd:YAG lasers with kilohertz repetition rates will be available in the near future. These devices will prove to be excellent sources for increasing the repetition rate of amplified pulses without a significant change in amplifier design. Recently, low repetition rate pulsed regenerative amplifiers (see Sec. III B) have also been designed.[310,311] Taylor *et al.* have reported output pulses of 0.2 mJ, 190 fs at 620 nm at a repetition rate of 10 Hz using such a design.[311]

A small increase in repetition rate, without sacrificing output power, can be obtained using excimer lasers as the pump source.[312,313] These commercially available systems provide high-energy pulses in the ultraviolet region (308 nm for XeCl), at repetition rates up to several hundred hertz with pulse energies of several hundred millijoules. In general, the amplifier design is similar to that used with the nanosecond Nd:YAG lasers. However, some important improvements have been incorporated into these design to take advantage of the properties of excimer pulses. Unlike the output of Nd:YAG lasers, excimer outputs are rectangular in shape with approximately uniform spatial intensity. Thus changes in cell design are required to effectively couple this light into the amplifying medium. In a recent design, single-sided quartz prisms are used for the gain cells. This design, originally proposed by Bethume,[304] provides the most efficient coupling of the rectangular excimer pulses into the dye. Using such a device, amplification of 70-fs pulses to 0.8 mJ with repetition rates up to 125 Hz was reported by Rolland and Corkum.[312] Recently, commercial XeCl lasers operating at 1 kHz have recently become available, suggesting that higher repetition rate systems can be built using excimer-pumped amplifiers. One drawback to this approach is that the pumping of visible dyes with excimer often degrades the amplification dye.

Recently, Hirlmann *et al.*[302] reported a compact all-reflective multipass amplifier for femtosecond light pulses. The optical scheme is shown in Fig. 11. Two concave mirrors, with centers at C_1 and C_2, are used to focus and recollimate the light beams. A flat mirror is located orthogonal to the symmetry axis; through translation of this optic, the number of passes through the gain medium can be changed. Total gains of 10^4 have been observed using 15 mJ of pump power from a 10-Hz Q-switched Nd:YAG laser (8-ns pulses). Similar results were reported by Georges *et al.*[314] for the amplification of ultrashort pulses from a CPM laser in a multipass geometry. Gains of 200 were reported with output

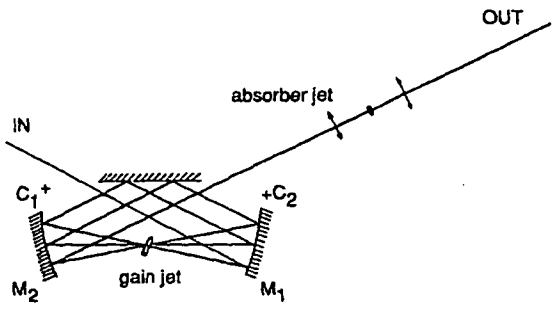

FIG. 11. The multipass amplifier system of Hirlmann *et al.* Using two concave mirrors and a flat high reflector, multiple passes through the gain medium are easily attained. Reprinted from Ref. 302 with permission.

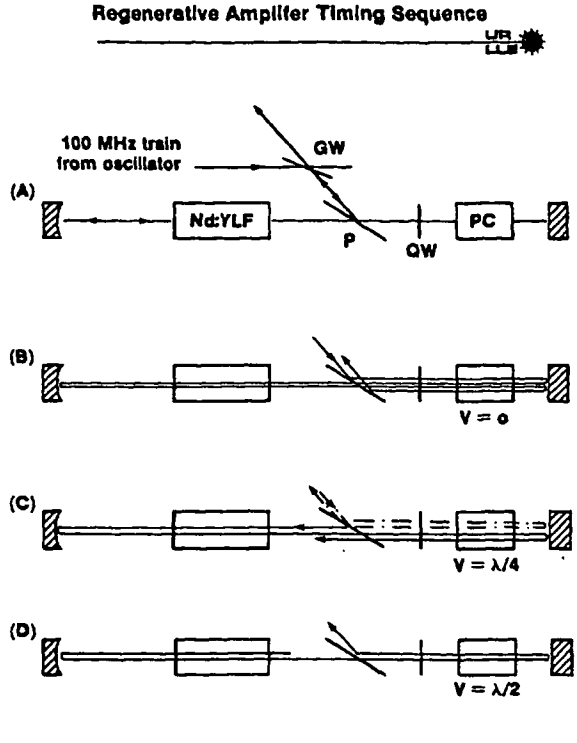

FIG. 12. The timing sequence of a cw Nd:YLF (or Nd:YAG) regenerative amplifier system (GW = glass wedge, P = dielectric polarizer). (A) With the Pockels cell (PC) off, the quarter-wave plate (QW) is rotated to prevent lasing in the cavity. (B) With no voltage on the Pockels cell, a seed pulse will travel through the gain medium twice before leaving the cavity, resulting in negligible amplification. (C) When a seed pulse passes through the gain medium once, the PC is switched to quarter-wave voltage. As a result, the pulse is trapped in the resonator and is amplified. (D) At maximum gain, the PC is switched to half-wave voltage, rotating the polarization of the amplified pulse, dumping it out of the cavity. Reprinted from Ref. 325 with permission.

pulses as short 20 fs.

B. 1–10-kHz repetition rates

Although the above-described techniques have proven useful in many areas of research, many applications of interest cannot be pursued using these systems. An example of the potential problems can be viewed by considering the possibility of unwanted multiphoton effects. Nonresonant multiphoton effects can be easily observed in many molecular species with powers as low as 6×10^6 W/cm^2. These energies are significantly lower than the output powers of the low repetition rate systems described above. In addition, because of the inherent instability of many systems to high peak powers (most notable applications in biology), a large number of experiments require using low-energy pulses. In order to effectively carry out such investigations, lower energies, high repetition rate systems are needed.

In the last few years, there has been significant progress in the development of amplifiers that can be operated in the kilohertz regime. In practice, two approaches are being used to amplify ultrashort dye-laser pulses in this repetition rate range: regenerative amplifiers and copper-vapor laser amplifiers.

Several researchers[315–324] have described Nd:YAG regenerative amplifiers that can be used to amplify low-power pulses from a synchronously pumped dye laser to microjoule levels. Before examining the dye amplification schemes, the basic design of a regenerative amplifier is reviewed. In this device, an ultrashort pulse is injected into a laser cavity, amplified in energy, and cavity dumped. The approach and timing sequence used in the regenerative Nd:YLF (also applicable to Nd:YAG) system developed by Bado, Bouvier, and Coe is shown schematically in Fig. 12.[325] The resonator shown consists of a Pockels cell, polarizer, quarter-wave plate, gain medium, and cavity mirrors. The output of a mode-locked Nd:YLF oscillator is reflected off the polarizer into the amplifier cavity. With the Pockels cell turned off, an input pulse passes through the gain medium twice, leaving the cavity before any significant amount of energy is extracted. At the time of injection, the Pockels cell is switched to $\lambda/4$ voltage. The single laser pulse that is between the Pockels cell and the end mirror is now trapped in the resonator. After multiple passes through the gain medium (≈ 50 round trips), the amplified pulse is cavity dumped by switching the Pockels cell to $\lambda/2$ voltage. The synchronization between the mode-locked oscillator and the regenerative cavity is easily achieved by locking the Pockels-cell driver to the frequency source of the acousto-optic mode locker. During the development of these devices, several approaches for seeding and cavity dumping the regenerative amplifier were reported. Designs involving a number of intracavity Pockels cells and polarizers were developed.[38,326,327] Recently, Postlewaite *et al.*[322] reported a technique in which seeding into the amplifier cavity was accomplished by an acousto-optic Q-switch, and a Pockels-cell–polarizer combination was used to cavity dump the amplified pulse. Nd:YAG regenerative amplifiers produce output pulses of $\approx$50–100 ps (FWHM) of ≈ 1 mJ/pulse with repetition rates up to 2 kHz.[225,321] Above this repetition rate, the peak power decreases, and instabilities are observed as the time between pulses is shorter than the time necessary to obtain stable population inversion. The outputs of regenerative amplifiers (>10 MW peak power) can be efficiently frequency doubled ($>60\%$) to produce synchronized light at 532 nm. This light can be used to pump a pulsed dye amplifier for

ultrashort light pulses. Average powers exceeding 1 W at 532 nm can be obtained. The dye amplifier design is similar to that used in the low repetition rate systems. Several significant advantages arise from this approach. First, the amplifier cells are now pumped by short picosecond pulses. This increases the efficiency of amplification and reduces the problem of ASE commonly associated with nanosecond pumped amplifiers. Second, the path length of the amplifier cells is greatly reduced (< 1- vs 10-cm cells for nanosecond amplifiers), decreasing the effects of GVD in the amplifier. The amplified output of these devices provide average powers of 10–50 mW at various wavelengths.

In the past two years, regenerative amplifier designs using Nd:YLF as the active medium have appeared.[221,325] Nd:YLF has been shown to lase at two wavelengths, 1.047 and 1.053 μm, corresponding to the two polarizations π ($E \| c$) and σ ($E \perp c$).[328,329] This material exhibits several properties which suggest that it is a superior choice to Nd:YAG for the generation of mode-locked pulses in the near-infrared region. First of all, Nd:YLF has a larger bandwidth than Nd:YAG [1.35 vs 0.45 nm (Ref. 328)], resulting in shorter pulse generation. In addition, thermal lensing is greatly reduced, providing a high ratio of TEM_{00} to multimode average power.[330] Finally, Nd:YLF exhibits a strong birefringence that overwhelms the thermal depolarization problems associated with isotropic media such YAG and glass.[331] Bado and co-workers have reported the generation of pulses as short as 37 ps from a mode-locked Nd:YLF oscillator.[332] Subsequent amplification of these pulses in a regenerative amplifier have resulted in pulse energies as high as 5 mJ at a 1-kHz repetition rate.[325] The use of mode-locked Nd:YLF systems to synchronously pump dye lasers has been inhibited by the lower output powers experimentally observed from various cavity designs. In the last year, Vanderzeele examined the thermal lensing properties of Nd:YLF and designed an optimized resonator for Nd:YLF that produces outputs comparable to that observed with Nd:YAG.[333–335] This has only recently opened up the exploration of using Nd:YLF systems for synchronously pumping dye lasers and the subsequent amplification of their ultrashort dye pulses using a Nd:YLF regenerative amplifier. A schematic of such a device that is currently running in the author's laboratory is shown in Fig. 13.[371] The generation of the ultrashort pulse is accomplished using a synchronously pumped hybrid mode-locked dye laser using R6G as the gain medium and DODCI as the saturable absorber. This laser generates pulses of 150-fs duration at a repetition rate of 100 MHz. A portion of the output from the mode-locked Nd:YLF oscillator is directed towards a second Nd:YLF cavity. At a repetition rate of 1 kHz, a single infrared pulse from the mode-locked train is injected into the second cavity, amplified up to $\approx$2 mJ/pulse, and cavity dumped. This amplified pulse is then frequency doubled using a 5-mm-long crystal of KTP producing > 0.8 mJ/pulse at 527 nm.

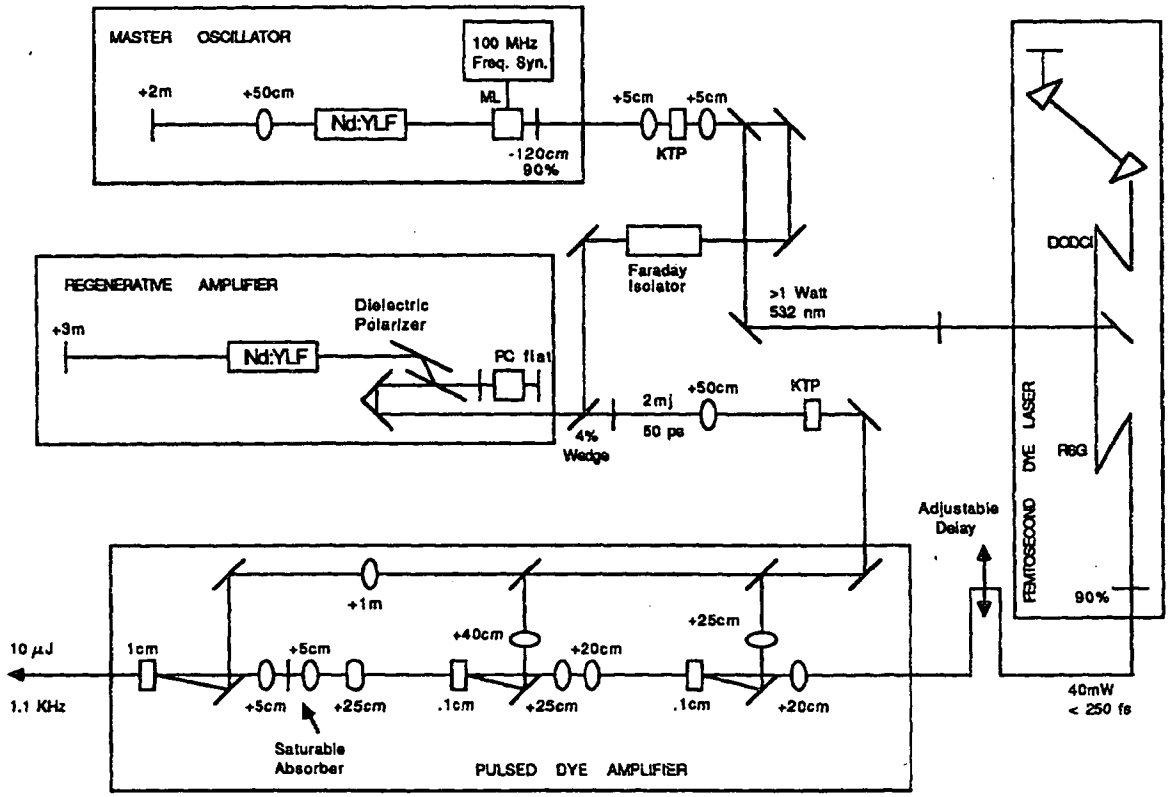

FIG. 13. A regeneratively amplified dye-laser system. A Nd:YLF oscillator is used to synchronously pump a HML dye laser as well as seed a the Nd:YLF regenerative amplifier. The output of the regenerative cavity is frequency doubled and used to pump a three-stage pulsed dye amplifier. This device can produce <0.2-ps pulses, 20 μJ/pulse, at repetition rates up to 1.1 kHz.

The green light is used to pump a three-stage pulsed dye amplified similar to the design reported by Newell *et al.*[228] Dye pulses can be amplified to energies on the order of 20 μJ/pulse using this approach.

Recently, Mourou and co-workers have taken advantage of the fact that the Nd:YLF line overlaps the gain of Nd:glass to generate TW/cm^2 1-ps (FWHM) laser pulses.[222,223,336] The device used is shown in Fig. 14. The effects of the gain saturation associated with short optical pulses is overcome by frequency chirping the mode-locked pulse in an optical fiber.[337] In the system developed by Mourou and co-workers, the output pulse from the mode-locked oscillator ($\approx$55 ps) is chirped in a 1.3-km optical fiber to produce pulses that are $\approx$300 ps. These pulses are seeded into a Nd:glass regenerative amplifier, then further amplified by several stages of pulsed amplification in Nd:glass. The output pulse is a 300-ps 1-J pulse, which can be easily recompressed to 1 ps (FWHM). This system combines advantages of regenerative amplification techniques with high-energy storage materials such as Nd:glass. Once amplified, the pulse can be recompressed to 1 ps, resulting in power levels and pulse widths that are not possible by direct amplification of a 1-ps laser pulse. Coe, Maine, and Bado[221] have reported pulse narrowing resulting from seeding a chirped optical pulse into a 1.0-kHz Nd:YLF regenerative amplifier. In this design, the output of a mode-locked Nd:YLF oscillator (44 ps) is chirped to 150 ps using an optical fiber. This pulse is seeded and amplified by a continuous-wave Nd:YLF regenerative amplifier. The output pulse is found to be 12 ps, which after passing through a grating pulse compressor produces a 8-ps FWHM laser pulse.

Regenerative amplification of dye-laser pulses from 750 to 770 nm has also been reported using a pulsed alexandrite laser as the gain medium.[338,339] Alexandrite is a very promising medium for high-power amplifiers. The saturation fluences are higher than Nd:glass, and combined with the large gain bandwidth, 700–800 nm, this material can potentially support amplification of pulses as short as a few femtoseconds. Mourou and co-workers have reported the generation of 300-fs 3.5-mJ pulses at 30 Hz using an alexandrite amplifier seeded by a positively chirped (50-ps) dye laser pulse.

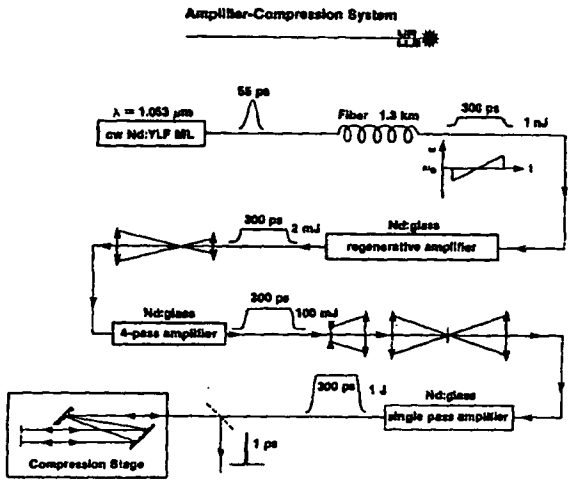

FIG. 14. The optical amplifier system of Maine *et al.* used to generate 1-TW 1-ps optical pulses. The output of a mode-locked Nd:YLF laser is chirped in a fiber optic and then amplified using both a Nd:glass regenerative amplifier and pulsed Nd:glass amplifiers. Once amplified, the pulse is recompressed using a grating pair. The advantages of chirped amplification are discussed in the text. Reprinted from Ref. 223 with permission.

In addition to regenerative amplifiers, phase locking the mode lockers in the oscillator and amplifier lasers has been reported.[228,340–344] The output of a mode-locked Q-switched and cavity-dumped Nd:YAG laser system is comparable to that observed in a regenerative amplifier. However, unlike the optical synchronization used in regenerative devices, rf locking allows one to synchronize different types of lasers (e.g., Nd:YAG and Nd:YLF). In addition, the synchronization of timing between the two coupled lasers can be easily adjusted using rf phase shifters. One drawback is that the relative timing of the two laser pulses at the gain medium is not exact. Cross-correlation studies between pulses generated from rf coupled mode-locked and Q-switched Nd:YAG lasers indicate a temporal jitter of $<$40 ps.[343] This can lead to problems in amplifying the output of ultrafast dye lasers. Newell *et al.* reported that such a timing jitter can have a dramatic effect on the stability of amplifier pulses when rf-coupled oscillators are combined with fiber-optic compression techniques.[22] The propagation time of the mode-locked pulse train through the optical fiber is dependent on the peak intensity of the laser pulses. Thus, pulse-to-pulse fluctuations give rise to significant instabilities in the amplification process. Newell *et al.* developed a method for reducing these effects by using an electronic feedback circuit to adjust the phase shifter that controls the mode locking in the amplifier laser.

To date, the highest repetition rate reported in the literature using a regenerative amplifier is 2 kHz.[225] Higher repetition rates can be achieved in amplifier systems that are driven by copper-vapor lasers (CVL).[345–351] In developing CVL dye amplifiers, four major problems had to be overcome in designing the device. First, the CVL pulse width (8–30 ns) was considerably longer than the natural fluorescence lifetime of most dyes (2–4 ns). Second, the energy output per pulse, $<$4 mJ, was substantially lower than the $\approx$350-mJ outputs of the Nd:YAG lasers that had been used for low repetition rate amplifiers. Third, the output of CVLs were longer than the interpulse separation of the mode-locked ultrashort pulse train. This required that the output repetition rate of the mode-locked laser be reduced. For synchronously pumped systems this could be accomplished using acousto-optic cavity dumpers. Unfortunately, these devices generally result in a broadening of the output pulse. These characteristics required new optical designs for efficient amplification. Recent advances in the design of CVLs have resulted in devices that can produce laser pulses that are $<$10 ns at repetition rates up to 12 kHz. As a result, the need to reduce the repetition rate of the ultrafast dye laser have been obviated. This enabled the development CVL-based amplifiers for CPM dye lasers. Similar to the low repetition rate amplifiers described above, electronic synchronization of the firing of the CVL with the dye-laser pulse is necessary. Many elec-

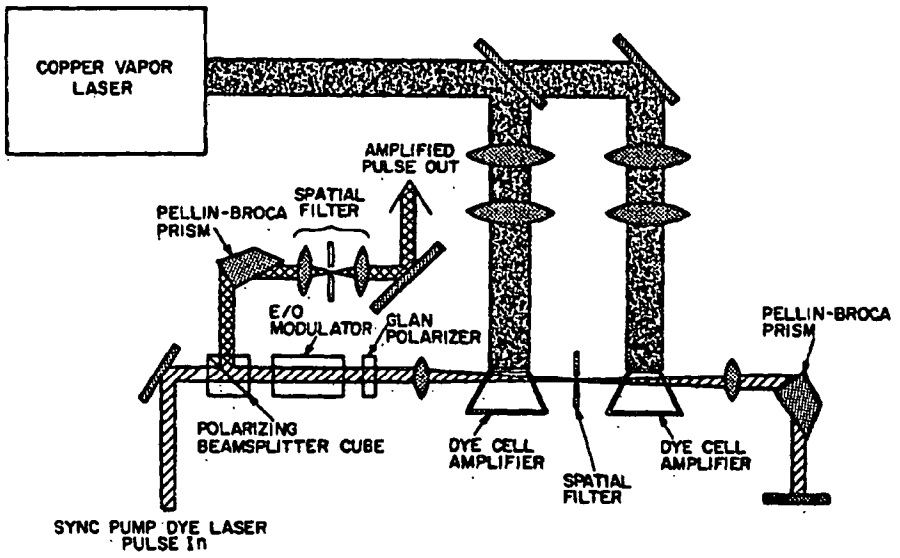

FIG. 15. The optical device developed by Hopkins and Rentzepis for amplifying ultrashort dye pulses with a copper-vapor laser. The electro-optic modulator ensures that only a single ultrashort light pulse is amplified by the nanosecond output of the CVL. Reprinted from Ref. 347 with permission.

tronic circuits have been developed; jitters as low as 1 ns have been reported.[347,379,351]

The first CVL amplifier was reported by McDonald and Jonah.[349] In their device a single multipass cell was used. A cavity-dumped dye laser was used to provide input pulses of 25-ps FWHM with pulse energies of 20 nJ. The amplifier cell was pumped by an 8-mJ 30-ns pulse from a Plasma Kinetics Model 451 CVL, operating at 5 kHz. The largest five-pass gain observed was a factor of 10^4, resulting in pulses with energies greater than 0.1 mJ/pulse. Hopkins and Rentzepis[347] introduced the multipass amplifier shown in Fig. 15. This device has several advantages over the single multipass cell. First of all, multiple cells with flowing dye are used in order to distribute the high average power of the pump laser. This reduces effects from both thermally induced turbulence in the dye solutions and ASE. Second, the focused waist of the pump laser, <0.5 mm, leads to a very high total gain. Finally, the retroreflected arrangement allows for easy and accurate alignment. The electro-optic element at the beginning of the amplifier is used to inject the dye pulse into the amplifier cells. This device served to guarantee that only a single dye pulse was amplified by the long pulse of the CVL. Amplification of a <5-ps 0.7-nJ pulse generated from a synchronously pumped dye laser using this device produced output pulse energies of $\approx 50\,\mu$J, representing a total gain on the order of 7×10^4. These values were reported pumping the amplifier with a 2-mJ/pulse output from a CVL. No evidence of gain saturation was observed; thus greater energies could be expected using more powerful CVLs.

The above two devices have significant problems when considering the amplification of femtosecond pulses. The large amount of dispersive materials used in these devices, i.e., glass, dye cells, and Pockels cells, would lead to substantial GVD and SPM. To overcome these problems, Knox and co-workers[348] developed the device shown in Fig. 16. In this case, the amplifier medium is a thick dye jet (≈ 1.2 mm). The CVL is focused to a small spot size (≈ 1 mm). The dye jet is produced using a sapphire plate n zzle, resulting in an interferometrically flat dye stream. The short optical path and high optical quality of this dye stream is important in maintaining good beam quality in the multipass system. The dye-laser pulses pass through the active medium six times. Two saturable absorber jets are used to eliminate unwanted ASE. Single-pass gains of ≈ 5 have been reported for amplifiers operating at several different wavelengths. For amplification of the output from a CPM laser, Sulphorhodamine 640 is used as the gain medium and malachite green is used as the saturable absorber. GVD in the amplifier broadens the output pulse to 150 fs; however,this is easily compensated using a prism or grating pair following amplification. Amplified 80-fs pulses at repetition rates between 6 and 8 kHz at 805 nm have also been reported using Styryl 9 as the gain medium.[345] The input to the amplifier was provided by a synchronously pumped hybrid mode-locked dye laser. Reports have also appeared which suggest that the characteristics of the amplified pulse are improved using a dye cell for

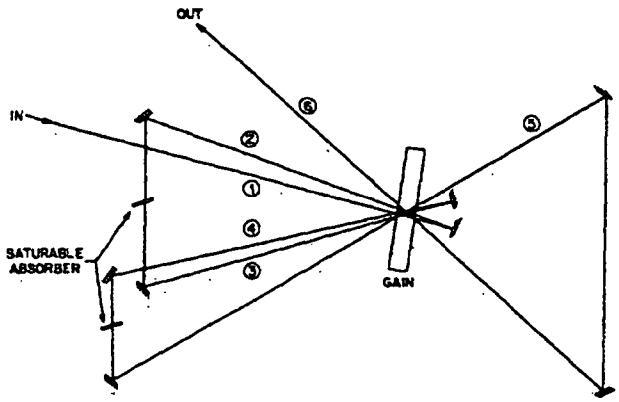

FIG. 16. The optical device developed by Knox *et al.* for amplifying femtosecond pulses with a copper-vapor laser. Six passes through the gain jet using reflective optics resulted in negligible GVD and appreciable gain. Two saturable absorber jets were used to control ASE. Reprinted from Ref. 348 with permission.

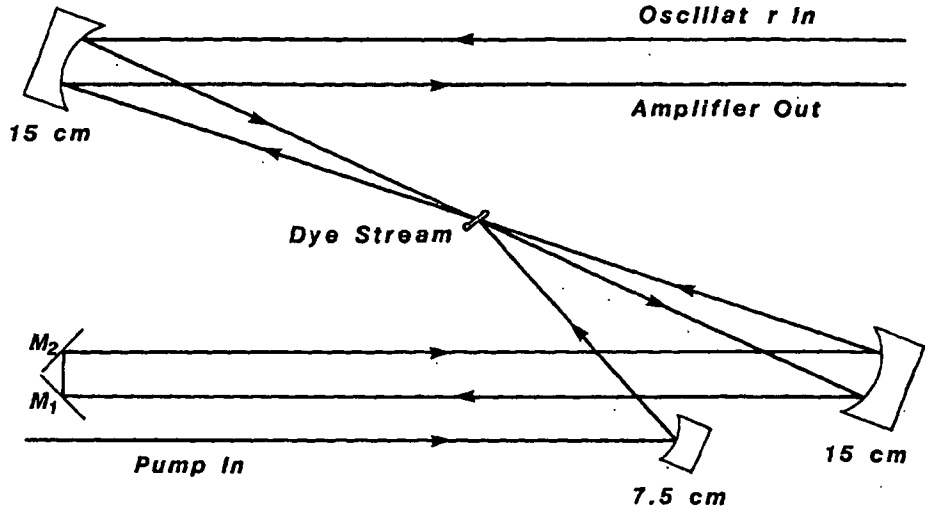

FIG. 17. The MHz repetition rate amplifier pumped by a cavity-dumped argon-ion laser developed by Gustafson and Roberts. This device utilizes a double pass of the ultrashort light pulse through the gain medium during the pulse width of the pump laser. Reprinted from Ref. 353 with permission.

the gain medium,[346] rather than a high-pressure jet stream. Recently, Kahlow *et al.*[351] have extended this technique to other wavelengths in the visible and near-infrared regions. Using the dye combination pyridine 2 and saturable absorbers of HITCI and DDI, microjoule pulses of < 100 fs duration have been generated at 720 nm. Using a gain medium of Styryl 8 and no other saturable absorber, pulses with energies as high as 6 μJ have been generated at 790 nm, with only a 15% broadening of the temporal width of the input laser pulse (70 fs) during the amplification process. Other optical arrangements for allowing multiple passes through the gain medium have been reported. Khoroshilov *et al.*[350] have used a dye jet located at the common focal point between two focusing mirrors. Using this approach, output pulse energies as high as 0.5 μJ in a 45-fs pulse at 10 kHz have been reported at 610 nm.

C. Megahertz amplifiers

The kilohertz repetition rate pulsed amplifiers described in Sec. IV B can provide high peak power at a moderate repetition rate. However, there are various experimental applications that would benefit considerably from even higher repetition rates. To accomplish this goal, amplifiers based on using cavity-dumped argon-ion lasers as the pump source have been investigated. Both picosecond and femtosecond amplification schemes have been reported. One such device, which was reported by Waldeck *et al.*[352] and further developed by Gustafson and Roberts,[353] is shown in Fig. 17. As in the case of amplifiers pumped by a CVL, a dye stream is used as the gain medium. An important feature of this amplifier is the double-pass configuration, enabling the picosecond pulse to travel through the gain medium twice during the pulse width of the pump laser. Using this device, amplified output energies of 140 nJ/pulse at 760 kHz were reported for input energies on the order of 1 nJ. This system has proved to be very effective in allowing one to measure picosecond time-resolved Raman spectra.

In addition, Downer, Fork and Islam[354] designed a device for the amplification of femtosecond pulses generated from a R6G-DODCI CPM laser. Shown schematically in Fig. 18, amplified output pulse energies of 10 nJ were obtained for < 100-fs pulses at a repetition rate of 3 MHz. The pump laser pulses from the cavity-dumped argon-ion laser were $\approx 1\,\mu$J, 15 ns at 514 nm. In this design, the pump beam is split into two parts, each part pumping a gain jet that contains a solution of SR640. By controlling the polarization of the laser pulse, each jet is double passed, resulting in a four-pass geometry. The collinear geometry between the pump and femtosecond beams in each jet requires careful mode matching. Amplifiers pumped by cavity-dumped argon-ion lasers have not been extensively used.

D. Amplification of ultrafast UV light using excimer laser cavities

In this section, we examine techniques that are used to amplify ultrashort pulses in the ultraviolet region. There is considerable interest in such systems for studies in surface science, atomic nonlinear phenomena, multiphoton processes, and x-ray lasers. The gain medium in these systems is provided by a excimer laser cavity. The seed pulses for such a device can be produced by frequency doubling the output of an ultrashort dye laser. Unfortunately, the spectral width of the gain in an excimer cavity is narrow, limiting the tunability of these devices. For example, in the case of KrF, the width of the gain curve is centered at 248 nm with a width of only 3.4 nm. Different excimers provide sources for amplification at different UV wavelengths. However, to take advan-

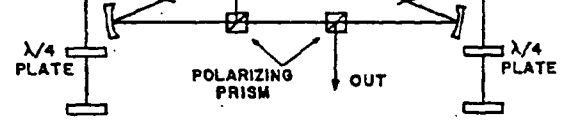

FIG. 18. The MHz repetition rate amplifier pumped by a cavity-dumped argon-ion laser developed by Downer, Fork, and Islam. The prism and wave plates enable the ultrafast pulse to be double passed through the two gain jets. Reprinted from Ref. 354 with permission.

tage of amplification by excimer modules, resonant ultrafast dye laser pulses need to be generated.

Using the technique of injection mode locking, Varghese[355] found that seeding XeCl cavity with the frequency-doubled output of a mode-locked R6G dye laser produced high-energy picosecond pulses. Related studies were also reported by Corkum and Taylor[356] and Glownia and co-workers.[203,357] Glownia, Misewich, and Sorokin examined the amplification of 350-fs pulses generated by frequency doubling the output of a fiber-optically compressed output from a mode-locked R6G dye laser. Pulse energies as high as 10 mJ were observed with ASE signals as low as 10%.[357] Similar pulse energies for 220-fs pulses were reported by Schaffer and co-workers.[358,359] XeCl modules have received considerable attention, as the gain wavelength is compatible with the second harmonic of the output of CPM lasers. Using the frequency-doubled output of a CPM laser as the seed pulse, Glownia, Misewich, and Sorokin designed an amplifier system based on two successive stages of XeCl gain modules.[360] This device generated 160-fs pulses, centered at 308 nm with energies of 12 mJ/pulse. The frequency spread of the input pulse from the doubled CPM laser was on the order of 100 cm^{-1}. However, the XeCl gain module only amplified light within $\approx \pm 50\ cm^{-1}$ of the 308-nm seed pulse. In this spectral region, the phase of the seed pulse is nearly constant; thus, at the beginning of the amplification process, the frequencies of the ultrashort UV pulse that are to be amplified in the gain module are essentially in phase. This enables bandwidth-limited pulses to be observed at the output of the gain module. Using a cyclohexane solution of 4,4″di(2-butyl-octoxy-1)-P-quarter-phenyl (BBQ) as a saturable absorber, Watanabe *et al.*[361] reported 1-TW peak powers for a XeCl cavity amplified 310-fs pulse with a pulse to ASE suppression ratio grater than 30:1.

On the other hand, the larger bandwidth of the KrF excimer suggests that shorter pulse widths can be obtained. Several reports of picosecond pulse amplification in KrF modules have appeared.[362-367] Output energies as high as 2.5 J in a pulse of 3.5 ps have been reported. Theoretical treatments of the ultrashort pulse propagation in KrF amplifiers have also appeared.[368] In 1987, Szatmari *et al.* succeeded in amplifying 80-fs pulses at 248 nm up to peak powers of 0.9 TW with repetition rates of 1 Hz.[365] A block diagram of this laser system is shown in Fig. 19. The system is designed around a XeCl-pumped picosecond dye-laser–amplifier system to produce 8-ps pulses at 365 nm with pulse energies of 3 μJ. This light was used to drive a distributed feedback dye laser (Sec. III B) at 497 nm, the output of which was amplified and frequency doubled. The pulse width of the resulting UV light was $\approx$ 80 fs with pulse energies of $\approx 5\,\mu$J. This light was amplified using a double-pass configuration of a KrF excimer cavity, generating 15-mJ pulses with essentially no temporal broadening. Using a second gain module, amplified energies as high as 75 mJ were reported. Unfortunately, the ASE from this double gain module device was $\approx$85 mJ, in excess of the pulse energy. Attenuation of the input to the second gain module by 10% resulted in an amplified pulse energy of 66 mJ, with a pulse-to-ASE ratio greater than 5:1. This observation indicates that with appropriate saturable absorbers, increased pulse-to-ASE discrimination can be achieved. Szatmari *et al.* suggest that ozone would be a good candidate for a saturable absorber in this region, although no results were reported. This drawback demonstrates the need for the development of saturable absorbers in the ultraviolet

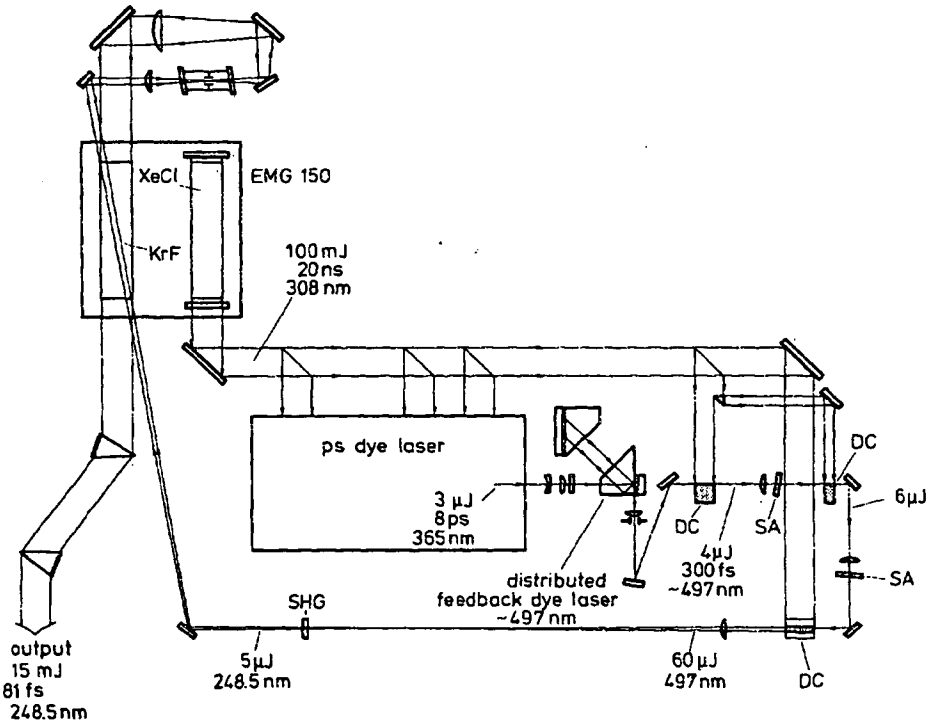

FIG. 19. The optical device used to generate high-energy ultrashort devices in the ultraviolet region designed by Szatmari *et al.* The seed pulse is generated using a DFL pumped by a picosecond dye laser. The output pulse, 4 μJ at 497 nm, is amplified to 60 μJ, and frequency doubled to 248.5 nm (5 μJ). The UV pulse is amplified using a pulsed KrF discharge, resulting in the generation of 81-fs 15-mJ pulses at 248.5 nm. Reprinted from Ref. 365 with permission.

region and it is likely that advances in this area will occur in the next few years. Recently, Endoh *et al.*[366] reported the generation of 390-fs 1.5-J pulses using KrF amplification. Only 1.8% of the total output energy was attributed to ASE.

ArF excimer cavities have also been used for pulsed amplification. In the study of Egger *et al.*,[369] the seed pulse for an ArF amplifier, 193 nm, was generated by producing the third harmonic of the amplified output of a synchronously pumped dye laser (580 nm, 6 ps, 1 mJ/pulse) in a strontium heat pipe. This approach generated a seed pulse of ≈ 2 nJ. After two stages of amplification, the output pulse was ≈ 40 mJ, 10 ps, riding on top of a 200-mJ background of ASE. Characteristics from another pulsed dye amplifier are presented in Table IV.[370] A related device using a double-pass XeF cavity has produced 1-mJ 550-fs pulses at 351 nm.[372]

V. EXTENSION OF WAVELENGTHS

As the outputs from ultrafast dye-laser systems are limited in tunability, novel approaches for extending the frequency range that can be generated have been developed. For the most part, the dye lasers and dye-laser amplifiers described in the previous sections (Secs. II–IV) provide short, intense radiation in the visible region of the spectrum. However, many applications require ultraviolet and/or infrared radiation. In this section, we examine techniques that are used to extend the ultrashort laser pulses into these spectral regions.

A. Harmonic generation, frequency-mixing techniques, and parametric oscillation

The most commonly used technique to generate new frequencies involves nonlinear frequency mixing. A complete discussion of nonlinear optical properties is beyond this review and excellent treatments of this subject can be found in a number of recently published books.[15,373,374] In this section, we will focus on the issues that are important in using nonlinear optics with ultrashort laser pulses. Research in this area has resulted in the availability of a large variety of nonlinear crystals. However, the optimal material of choice depends on several factors. Different nonlinear materials have different wavelength ranges over which phase matching can be achieved, different requirements as to the acceptance angles, and a wide range of efficiencies and dispersion properties.

The birefringence of the crystal determines the phase-matching properties. In general, phase matching requires that the wave vector of the sum- (or difference-) frequency generated in the nonlinear optical material, k_3, be the sum (or difference) of the wave vectors k_1 and k_2 of the two input beams. The acceptance angle of the crystal, $\Delta\theta$, can be expressed as

$$\Delta\theta = \frac{4\pi}{L}\left(\frac{\partial \Delta k}{\partial \theta}\right)^{-1}, \tag{5}$$

where L is the crystal length, and the derivative represents the change of phase mismatch ($\Delta k = k_3 - k_2 - k_1$, in the case of sum-frequency generation) with respect to θ. The above equation indicates that shorter crystals have greater acceptance angles. This is a very important consideration in using nonlinear materials with ultrashort laser pulses. In order to maintain Fourier-transform-limited pulses, the entire frequency spread of the short pulse must satisfy the phase-matching condition. Thus, short crystals are required. Kahlow *et al.*[351] have recently discussed the importance of considering the acceptance angles for various crystals of thickness 1 mm for sum-frequency generation where one of the input beams is at 800 nm.

In addition to phase-matching considerations, group-velocity mismatch in the nonlinear material can also result in substantial broadening of the laser pulse. For frequency doubling, the mismatch in velocities of the frequency comp - nents of the pulse, $\Delta\nu_g$, can be calculated from (in units of time/distance)

$$\Delta\nu_g = |\nu_g(\omega_0)^{-1} - \nu_g(\omega_0/2)^{-1}|^{-1}, \tag{6}$$

where $\nu_g(\omega_0)$ is the velocity at the center frequency of the pulse. In order to prevent temporal broadening, the crystal length must be shorter than the product of the pulse width and $\Delta\nu_g$. Kahlow *et al.*[351] have examined this effect for second-harmonic generation in KDP, β-BBO, and $LiIO_3$ crystals. These results are shown in Fig. 20. In light of these issues, efficiencies for these nonlinear processes using subpicosecond laser pulses are generally smaller than what is commonly observed in related nanosecond devices. In a recent study by Kuhlke and Herpers, the intensity dependence of the second-harmonic efficiency of femtosecond pulses was examined in detail.[375] Using a 10-Hz amplified CPM laser systems (0.3 mJ at 620 nm), the maximum efficiency observed was 15% and 21% for pulses of 100-fs and 150-fs duration. In the case of the 100-fs pulses, the conversion efficiency was constant for input intensities greater than 6×10^{10} W/cm^2. However, for intensities between 2×10^{10} W/cm^2 and 6×10^{10} W/cm^2, the conversion efficiency increased linearly with input intensity. The saturation effect was attributed to the reduction of the phase-matching bandwidth at high intensities.

β-BBO offers to be a promising material for ultrashort pulse applications due to its wide transparency range (190–2500 nm), large second-order nonlinear susceptibility, high

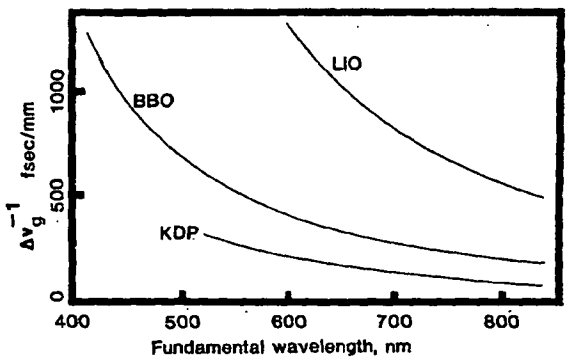

FIG. 20. The group-velocity dispersion for $LiIO_3$ (LIO), β-BBO (BB), and KDP are plotted as a function of wavelength. These data demonstrate the need to use thin crystals with ultrafast pulses. Reprinted with permission from Ref. 351.

damage threshold, and low GVD.[376] Only a few reports using β-BBO have appeared.[85,377-379] In particular, Edelstein *et al.* have recently demonstrated the generation of femtosecond UV pulses by intracavity frequency doubling using β-BBO in a CPM laser.[85] Pulse widths as short as 43 fs were reported with output powers as high as 20 mW. In addition, Chen *et al.*[380] have recently described a new optical material, LiB_3O_5 (LBO), which may prove to be useful in generating ultrashort pulses in the vacuum-ultraviolet region.

In addition to harmonic generation, difference-frequency techniques have been used to generate picosecond infrared light. Spears *et al.*[160] reported a system capable of producing infrared light through difference-frequency generating between the output of a tunable short-cavity picosecond dye laser and the fundamental of an active and passive mode-locked pulsed Nd:YAG laser

In addition, parametric oscillators have been used to generate tunable infrared and visible radiation.[381-384] Laubereau *et al.*[385] have described a system using lithium niobate as the parametric material to generate tunable pulses from 2500 cm^{-1} (4 μm) to 7000 cm^{-1} (1.43 μm), and from 800 to 588 nm using the fundamental and second-harmonic wavelengths of a mode-locked flash-lamp-pumped Nd:glass laser as the input beam. In parametric generation in a pair of proustite crystals (Ag_3AsS_3), Elsaesser, Seilmeier, and Kaiser[386] reported tunable infrared light from 1.2 to 8 μm. Campillo, Hyer, and Shapiro have observed light in the range from 10–20 μm by down conversion in CdSe of infrared light generation by parametric oscillation in $LiNbO_3$.[384] Amplification of subpicosecond 10-μm light has been observed in multiatmospheric CO_2 lasers.[387] In this study, the seed light was generated by semiconductor switching techniques; however, the approach should be applicable to light generated by parametric oscillation. Takagi *et al.*[388] have reported tunable $\approx$10-ps pulses with energies greater than 100 μJ over the wavelength range from 215 to 245 nm. Their approach involved summing Raman and optical parametrically generated light. Tanaka, Kuroda, and Shionoya reported mixing harmonics of a mode-locked Nd:YAG laser with tunable pulses from a $LiNbO_3$ parametric oscillator to generate high-energy picosecond pulses, >20 kW peak power, as deep as 197 nm in the ultraviolet region.[389] Angle-tuned KDP has been used to parametrically generate light from 450–650- and 800–1600-nm pumping with the second and third harmonics of an active-passive mode-locked Nd:YAG laser (30 ps).[390] Parametric oscillation in ADP has also been used to generate tunable ultrashort pulses from 5700 to 22 700 cm^{-1},[391] In 1984, Fan, Eckardt, and Byer[392] reported the generation of infrared light by parametric oscillation in $AgGaS_2$. Light from 1.4 to 4 μm was generated, pumping with the fundamental of the Nd:YAG laser. Elsaesser, Seilmeier, and Kaiser have reported generation of infrared pulses from 1.2 to 10 μm using parametric oscillation in a series of two $AgGaS_2$ crystals.[393] The bandwidth of the idler pulses between 6 and 10 μm was $\approx$10 cm^{-1}. Using 20-ps pump pulses from a pulsed Nd:YAG laser, infrared pulses of 8 ps were observed. In addition, ultrashort light pulses in the far-infrared region (20–200 cm^{-1}) have been generated using $LiNbO_3$.[394]

B. Continuum generation

One of the most common methods for extending the wavelength range of amplified ultrafast laser systems is by white-light continuum generation.[395-397] White-light continuum was first observed by focusing intense short laser pulses in glass. More recently, a variety of liquids have been used, including water, ethylene glycol, phosphoric acid, and several solvent mixtures. The dominant mechanism giving rise to continuum generation using femtosecond optical pulses involves SPM. As described in the first section of this review, the index of refraction of any medium is intensity dependent. Thus, in the case of continuum generation, as the pulse travels through the liquid, the intensity dependence of the index of refraction causes a time-dependent change in the phase and thus alters the frequency distribution. The rising edge of the pulse would give rise to redder wavelengths and the trailing edge would generate bluer wavelengths. In the limit where SPM plays a dominant role in the continuum generation process, stable and spatially uniform pulses are expected. Experimental studies confirm these predictions.[398]

Using the 80-fs amplified output of a CPM laser, Fork *et al.*[398] reported the generation of a white-light continuum in a jet of ethylene glycol that extended from 190 to 1600 nm. Studies on the temporal evolution of different wavelengths in the pulse confirmed that SPM was the dominant mechanism responsible for the formation of the white light. In addition, the chirp of the continuum was small, < 10 fs/1000 Å in the red and < 30 fs/1000 Å in the blue. In addition, effects due to GVD in the ethylene glycol jet were also small in comparison with the 80-fs pulse width. Using femtosecond pulses, Fork and co-workers also found that the white light was generated with high efficiency ($\approx$50%). Earlier studies using longer picosecond pulses reported much smaller efficiencies.

This approach enables one to produce femtosecond pulses that are tunable throughout a large portion of the optical spectrum. Selected wavelengths can be chosen using interference filters, greatly extending the applications of these devices in research. In addition, the amplification techniques described in Sec. II can be used to amplify sections of the femtosecond continuum.[309,399] Migus *et al.*[309] have used this approach to generate high-energy pulses in the region of 800 nm. In this device, a single gain stage pumped by a 10-Hz Nd:YAG laser is double passed, resulting in the production of microjoule pulses. Becker *et al.* extended these ideas to produce high-energy tunable 9-fs pulses in the near-infrared region, 800–840 nm.[400] The infrared radiation was produced through continuum generation using a 8-kHz CVL pumped amplifier and a CPM dye laser. The near-infrared light was selected and amplified by a second CVL pumped amplifier. The output was then compressed (Sec. II D) to 9 fs. To reduce ASE in the amplification of the continuum light, a 5-μm piece of GaAs was used as a saturable absorber. Before pulse compression, amplified outputs on the order of 0.5 μJ were reported.

Jedju and Rothberg[401] also reported the generation of a broadband infrared continuum by frequency-difference generation between the white-light continuum and the laser fun-

damental in a $LiIO_3$ crystal. This development opens up the possibility of collecting broadband time-resolved infrared spectra. Continuum light in the infrared region has also been achieved in optical fibers. Islam *et al.*[402] have reported the generation of a continuum between 1.55 and 1.85 μm by focusing the output of a mode-locked NaCl color-center laser (1.5 μm) into a 100- or 500-m length of single-mode polarization-preserving fiber. The autocorrelation of the 1.7-μm output from the 100-m fiber revealed a pulse length of 153 fs. Infrared continuum generated from $LiNbO_3$ (1.5–4.5 μm) (Ref. 403) and $LiIO_3$ (1.7–3 μm) (Ref. 404) has been reported. In addition, by focusing picosecond output from a CO_2 laser (2.9 ps, 9μm) on crystals of GaAs, AgBr, ZnSe, and CdS, infrared continuum ranging from 3 to 14 μm has been reported.[405]

C. Stimulated Raman scattering

In 1980, Wyatt and Cotter[406] reported the generation of tunable nanosecond infrared light using stimulated Raman scattering of the output from a Nd:YAG pumped dye laser from the 6*s*-5*d* Raman transition of cesium in a cesium-vapor heat pipe. In 1984, Berg *et al.*[303] extended this technique to the picosecond domain. Using the tunable 1-ps output from a 10-Hz amplified synchronously pumped dye-laser system, Raman scattering from the 6*s*-5*d* transition in a superheated cesium vapor produced pulses between 3040 cm^{-1} (3.3 μm) and 2320 cm^{-1} (4.3 μm). In order to cover this range of frequencies, four different laser dyes needed to be used: R6G, Rhodamine 610, Kyton red 620, and R640. Peak infrared intensities up to 11-μJ pulses were observed. The generation of light lower than 2320 cm^{-1} was limited by the absorption of cesium dimers.

May and Sibbett[407] reported generation of Stokes-shifted radiation by focusing the output of an amplified CPM into capillary waveguides of H_2 and CH_4. This produced light at 830 and 1265 nm and 752, 964, and 1034 nm, respectively.

VI. CONCLUDING REMARKS

The last decade has seen a significant advance in the devices used to generate and amplify ultrashort light pulses. The identification of saturable absorbers coupled with developments in nonlinear optical materials now enable one to generate high-energy femtosecond pulses in the ultraviolet, visible, and infrared regions of the spectrum. These light pulses are currently being used to study a wide variety of fundamental problems in the physical sciences. Novel high-speed optical devices (i.e., switches, electro-optic sampling) that use ultrashort light pulses are currently being developed. In addition, in the last few years there have been considerable advances in the medical applications of ultrashort pulsed lasers. The future is bound to bring new and exciting applications of these devices.

VII. ACKNOWLEDGMENTS

This work is supported by the Chemistry Division at the National Science Foundation, the Petroleum Research Foundation administered by the American Chemical Society, and the Materials and Medical Free Electron Laser Program administered by the Office of Naval Research.

[a] NSF Presidential Young Investigator 1985-1990, Alfred P. Sloan Fellow 1988–1990.
[1] G. R. Fleming, *Chemical Applications of Ultrafast Spectroscopy* (Oxford University Press, Oxford, 1986).
[2] *Ultrashort Laser Pulses*, edited by W. Kaiser (Springer-Verlag, New York, 1988).
[3] *Ultrashort Light Pulses*, edited by S. L. Shapiro (Springer-Verlag, New York, 1977).
[4] See *Ultrafast Spectroscopy of Chemical and Biological Processes*, J. Opt. Soc. Am. B (to be published).
[5] See "Ultrafast Phenomena," IEEE J. Quantum Electron. **QE-25** (December 1989).
[6] *Picosecond Optoelectronics*, edited by G. Mourou (Proc. Soc. Photo-Opt. Instrum. Eng. **439** (1983).
[7] *Applications of Picosecond Spectroscopy to Chemistry*, edited by K. B. Eisenthal (Reidel, Boston, 1984).
[8] *Picosecond Phenomena*, edited by C. V. Shank, E. P. Ippen, and S. L. Shapiro (Springer, New York, 1978).
[9] *Picosecond Phenomena II*, edited by R. M. Hochstrasser, W. Kaiser, and C. V. Shank (Springer, New York, 1980).
[10] *Picosecond Phenomena III*, edited by K. B. Eisenthal, R. M. Hochstrasser, W. Kaiser, and A. Laubereau (Springer, New York, 1982).
[11] *Ultrafast Phenomena IV*, edited by D. H. Auston and K. B. Eisenthal (Springer, New York, 1984).
[12] *Ultrafast Phenomena V*, edited by G. R. Fleming and A. E. Siegman (Springer, New York, 1986).
[13] *Ultrafast Phenomena VI*, edited by T. Yajima, K. Yoshihara, C. B. Harris, and S. Shioniya (Springer, New York, 1988).
[14] A. E. Siegman, *Lasers* (University Science, San Francisco, CA, 1986).
[15] A. Yariv, *Quantum Electronics* (Wiley, New York, 1975), Chap. 11.
[16] D. von der Linde, Appl. Phys. **2**, 281 (1983).
[17] N. H. Schiller, M. Foresti, and R. R. Alfano, J. Opt. Soc. Am. B **2**, 729 (1985).
[18] J. A. Valdmanis, R. L. Fork, and J. P. Gordon, Opt. Lett. **10**, 131 (1985).
[19] F. A. Hopf and G. I. Stegeman, *Linear Optics* Vol. 1 of *Applied Classical Electrodynamics* (Wiley, New York, 1985).
[20] P. G. May, W. Sibbett, K. Smith, J. R. Taylor, and J. P. Wilson, Opt. Commun. **42**, 285 (1982).
[21] L. L. Steinmetz, J. H. Richardson, and B. W. Wallin, Appl. Phys. Lett. **33**, 163 (1978).
[22] E. W. Roschger, A. P. Schwarzenbach, J. E. Balmer, and H. P. Weber, IEEE J. Quantum Electron. **QE-21**, 465 (1985).
[23] G. F. Albrecht, M. T. Gruneisen, and S. Smith, IEEE J. Quantum Electron. **QE-21**, 1189 (1985).
[24] U. Keller, J. A.Valdmanis, M. C. Nuss, and A. M. Johnson, IEEE J. Quantum Electron. **QE-24**, 427 (1988).
[25] S. De Silvestri, P. Laporta, and V. Magni, Opt. Lett. **11**, 785 (1986).
[26] H. Vanherzeele, Opt. Lett. **13**, 369 (1988).
[27] S. De Silvestri, P. Laporta, and V. Magni, Opt. Commun. **57**, 339 (1986).
[28] M. D. Dawson, A. S. L. Gomes, W. Sibbett, and J. R. Taylor, Opt. Commun. **52**, 295 (1984).
[29] H. J. Eichler, Opt. Commun. **56**, 351 (1986).
[30] B. Luther-Davies, Opt. Commun. **57**, 345 (1986).
[31] F. Patterson, Ph.D. thesis, Department of Chemistry, Stanford University, Stanford, CA, 1986.
[32] R. J. Dwayne Miller, L. Min, and M. A. Shragowitz, Opt. Commun. **62**, 185 (1987).
[33] L. Yan, J. D. Ling, P.-T. Ho, and C. H. Lee, Opt. Lett. **11**, 502 (1986).
[34] S. A. Strobel, P. Ho, and C. Lee, Appl. Phys. Lett. **45**, 1171 (1984).
[35] J. M. Dawes and M. G. Sceats, Opt. Commun. **65**, 275 (1988).
[36] X. Xie and J. D. Simon, Opt. Commun. **69**, 303 (1989).
[37] L. Min, Q. Bao, and R. J. D. Miller, Opt. Commun. **68**, 427 (1988).
[38] T. Sizer II and I. N. Duling III, IEEE J. Quantum Electron. **QE-24**, 404 (1988).
[39] P. Heinz, M. Fickenscher and A. Laubereau, Opt. Commun. **62**, 343 (1987).
[40] J. Weston, P. H. Chiu, and R. Aubert, Opt. Commun. **61**, 208 (1987).
[41] H. P. Kortz, IEEE J. Quantum Electron. **QE-19**, 578 (1983).
[42] I. P. Alcock and A. I. Ferguson, Opt. Commun. **58**, 417 (1986).
[43] J. A. Valdmanis and R. L. Fork, IEEE J. Quantum Electron. **QE-22**, 112 (1986).

[44] D. Kuhlke, U. Herpers, and D. von der Linde, Opt. Commun. **63**, 275 (1987).
[45] D. Kuhlke, W. Rodolph, and B. Wilhelmi, IEEE J. Quantum Electron. **QE-19**, 526 (1983).
[46] E. B. Treacy, IEEE J. Quantum Electron. **QE-5**, 454 (1969).
[47] R. L. Fork, O. E. Martinez, and J. P. Gordon, Opt. Lett. **9**, 150 (1984).
[48] F. Gires and P. Tournois, C. R. Acad. Sci. **258**, 6112 (1964).
[49] M. I. Lambsdorff and J. Kuhl, J. Opt. Soc. Am. B **5**, 2311 (1988).
[50] P. M. W. French, G. F. Chen, and W. Sibbett, Opt. Commun. **57**, 263 (1986).
[51] R. L. Fork, C. V. Shank, R. Yen, and C. A. Hirlmann, IEEE J. Quantum Electron. **QE-19**, 500 (1983).
[52] D. H. Auston, in *Ultrashort Light Pulses*, Ref. 3.
[53] R. H. Stolen and C. Lin, Phys. Rev. A **17**, 1448 (1978).
[54] C. V. Shank, R. L. Fork, and R. T. Yen, in *Picosecond Phenomena III*, Ref. 10, p.2.
[55] S. De Silvestri, P. Laporta, and O. Svelto, IEEE J. Quantum Electron. **QE-20**, 533 (1984).
[56] M. Yamashita, M. Ishikawa, K. Torizuka, and T. Sato, Opt. Lett. **11**, 504 (1986).
[57] M. Yamashita, K. Torizuka, and T. Sato, IEEE J. Quantum Electron. **QE-23**, 2005 (1987).
[58] M. Yamashita, K. Torizuka, T. Sato, and M. Ishikawa in *Ultrafast Phenomena V*, Ref. 12, p.8.
[59] H. Harri, S. Leutwyler, and E. Schumacher, Rev. Sci. Instrum. **53**, 1855 (1982).
[60] Z. A. Yasa and N. M. Amer, Opt. Lett. **6**, 67 (1981).
[61] C. V. Shank and E. P. Ippen, Appl. Phys. Lett. **24**, 373 (1974).
[62] Z. A. Yasa and N. M. Amer, Opt. Commun. **42**, 281 (1982).
[63] R. L. Fork, B. I. Greene, and C. V. Shank, Appl. Phys. Lett. **38**, 671 (1981).
[64] N. J. Frigo, IEEE J. Quantum Electron. **QE-19**, 511 (1983).
[65] O. E. Martinez, R. L. Fork, and J. P. Gordon, Opt. Lett. **9**, 156 (1984).
[66] M. S. Stix and E. P. Ippen, IEEE J. Quantum Electron. **QE-19**, 520 (1983).
[67] D. Kuhlke and W. Rudolph, Opt. Quantum Electron. **QE-16**, 57 (1984).
[68] D. Kuhlke, T. Bonkhofer, and D. Von Der Linde, Opt. Commun. **59**, 208 (1986).
[69] R. L. Fork, Opt. Lett. **11**, 629 (1986).
[70] G. R. Jacobovitz, C. H. Brito Cruz, and M. A. Scarparo, Opt. Commun. **57**, 133 (1986).
[71] M. C. Nuss, R. Leonhardt, and W. Zinth, Opt. Lett. **10**, 16 (1985).
[72] P. M. W. French and J. R. Taylor, Opt. Commun. **61**, 224 (1987).
[73] P. M. W. French and J. R. Taylor, Opt. Lett. **13**, 470 (1986).
[74] P. M. W. French and J. R. Taylor, Opt. Commun. **67**, 51 (1988).
[75] P. M. W. French, M. M. Opalinska, and J. R. Taylor, Opt. Lett. **14**, 217 (1989).
[76] J. Dobler, H. H. Schulz, and W. Zinth, Opt. Commun. **57**, 407 (1986).
[77] M. Mihailidi, Y. Budansky, X. M. Zhao, Y. Takiguchi, and R. R. Alfano, Opt. Lett. **13**, 987 (1988).
[78] P. Georges, F. Salin, G. Le Saux, G. Roger, and A. Brun, Opt. Commun. **69**, 281 (1989).
[79] N. Michailov, T. Deligeorgiev, V. Petrov, and I. Tomov, Opt. Commun. **70**, 137 (1989).
[80] P. M. W. French and J. R. Taylor, in *Ultrafast Phenomena VI*, Ref. 13, p. 94.
[81] M. Manherzeele, J.-C. Diels, and R. Torti, Opt. Lett. **9**, 549 (1984).
[82] H. Vanherzeele, R. Torti, and J. Diels, J. Appl. Opt. **23**, 4182 (1984).
[83] G. Focht and M. C. Downer, IEEE J. Quantum Electron. **QE-24**, 431 (1988).
[84] M. C. Downer, G. Focht, T. R. Zhang, W. M. Wood, D. H. Reitze, and G. W. Burdick, in *Ultrafast Phenomena VI*, Ref. 13, p. 101.
[85] D. C. Edelstein, E. S. Wachman, L. K. Cheng, W. R. Bosenberg, and C. L. Tang, Appl. Phys. Lett. **52**, 2211 (1988).
[86] T. R. Zhang, G. Focht, P. E. Williams, and M. C. Downer, IEEE J. Quantum Electron. **QE-24**, 1877 (1988).
[87] P. M. W. French and J. R. Taylor, Appl. Phys. Lett. **50**, 1708 (1987).
[88] P. M. W. French and J. R. Taylor, Opt. Lett. **11**, 297 (1986).
[89] P. M. W. French, M. D. Dawson, and J. R. Taylor, Opt. Commun. **56**, 430 (1986).
[90] A. Wantanabe, H. Tahemura, S. Tamaka, H. Kobayashi, and M. Hara, IEEE J. Quantum Electron. **QE-19**, 533 (1983).
[91] J. C. Diels, W. Deitel, J. J. Fontaine, W. Rudolph, and B. Wilhelmi, J. Opt. Soc. Am. B. **2**, 680 (1985).
[92] J.-C. Diels, N. Jamasbi, and L. Sarger in *Ultrafast Phenomena V*, Ref. 12, p.2.
[93] P. M. W. French and J. R. Taylor, J. Appl. Phys. B **41**, 53 (1986).
[94] P. M. W. French and J. R. Taylor, Opt. Commun. **58**, 53 (1986).
[95] P. M. W. French and J. R. Taylor, IEEE J. Quantum Electron. **QE-22**, 1162 (1986).
[96] K. Smith, N. Langford, W. Sibbett, and J. R. Taylor, Opt. Lett. **10**, 559 (1985).
[97] P. M. W. French and J. R. Taylor, in *Ultrafast Phenomena VI*, Ref. 13, p. 94.
[98] B. C. Johnson, P. F. Moulton, and A. Mooradian, Opt. Lett. **10**, 116 (1984).
[99] H. Ansari, A. Dienes, and J. R. Whinnery, J. Opt. Lett. **10**, 19 (1985).
[100] N. Langford, R.S. Grant, C. I. Johnston, K. Smith, and W. Sibbett, Opt. Lett. **14**, 45 (1989).
[101] B. H. Soffer and L. W. Lin, J. Appl. Phys. **39**, 5959 (1968).
[102] D. J. Bradley, A. Durrant, G. Gale, M. Moore, and P. D. Smith, IEEE J. Quantum Electron. **QE-4**, 707 (1968).
[103] D. J. Bradley and A. Durrant, Phys. Lett. **27A**, 73 (1968).
[104] M. R. Topp and P. M. Rentzepis, Phys. Rev. A **3**, 358 (1971).
[105] L. Goldberg and C. Moore, Appl. Phys. Lett. **27**, 217 (1975).
[106] C. Moore and L. Goldberg, Opt. Commun. **16**, 21 (1976).
[107] A. Dienes, E. P. Ippen, and C. V. Shank, Appl. Phys. Lett. **19**, 258 (1971).
[108] C. K. Chan and S. O. Sari, Appl. Phys. Lett. **25**, 403 (1974).
[109] J. J. Kasinski, R. J. D. Miller, P. Geist, F. Hiesel, A. Martz, and J. A. Miehe, Opt. Commun. **55**, 450 (1985).
[110] J. J. Kasinski, L. A. Gomez-Jahn, R. J. Dwayne Miller, P. Geist, B. Geoffroy, F. Heisel, A. Martz, and J. A. Miehe, J. Opt. Soc. Am. B **3**, 1566 (1986).
[111] J. Herrmann and U. Metschmann, Appl. Phys. B **27**, 27 (1982).
[112] J. V. Hryniewicz, G. M. Carter, and Y. J. Chen, Opt. Commun. **54**, 230 (1985).
[113] R. K. Jain, Appl. Phys. Lett. **40**, 295 (1982).
[114] G. W. Fehrenbach, K. J. Gruntz, and R. G. Ulbrich, Appl. Phys. Lett. **33**, 159 (1978).
[115] D. J. Eilenberger, E.D. Isaacs, and G. D. Aumiller, Opt. Commun. **44**, 350 (1981).
[116] F. S. Choa and P. L. Liu, Opt. Lett. **13**, 743 (1988).
[117] J. M. Cemens, J. Najbar, I. Bronstein-Bonte, and R. M. Hochstrasser, Opt. Commun. **47**, 271 (1983).
[118] T. Sizer II and G. Mourou, Opt. Commun. **37**, 207 (1981).
[119] F. S. Choa, U. Liu, and P. L. Liu, Opt. Lett. **14**, 222 (1989).
[120] A. Seilmeier, W. Kaiser, B. Sens, and K. H. Drexhage, Opt. Lett. **8**, 205 (1983).
[121] P. M. W. French, A. L. Gones, A. S. Gouveia-Neto, and J. R. Taylor, Opt. Commun. **60**, 389 (1986).
[122] M. D. Dawson, W. A. Schroeder, D. P. Norwood, and A. L. Smirl, Opt. Lett. **14**, 364 (1989).
[123] H. Roskos, S. Optiz, A. Seilmeier, and W. Kaiser, IEEE J. Quantum Electron. **QE-22**, 697 (1986).
[124] A. M. Johnson and W. M. Simpson, Opt. Lett. **8**, 854 (1983).
[125] P. Beaud, B. Zysset, A. P. Schwarzenbach, and H. P. Weber, Opt. Lett. **11**, 24 (1986).
[126] G. A. Mourou and T. Sizer II, Opt. Commun. **41**, 47 (1982).
[127] P. M. W. French, A. S. L. Gomes, A. S. Gouveia-Neto, and J. R. Taylor, Opt. Commun. **59**, 366 (1986).
[128] Y. Ishida, K. Naganuma, and T. Yajima, IEEE J. Quantum Electron. **QE-21**, 69 (1985).
[129] D. L. MacFarlane and L. W. Casperson, Opt. Lett. **14**, 314 (1989).
[130] D. Kuhlke, U. Herpers, and D. von der Linde, Appl. Phys. B **38**, 233 (1985).
[131] P. G. May, W. Sibbett, and J. R. Taylor, Appl. Phys. B **26**, 179 (1981).
[132] D. Dawson, T. F. Boggess, and D. W. Garvey, Opt. Commun. **60**, 79 (1986).
[133] M. D. Dawson, T. F. Boggess, and A. L. Smirl, Opt. Lett. **12**, 254 (1987).
[134] M. D. Dawson, T. F. Boggess, D. W. Garvey, and A. L. Smirl, IEEE J. Quantum Electron. **QE-23**, 290 (1987).
[135] H. Kubota, K. Kurokawa, and M. Nakazawa, Opt. Lett. **13**, 749 (1988).
[136] J. Chesnoy and L. Fini, Opt. Lett. **11**, 635 (1986).
[137] T. Norris, T. Sizer II, and G. Mourou, J. Opt. Soc. Am. B **2**, 613 (1985).
[138] A. E. Siegman, Opt. Lett. **6**, 334 (1981).
[139] A. E. Siegman and H. Vanherzeele, in *Picosecond Phenomena III*, Ref.

10, p. 14.
[140] H. Vanherzeele, J. L. Van Eck, and A. E. Siegman, Appl. Opt. 20, 3483 (1981).
[141] S. Ruhman, A. G. Joly, B. Kohler, L. R. Williams,and K. A. Nelson, Rev. Phys. Appl. 22, 1717 (1987).
[142] D. K. Negus, B. C. Couillaud, and R. Brady, in *Ultrafast Phenomena VI*, Ref. 13, p. 97.
[143] D. B. McDonald, J. L. Rossel, and G. R. Fleming, IEEE J. Quantum Electron. QE-17, 1134 (1981).
[144] F. Minami and K. Era, Opt. Commun. 56, 46 (1985).
[145] K. L. Sala, G. A. Kenney-Wallace, and G. E. Hall, IEEE J. Quantum Electron. QE-16, 990 (1980).
[146] C. P. Ausschnitt, R. K. Jain, and J. P. Heritage, IEEE J. Quantum Electron. QE-15, 912 (1979).
[147] D. B. McDonald, D. Waldeck, and G. R. Fleming, Opt. Commun. 34, 127 (1980).
[148] S. L. Shapiro, R. R. Cavanagh, and J. C. Stephenson, Opt. Lett. 6, 470 (1981).
[149] K. Smith, J. M. Catherall, and G. H. C. New, Opt. Commun. 58, 118 (1986).
[150] R. Illingworth and I. S. Ruddock, Opt. Commun. 59, 375 (1986).
[151] M. D. Dawson, D. Maxson, T. F. Boggess, and A. L. Smirl. Opt. Lett. 13, 126 (1988).
[152] A. I. Ferguson and R. A. Taylor, in *Picosecond Phenomena III*, Ref. 10, p. 31.
[153] S. R. Rotman, C. Roxlo, D. Bebelaar, and T. K. Yee, Appl. Phys. B 28, 319 (1982).
[154] S. Kishida, K. Inoue, and K. Washio, Opt. Lett. 5, 191 (1980).
[155] M. J. W. Rodwell, K. J. Weingarten, D. M. Bloom, T. Baer, and B. H. Kolner, Opt. Lett. 11, 638 (1986).
[156] M. J. W. Rodwell, D. M. Bloom, and K. J. Weingarten, IEEE J. Quantum Electron. QE-25, 817 (1989).
[157] K. Yamada, K. Miyazaki, T. Hasama, and T. Sato, J. Appl. Opt. 25, 634 (1986).
[158] L. J. Qian, Y. X. Liu, and F. M. Li, Opt. Commun. 69, 398 (1989).
[159] H. P. Kortz, A. J. Cox, G. W. Scott, D. M. Guthals, H. Nathel, S. W. Yeh, S. P. Webb, and J. H. Clark, IEEE J. Quantum Electron. QE-21, 1795 (1985).
[160] K. G. Spears, X. Zhu, X. Yang, and L. Wang, Opt. Commun. 66, 167 (1988).
[161] G. W. Scott, S. G. Shen, and A. J. Cox, Rev. Sci. Instrum. 55, 358 (1984).
[162] I. A. McIntyre, K. Boyer, and C. K. Rhodes, Opt. Commun. 67, 225 (1988).
[163] M. D. Dawson, T. F. Boggess, and A. L. Smirl, Opt. Lett. 12, 590 (1987).
[164] T. S. Stork, M. D. Dawson, and A. L. Smirl, Opt. Commun. 68, 361 (1988).
[165] S. Kelly, G. H. C. New, and D. Wood, J. Appl. Phys. B 47, 349 (1988).
[166] C. R. Pollock, J. F. Pinto, and E. Georgiou, J. Appl. Phys. B 48, 287 (1989).
[167] L. Isganitis, M. G. Sceats, and K. R. German, Opt. Lett. 5, 7 (1980).
[168] T. Basiev, B. Mirov, and V. V. Osiko, IEEE J. Quantum Electron. QE-91, 1052 (1988).
[169] P. N. Kean, X. Zhu, D. W. Crust, R. S. Grant, N. Langford, and W. Sibbett, Opt. Lett. 14, 39 (1989).
[170] L. F. Mollenauer, N. D. Vieira, and L. Szeto, Opt. Lett. 7, 414 (1982).
[171] L. F. Mollenauer and D. M. Bloom, Opt. Lett. 4, 247 (1979).
[172] L. F. Mollenauer, D. M. Bloom, and A. M. DelGaudio, Opt. Lett. 3, 48 (1978).
[173] L. F. Mollenauer and R. H. Stolen, Opt. Lett. 9, 13 (1984).
[174] L. F. Mollenauer, Philos. Trans. R. Soc. London A 315, 437 (1985).
[175] A. Hasegawa and F. Tappert, Appl. Phys. Lett. 23, 142 (1973).
[176] L. F. Mollenauer, R. H. Stolen, J. P. Gordon, and W. J. Tomilson, Opt. Lett. 8, 289 (1983).
[177] L. F. Mollenauer, R. H. Stolen, and J. P. Gordon, Phys. Rev. Lett. 45, 1095 (1980).
[178] R. H. Stolen, L. F. Mollenauer, and W. J. Tomilson, Opt. Lett. 8, 186 (1983).
[179] F. M. Mitschke and L. F. Mollenauer, in *Ultrafast Phenomena V*, Ref. 12, p. 58.
[180] A. S. Gouveia-Neto, A. S. L. Gomes, and J. R. Taylor, IEEE J. Quantum Electron. QE-24, 332 (1988).
[181] E. M. Dianov, A. Ya. Karasik, P. V. Mamyshev, A. M. Prokhorov, V. N. Serkin, M. F. Stelmaich, and A. A. Fomichec, Pisma Zh. Eksp. Teor. Fiz. 41, 242 (1985).
[182] A. Hasegawa, Opt. Lett. 8, 650 (1983).
[183] R. H. Stolen, Fiber Integrated Opt. 3, 21 (1980).
[184] C. Lin and W. G. French, Appl. Phys. Lett. 34, 666 (1979).
[185] R. H. Stolen and E. P. Ippen, Appl. Phys. Lett. 22, 276 (1973).
[186] J. D. Kafka, D. F. Head, and T. Baer, in *Ultrafast Phenomena V*, Ref. 12, p. 51.
[187] B. Zysset, P. Beaud, W. Hodel, and H. P. Weber, in *Ultrafast Phenomena V*, Ref. 12, p. 54.
[188] V. A. Vysluolch and V. N. Serkin, Pisma Zh. Eksp. Teor. Fiz. 38, 170 (1983).
[189] M. N. Islam, L. F. Mollenauer, and R. H. Stolen, in *Ultrafast Phenomena V*, Ref. 12, p. 46.
[190] C. P. Yakymyshyn, J. F. Pinto, and C. R. Pollock, Opt. Lett. 14, 621 (1989).
[191] P. N. Kean, R. S. Grant, X. Zhu, D. W. Crust, D. Burns, and W. Sibbett, in Conference on Lasers Electrooptics (CLEO), Opt. Soc. Am. 1988, paper PD7-1.
[192] K. J. Blow and B. P. Nelson, Opt. Lett. 13, 1026 (1988).
[193] J. Mark, L. Y. Liv, K. Hall, H. A. Haus, and E. P. Ippen (unpublished).
[194] H. Nakatsuka and D. Grischkowsky, J. Opt. Lett. 6, 13 (1981).
[195] N. J. Halas and D. Grischkowsky, Appl. Phys. Lett. 48, 823 (1986).
[196] M. Nakazawa, T. Nakashima, H. Kubota, and S. Seikai, J. Opt. Soc. Am. B 5, 215 (1988).
[197] B. Nikolaus and D. Grischkowsky, Appl. Phys. Lett. 43, 228 (1983).
[198] S. L. Palfrey and D. Grischkowsky, J. Opt. Lett. 10, 562 (1985).
[199] Y. Ishida and T. Yajima, Opt. Commun. 58, 355 (1986).
[200] T. C. Damen and J. Shah, Appl. Phys. Lett. 52, 1291 (1988).
[201] B. Nikolaus and D. Grischkowsky, Appl. Phys. Lett. 42, 1 (1983).
[202] M. Nakazawa, T. Nakashima, H. Kubota, and S. Seikai, Appl. Phys. Lett. 51, 728 (1987).
[203] J. H. Glownia, G. Arjavalingam, P. P. Sorokin, and J. E. Rothenberg, Opt. Lett. 11, 79 (1986).
[204] A. P. Schwarzenbach, T. S. Luk, I. A. McIntyre, U. Johann, A. McPherson, K. Boyer, and C. K. Rhodes, Opt. Lett. 11, 499 (1986).
[205] B. Valk, K. Vilhelmsson, and M. M. Salour, J. Appl. Phys. Lett. 50, 656 (1987).
[206] B. Zysset, W. Hodel, P. Beaud, and H. P. Weber, J. Opt. Lett. 11, 156 (1986).
[207] M. Kuckartz, R. Schulz, and H. Harde, J. Opt. Soc. Am. B 5, 1353 (1988).
[208] A. S. L. Gomes, U. Osterberg, W. Sibbett, and J. R. Taylor, Opt. Commun. 54, 377 (1985).
[209] A. S. L. Gones, W. Sibbett, and J. R. Taylor, J. Opt. Lett. 10, 338 (1985).
[210] J. D. Kafka, B. H. Kolner, T. Baer, and D. M. Bloom, J. Opt. Lett. 9, 505 (1984).
[211] K. J. Blow, N. J. Doran, and B. P. Nelson, Opt. Lett. 10, 393 (1985).
[212] A. S. L. Gomes, W. E. Sleat, W. Sibbett, and J. R. Taylor, Opt. Commun. 57, 257 (1986).
[213] E. M. Dianov, L. M. Ivanov, P. V. Mamyshev, and A. M. Prokhorov, IEEE J. Quantum Electron. QE-25, 828 (1989).
[214] L. A. Gomez Jahn, J. J. Kasinski, and R. J. Dwayne Miller, J. Appl. Phys. A 43, 41 (1987).
[215] A. S. L. Gomes and J. R. Taylor, Opt. Commun. 55, 435 (1985).
[216] R. L. Fork, C. H. Brito Cruz, P. C. Becker, and C. V. Shank, Opt. Lett. 12, 483 (1987).
[217] T. Sizer, J. D. Kafka, I. N. Duling, C. W. Gabel, and G. A. Mourou, IEEE J. Quantum Electron. QE-19, 506 (1983).
[218] C. V. Shank, R. L. Fork, R. Yen, R. H. Stolen, and W. J. Tomlinson, Appl. Phys. Lett. 40, 761 (1982).
[219] J. M. Halbout and D. Grischkowsky, Appl. Phys. Lett. 45, 1281 (1984).
[220] G. Boyer, M. Franco, J. P. Chanbaret, A. Migus, A. Antonetti, P. Georges, F. Salin, and A. Brun, Appl. Phys. Lett. 53, 823 (1988).
[221] J. S. Coe, P. Maine, and P. Bado, J. Opt. Soc. Am. B 5, 2560 (1988).
[222] P. Maine and G. Mourou, Opt. Lett. 13, 467 (1988).
[223] P. Maine, D. Strickland, P. Bado, M. Pessot, and G. Mourou, IEEE J. Quantum Electron. QE-24, 398 (1988).
[224] T. Damm, M. Kaschke, F. Noack, and B. Wilhelmi, J. Opt. Lett. 10, 176 (1985).
[225] Y. J. Chang, C. Veas, and J. B. Hopkins, Appl. Phys. Lett. 49, 1758 (1986).
[226] W. J. Tomlinson, R. H. Stolen, and C. V. Shank, J. Opt. Soc. Am. B 1, 139 (1984).
[227] J. D. Kafka and T. M. Baer, IEEE J. Quantum Electron. QE-24, 341 (1988).

[228] V. J. Newell, F. W. Deeg, S. R. Greenfield, and M. D. Fayer, J. Opt. Soc. Am. B 6, 257 (1989).
[229] C. H. Brito Cruz, P. C. Becker, R. L. Fork, and C. V. Shank, Opt. Lett. 13, 123 (1988).
[230] K. D. Li, W. H. Knox, and N. M. Pearson, Opt. Lett. 14, 450 (1989).
[231] M. A. Duguay and J. W. Hanson, Appl. Phys. Lett. 14, 14 (1968).
[232] A. M. Johnson, R. H. Stolen, and W. M. Simpson, Appl. Phys. Lett. 44, 729 (1984).
[233] K. Tai and A. Tomita, Appl. Phys. Lett. 48, 309 (1986).
[234] K. Tai and A. Tomita, Appl. Phys. Lett. 48, 1033 (1986).
[235] P. Maine, D. Strickland, M. Pessot, J. Squier, P. Bado, G. Mourou, and D. Hurter, in *Ultrafast Phenomena VI*, Ref. 13, p. 2.
[236] A. M. Weiner, J. P. Heritage, and E. M. Kirschner, J. Opt. Soc. Am. B 5, 1563 (1988).
[237] R. N. Thurston, J. P. Heritage, A. M. Weiner, and W. J. Tomlinson, IEEE J. Quantum Electron. QE-22, 682 (1986).
[238] M. Haner and W. S. Warren, Appl. Phys. Lett. 52, 1458 (1988).
[239] W. Warren, Science 242, 878 (1988).
[240] A. Sanchez, R. E. Fahey, A. J. Strauss, and R. L. Aggarwal, Opt. Lett. 11, 363 (1986).
[241] J. D. Kafka, A. J. Alfrey, and T. Baer, in *Ultrafast Phenomena VI*, Ref. 13, p. 64.
[242] R. Roy, P. A. Schultz, and A. Walther, Opt. Lett. 12, 672 (1987).
[243] J. T. Darrow and R. K. Jain, in Digest of Conference on Lasers Electrooptics, paper ME1 (1988).
[244] P. A. Schultz, IEEE J. Quantum Electron. QE-24, 1039 (1988).
[245] A. C. Maciel, P. Maly, and J. F. Ryan, Opt. Commun. 61, 125 (1987).
[246] J. Klebniczki, Z. Bor, and G. Szabo, J. Appl. Phys. B 46, 151 (1988).
[247] J. Hebling and J. Kuhl, Opt. Lett. 14, 278 (1989).
[248] Z. Bor, S. Szatmari, and A. Muller, J. Appl. Phys. B 32, 101 (1983).
[249] Z. Bor and B. Racz, Opt. Commun. 54, 165 (1985).
[250] P. O. Scherer, A. Seilmeir, and W. Kaiser, J. Chem. Phys. 83, 3948 (1985).
[251] H. J. Polland, T. Elsaesser, A. Seilmeier, and W. Kaiser, J. Appl. Phys. B 32, 53 (1983).
[252] T. Elsaesser, J. H. Polland, A. Seilmeier, and W. Kaiser, IEEE J. Quantum Electron. QE-20, 191 (1984).
[253] H. Lobentanzer and T. Elsaesser, J. Appl. Phys. B 41, 139 (1986).
[254] J. Jasny, Rev. Sci. Instrum. 57, 1303 (1986).
[255] Z. Bor, IEEE J. Quantum Electron. QE-16, 517 (1980).
[256] S. Szatmari, B. Racz, J. Appl. Phys. B 43, 173 (1987).
[257] J. Hebling, J. Appl. Phys. B 47, 267 (1988).
[258] G. Szabo and Z. Bor, J. Appl. Phys. B 47, 299 (1988).
[259] Z. Bor and G. Szabo, J. Appl. Phys. B 47, 135 (1988).
[260] C. V. Shank, J. E. Bjorkholm, and H. Kogelnik, Appl. Phys. Lett. 18, 396 (1971).
[261] J. S. Bakos, Z. Fuzessy, Z. Sorlei, and J. Szigeti, Phys. Lett 50A, 227 (1983).
[262] J. S. Bakos and Z. Sorlei, Opt. Commun. 22, 258 (1977).
[263] S. Chandra, N. Takeuchi, and S. R. Hartman, Appl. Phys. Lett. 21, 144 (1972).
[264] T. Sh. Efendiev and A. N. Rubinov, Zh. Prikl. Spektrosk. 21, 526 (1974).
[265] A. N. Rubinov, T. Sh. Efendiev, A. V. Adamushko, Z. Bor, and N. A. Nemkovich, Pisma Zh. Teh. Fiz. 2, 704 (1976).
[266] V. A. Zhaporozhcenko, A. N. Rubinow, and T. Sh. Efendiev, Pisma Zh. Teh. Fiz. 8, 114 (1977).
[267] I. Ketskemety, Z. Bor, B. Racz, L. Kozma, and A. N. Runinov, Opt. Commun. 22, 275 (1977).
[268] Z. Bor, B. Racz, L. Kozma, A. M. Rubinov, and T. Sh. Efendiev, Opt. Commun. 24, 265 (1978).
[269] V. I. Vashchuk, E. I. Zabello, and E. I. Tikhonov, Sov. J. Quantum Electron. 8, 859 (1978).
[270] V. M. Katarkevich, A. N. Rubinov, and T. Sh. Efendiev, Zh. Prikl. Spektrosk. 43, 559 (1985).
[271] Z. Bor, Opt. Commun. 29, 103 (1979).
[272] See IEEE J. Quantum Electron. QE-23, Special Issue on Free-Electron Lasers (Sept. 1987).
[273] See J. Opt. Soc. Am. B 6, (May 1989).
[274] A. Cutolo, S. V. Benson, B. Hooper, J. F. Schultz, and J. M. Madey, J. Appl. Opt. 28, 97 (1989).
[275] J. Stone, J. M. Wiesenfeld, A. G. Dentai, T. C. Damen, M. A. Duguay, T. Y. Chang, and E. A. Caridi, Opt. Lett. 6, 534 (1981).
[276] L. A. Glasser, Electron. Lett. 14, 725 (1978).
[277] Y. Arakawa, A. Larsson, J. Paslaki, and A. Yariv, Appl. Phys. Lett. 48, 561 (1981).
[278] T. Paoli and J. E. Ripper, Appl. Phys. Lett. 16, 96 (1970).
[279] K. Y. Lau and A. Yariv, Appl. Phys. Lett. 45, 124 (1984).
[280] E. Scholl, J. Appl. Phys. B 46, 69 (1988).
[281] C. Rolland and P. B. Corkum, J. Opt. Soc. Am. B 3, 1625 (1986).
[282] A. Takada, T. Sugie, and M. Saruwatari, IEEE J. Light. Technol. LT-5, 1525 (1987).
[283] A. Takada, T. Sugie, and M. Saruwatari, Electron. Lett. 22, 1347 (1986).
[284] E. P. Ippen, D. J. Eilenberger, and R. W. Dixon, Appl. Phys. Lett. 37, 267 (1980).
[285] Y. Silberberg and P. W. Smith, IEEE J. Quantum Electron. QE-22, 759 (1986).
[286] T. L. Paoli and J. E. Ripper, Appl. Phys. Lett. 16, 96 (1970).
[287] J. P. van der Ziel, R. A. Logan, and R. M. Mikulyak, Appl. Phys. Lett. 39, 867 (1981).
[288] M. A. Duguay, T. C. Damen, J. Stone, J. M. Wiesenfeld, and C. A. Burrus, Appl. Phys. Lett. 37, 369 (1980).
[289] Pao-Lo Liu, C. Lin, I. P. Kaminow, and J. J. Hsieh, IEEE J. Quantum Electron. QE-17, 671 (1981).
[290] T. Sogawa, Y. Arakawa, and T. Kamiya, in *Ultrafast Phenomena VI*, Ref. 13, p. 70.
[291] P. W. Smith, Y. Silberberg, and D. A. B. Miller, J. Opt. Soc. Am. B 2, 1228 (1985).
[292] Y. Silberberg and P. W. Smith, IEEE J. Quantum Electron. QE-22, 759 (1986).
[293] P. P. Vasil'ev, IEEE J. Quantum Electron. QE-24, 2386 (1988).
[294] A. Migus, C. V. Shank, E. P. Ippen, and R. L. Ford, IEEE J. Quantum Electron. QE-18, 101 (1982).
[295] W. H. Knox, IEEE J. Quantum Electron. QE-24, 388 (1988).
[296] A. Migus, J. L. Martin, R. Astier, and A. Orszag in *Picosecond Phenomena II*, Ref. 9, p. 296.
[297] A. Penzhofer and W. Kaiser, Opt. Quantum Electron. 9, 315 (1977).
[298] T. L. Koch, L. C. Chiu, and A. Yariv, Opt. Commun. 40, 364 (1982).
[299] T. L. Koch, L. C. Chiu, and A. Yariv, J. Appl. Phys. 53, 6047 (1982).
[300] R. L. Ford, C. V. Shank, and R. T. Yen, Appl. Phys. Lett. 41, 223 (1982).
[301] M. M. Murnane and R. W. Falcone, J. Opt. Soc. Am. B 5, 1573 (1988).
[302] C. Hirlmann, O. Seddiki, J.-F. Morhange, R. Mounet, and A. Goddi, Opt. Commun. 59, 52 (1986).
[303] M. Berg, A. L. Harris, J. K. Brown, and C. B. Harris, Opt. Lett. 9, 50 (1984).
[304] D. S. Bethume, Appl. Opt. 20, 1897 (1981).
[305] M. M. Murname and R. W. Falcone, J. Opt. Soc. Am. B 5, 1575 (1988).
[306] W. M. Wood, G. Focht, and M. C. Downer, Opt. Lett. 13, 984 (1986).
[307] R. H. Austin and J. D. LeGrange, Rev. Sci. Instrum. 56, 630 (1985).
[308] E. L. Quitevis and G. A. Kenney-Wallace, Rev. Sci. Instrum. 55, 1265 (1984).
[309] A. Migus, A. Antonetti, J. Etchepare, D. Hulin, and A. Orszag, J. Opt. Soc. Am. B 2, 584 (1985).
[310] M. D. Perry, O. L. Landen, J. Weston, and R. Ettlebrick, Opt. Lett. 14, 42 (1989).
[311] A. J. Taylor, J. P. Roberts, T. R. Gosnell, and C. S. Lester, Opt. Lett. 14, 444 (1989).
[312] C. Rolland and P. B. Corkum, Opt. Commun. 59, 64 (1986).
[313] T. Turner, M. Chatelet, D. S. Moore, and S. C. Schmidt, Opt. Lett. 11, 357 (1986).
[314] P. Georges, F. Salin, G. LeSaux, G. Roger, and A. Brun, Opt. Commun. 67, 297 (1988).
[315] T. Juhasz, J. Kuhl, and W. E. Bron, Opt. Lett. 13, 577 (1988).
[316] J. E. Murray and D. J. Kuizenga, Appl. Phys. Lett. 37, 27 (1980).
[317] T. Sizer II, J. D. Kafka, A. Krisiloff, and G. Mourou, Opt. Commun. 39, 259 (1981).
[318] M. D. Dawson, W. A. Schroeder, D. P. Norwood, A. L. Smirl, J. Weston, R. N. Ettelbrick, and R. Aubert, Opt. Lett. 13, 990 (1988).
[319] T. A. Hall and W. Hamudi, Opt. Commun. 55, 66 (1985).
[320] D. F. Voss and L. S. Goldberg, Opt. Lett. 11, 210 (1986).
[321] I. N. Duling III, T. Norris, T. Sizer II, P. Bado, and G. A. Mourou, J. Opt. Soc. Am. B 2, 616 (1985).
[322] J. C. Postlewaite, J. B. Miers, C. C. Reiner, and D. D. Dlott, IEEE J. Quantum Electron. QE-24, 411 (1988).
[323] J. E. Murray and W. H. Lowdermilk, J. Appl. Phys. 51, 3548 (1980).
[324] J. E. Murray and D. J. Kuizenga, Appl. Phys. Lett. 37, 27 (1980).

[325] P. Bado, M. Bouvier, and J. S. Coe, Opt. Lett. **12**, 319 (1987).
[326] P. Bado and M. Bouvier, Rev. Sci. Instrum. **59**, 1744 (1985).
[327] S. Dong, W. Krause, F. Volker, and H. Weber, Rev. Sci. Instrum. **57**, 539 (1986).
[328] A. L. Harmer, A. Linz, and D. R. Gabbe, J. Phys. Chem. Solids **30**, 1483 (1969).
[329] E. J. Sharp, D. J. Horowitz, and J. E. Miller, J. Appl. Phys. **44**, 5399 (1973).
[330] J. E. Murray, IEEE J. Quantum Electron. **QE-19**, 488 (1983).
[331] T. M. Pollak, W. F. Wing, R. J. Grasso, E. P. Chicklis, and H. P. Jenssen, IEEE J. Quantum Electron. **QE-18**, 159 (1982).
[332] P. Bado (personal communication).
[333] H. Vanderzeele, Rev. Sci. Instrum. **60**, 592 (1989).
[334] H. Vanderzeele, Opt. Lett. **13**, 369 (1988).
[335] H. Vanderzeele, Appl. Opt. **27**, 3608 (1988).
[336] D. Strickland and G. Mourou, Opt. Commun. **55**, 447 (1985).
[337] M. Pessot, P. Maine, and G. Mourou, Opt. Commun. **62**, 419 (1987).
[338] M. Pessot, J. Squier, P. Bado, G. Mourou, and D. J. Harter, IEEE J. Quantum Electron. **QE-25**, 61 (1989).
[339] P. Maine, D. Strickland, M. Pessot, J. Squier, P. Bado, G. Mourou, and D. Harter, in *Ultrafast Phenomena VI*, Ref. 13, p. 2.
[340] D. J. Kuizenga, IEEE J. Quantum Electron. **QE-17**, 1694 (1981).
[341] G. T. Harvey, C. W. Gabel, and G. A Mourou, Opt. Commun. **36**, 213 (1981).
[342] J. M. Bostick, S. A. Mounter, and C. K. Johnson, Opt. Commun. **69**, 54 (1988).
[343] T. Sizer II, J. D. Karka, I. N. Duling III, C. W. Gabel, and G. A Mourou, IEEE J. Quantum Electron. **QE-19**, 506 (1983).
[344] I. N. Duling III and T. Sizer II, in Proceedings of the Optical Society of America, Annual Meeting, Seattle, WA October, 1986, paper I-PD6.
[345] W. H. Knox, J. Opt. Soc. Am. B **4**, 1771 (1987).
[346] D. Nickel, D. Kuhlke, and D. von der linde, Opt. Lett. **14**, 36 (1989).
[347] J. B. Hopkins and P. M. Rentzepis, Appl. Phys. Lett. **47**, 776 (1985).
[348] W. H. Knox, M. C. Downer, R. L. Fork, and C. V. Shank, Opt. Lett. **9**, 552 (1984).
[349] D. B. McDonald and C. D. Jonah, Rev. Sci. Instrum. **55**, 1166 (1984).
[350] E. V. Khoroshilov, I. V. Kryukov, P. G. Kryukov, and A. V. Sharkov, in *Ultrafast Phenomena VI*, Ref. 13, p. 22.
[351] M. A. Kahlow, W. Jarzeba, T. P. DuBruil, and P. F. Barbara, Rev. Sci. Instrum. **59**, 1098 (1988).
[352] D. H. Waldeck, W. T. Lotshaw, D. B. McDonald, and G. R. Fleming, Chem. Phys. Lett. **88**, 297 (1982).
[353] T. L. Gustafson and D. M. Roberts, Opt. Commun. **43**, 141 (1982).
[354] M. C. Downer, R. L. Fork, and M. Islam, in *Ultrafast Phenomena VI*, Ref. 11, p. 27.
[355] T. Varghese, Appl. Phys. Lett. **40**, 127 (1982).
[356] P. B. Corkum and R. S. Taylor, IEEE J. Quantum Electron. **QE-18**, 1962 (1982).
[357] J. H. Glownia, J. Misewich, and P. P. Sorokin, J. Opt. Soc. Am. B **3**, 1573 (1986).
[358] B. Dick, S. Szatmari, B. Racz, and F. P. Schafer, Opt. Commun. **62**, 277 (1987).
[359] S. Szatmari, B. Racz, and F. P. Schafer, Opt. Commun. **62**, 271 (1987).
[360] J. H. Glownia, J. Misewich, and P. P. Sorokin, J. Opt. Soc. Am. B **4**, 1061 (1987).
[361] M. Watanabe, A. Endoh, N. Sarakura, and S.Watanabe, J. Appl. Phys. **65**, 428 (1989).
[362] J. R. M. Barr, N. J. Everall, C. J. Hooker, I. N. Ross, M. J. Shaw, and W. T. Toner, Opt. Commun. **66**, 127 (1988).
[363] C. J. Hooker, F. Kannari, and M. J. Shaw, Opt. Commun. **65**, 269 (1988).
[364] A. J. Taylor, R. B. Gibson, and J. P. Roberts Appl. Phys. Lett. **52**, 773 (1988).
[365] S. Szatmari, F. P. Schafer, E. Muller-Horsche, and W. Muckenheim, Opt. Commun. **63**, 305 (1987).
[366] A. Endoh, M. Watanabe, N. Sarukura, and S. Watanabe, Opt. Lett. **14**, 353 (1989).
[367] W. Tighe, C. H. Nam, J. Robinson, and S. Suckewer, Rev. Sci. Instrum. **59**, 2235 (1988).
[368] P. W. Milonni, R. B. Gibson, and A. J. Taylor, J. Opt. Soc. Am. B **5**, 1360 (1988).
[369] H. Egger, T. S Luk, K. Boyer, D. F. Muller, H. Pummer, T. Srinivasan, and C. K. Rhodes, Appl. Phys. Lett. **41**, 1032 (1982).
[370] J.-M. Halbout and D. Grischkowsjy, Appl. Phys. Lett. **45**, 1281 (1984).
[371] M. Messmer and J. D. Simon (unpublished).
[372] Q. Zhao, S. Szatmari, and F. P. Schafer, J. Appl. Phys. B **47**, 325 (1988).
[373] J. F. Reintjes, *Nonlinear Optical Parametric Processes in Liquids and Gases* (Academic, New York, 1984).
[374] Y. R. Shen, *The Principles of Nonlinear Optics* (Wiley, New York, 1984).
[375] D. Kuhlke and U. Herpers, Opt. Commun. **69**, 75 (1988).
[376] Y. Ishida and T. Yajima, Opt. Commun. **62**, 197 (1987).
[377] P. Qiu and A. Penzkofer, J. Appl. Phys. B **45**, 225 (1988).
[378] K. L. Cheng, W. Bosenberg, F. W. Wise, I. A. Waimsley, and C. L. Tang, Appl. Phys. Lett. **52**, 519 (1988).
[379] T. L. Gustafson, Opt. Commun. **67**, 53 (1988).
[380] C. Chen, Y. Wu, A. Jiang, B. Wu, G. You, R. Li, and S. Lim, J. Opt. Soc. Am. B **6**, 616 (1989).
[381] R. A Baumgartner and R. L. Byer, IEEE J. Quantum Electron. **QE-15**, 432 (1979).
[382] S. J. Brosnan and R. L. Byer, IEEE J. Quantum Electron. **QE-15**, 415 (1979).
[383] M. J. Rosker, K. Cheng, and C. L. Tang, IEEE J. Quantum Electron. **QE-21**, 1600 (1985).
[384] A. J. Campillo, R. C. Hyer, and S. L. Shapiro, Opt. Lett. **4**, 325 (1979).
[385] A. Laubereau, A. Fendt, A. Seilmeier, and W. Kaiser, in *Picosecond Phenomena*, Ref. 8, p. 89.
[386] T. Elsaesser, A. Seilmeier, and W. Kaiser, Opt. Commun. **44**, 293 (1983).
[387] P. B. Corkum, IEEE J. Quantum Electron. **QE-21**, 216 (1985).
[388] Y. Takagi, M. Sumitani, N. Nakashima, D. V. O'Connor, and K. Yoshihara, Appl. Phys. Lett. **42**, 489 (1983).
[389] Y. Tanaka, H. Kuroda, and S. Shionoya, Opt. Commun. **41**, 434 (1982).
[390] D. W. Anthon, H. Nathel, D. M. Guthals, and J. H. Clark, Rev. Sci. Instrum. **58**, 2054 (1987).
[391] F. Wondrazek, A. Seilmeier, and W. Kaiser, Appl. Phys. B **32**, 39 (1983).
[392] Y. X. Fan, R. C. Eckardt, and R. L. Byer, Appl. Phys. Lett. **45**, 313 (1984).
[393] T. Elsaesser, A. Seilmeier, and W. Kaiser, Appl. Phys. Lett. **44**, 383 (1984).
[394] M. Berg and C. B. Harris, Appl. Phys. Lett. **47**, 206 (1985).
[395] R. Alfano and S. L. Shapiro, Phys. Rev. Lett. **24**, 584 (1970).
[396] R. Alfano and S. L. Shapiro, Phys. Rev. Lett. **24**, 592 (1970).
[397] E. Yablonovich and N. Bloembergen, Phys. Rev. Lett. **29**, 907 (1972).
[398] R. L. Fork, C. V. Shank, C. Hirlimann, R. Yen, and W. J. Tomlinson, Opt. Lett. **8**, 1 (1983).
[399] A. Migus, J. L. Martin, R. Astier, A. Antonetti, and A. Orszag, in *Picosecond Phenomena III*, Ref. 10, p. 6.
[400] P. C. Becker, H. L. Fragnito, R. L. Fork, F. A. Beisser, and C. V. Shank, in *Ultrafast Phenomena VI*, Ref. 13, p. 12.
[401] T. M. Jedju and L. Rothberg, J. Appl. Opt. **27**, 615 (1988).
[402] M. N. Islam, G. Sucha, I. Bar-Joseph, M. Wegener, J. P. Gordon, and D. S. Chemla, Opt. Lett. **14**, 370 (1989).
[403] A. J. Campillo, R. C. Hyer, and S. L. Shapiro, Opt. Lett. **4**, 357 (1979).
[404] K. M. Pokhsraryan, Opt. Commun. **55**, 439 (1985).
[405] P.B. Corkum, P. P. Ho, R. R. Alfano, and J. T. Manassah, Opt. Lett. **10**, 624 (1985).
[406] R. Wyatt and D. Cotter, J. Appl. Phys. **21**, 199 (1980).
[407] P. G. May and W. Sibbett, Appl. Phys. Lett. **43**, 634 (1983).

REVIEW

Frontiers in Ultrashort Pulse Generation: Pushing the Limits in Linear and Nonlinear Optics

G. Steinmeyer,* D. H. Sutter, L. Gallmann, N. Matuschek, U. Keller

Optical pulses in the 5-femtosecond range are produced by a variety of methods. Although different in technical detail, each method relies on the same three key components: spectral broadening due to the nonlinear optical Kerr effect, dispersion control, and ultrabroadband amplification. The state of the art of ultrashort pulse generation is reviewed with a focus on direct laser oscillator schemes.

Our ability to perceive the dynamics of nature is ultimately limited by the temporal resolution of the instruments available to us. Mechanical shutters allow for resolution in the millisecond range, whereas stroboscopic illumination allows us to probe the microsecond range. Modern electronic sampling oscilloscopes eventually brought the limit down into the picosecond range. Ultrafast lasers have advanced the temporal resolution of measurements another three orders of magnitude into the sub–10-fs (1 fs = 10^{-15} s) regime, allowing for the direct observation of vibrational molecular dynamics (*1*). The broad spectral content can be used in medical diagnostics (*2*), and the extreme concentration of energy in femtosecond pulses is useful for material processing because much finer structures can be created in the absence of thermal interaction caused by longer pulses (*3*).

Figure 1 shows the historical development of ultrafast pulse generation. In the late 1980s, the pulse duration of dye lasers was as low as 27 fs (*4*), which was later compressed to 6 fs (*5*). At a wavelength of 600 nm, only three optical cycles fit under the full width at half maximum of the intensity envelope of such a pulse. It took almost a decade to surpass these results with solid-state lasers. Our goal is to review this recent progress with ultrafast solid-state lasers.

Measurement of ultrashort pulses is also a demanding task. Whereas traditionally, a short event has been characterized with the aid of an even shorter event, this is not an option for the characterization of the shortest event. Nonlinear autocorrelation techniques have been used in ultrafast optics because they use a short event to measure itself. In this type of measurement, two replicas of the pulse are generated, which are delayed with respect to each other. An instantaneous nonlinear optical effect, such as second-harmonic generation or two-photon absorption, is used to form the product of the two replicas, which depends on the temporal overlap of the replicas. Effectively, this allows converting measurement of a time into the measurement of a distance. Examples of autocorrelation measurements of some of the shortest pulses generated to date are shown (Fig. 2). Although completely different pulse generation techniques were employed in these examples, the autocorrelation traces are very similar, as indicated by the relative magnitude of the first- and second-side maximum of the traces shown.

Here, we describe methods that can be used to generate pulses as short as those displayed in Fig. 2, with a full width at half maximum of only about 5 fs (*6–10*). For a wavelength in the visible or near-infrared spectral range, as in the examples we discuss, this corresponds to about two optical cycles. We will show that pulse generation techniques demonstrated in the two-cycle regime rely essentially on three identical ingredients: the nonlinear optical Kerr effect acting as a spectral broadening process, precise control of dispersion, and an ultrabroadband amplifying process. Here, we review these key ingredients comprehensively and focus on the interaction between nonlinear pulse-shaping processes and linear phase correction. We emphasize how these effects can be used inside a laser to directly generate extremely short pulses.

The Kerr Effect, Dispersion, and Pulse Compression

At high intensities, the polarization inside a dielectric medium does not proportionally follow the electric field, and a nonlinear component at the frequency of the exciting wave is induced, giving rise to an instantaneous change of the refractive index n proportional to the time- and space-dependent intensity $I(t, \vec{x})$

$$n(t,\vec{x}) = n_0 + n_2 I(t,\vec{x}) \qquad (1)$$

This is called the optical Kerr effect (*11*), which is essential for all the concepts delivering pulses in the two-cycle regime. For typical solid-state materials, the nonlinear index n_2 is on the order of several 10^{-16} cm^2/W. The index change causes a temporal delay or phase shift for the most intense parts of a beam. Assuming Gaussian spatial and temporal profiles, the effects caused by this index change are shown (Fig. 3) longitudinal and transverse to the propagation direction. Retardation of the most intense part of a plane wavefront transversely acts like a focusing lens, whereas along the axis of propagation, the Kerr effect retards the center of an optical pulse. This longitudinal effect produces a red shift of the leading part of the pulse, and a blue shift in the trailing part and has also been named self-phase modulation (SPM). It is important to note that SPM generates extra bandwidth, that is, it spectrally broadens the pulse.

SPM alone does not modify the pulse envelope, but a much shorter pulse can be created with the extra bandwidth generated, as follows from the Fourier transform of the wider spectrum. To exploit the broadened bandwidth for the generation of a shorter pulse, the red and blue components in the temporal wings of the pulse have to be temporarily delayed and advanced, respectively. The spectral dependence of the speed of light needed to shorten the

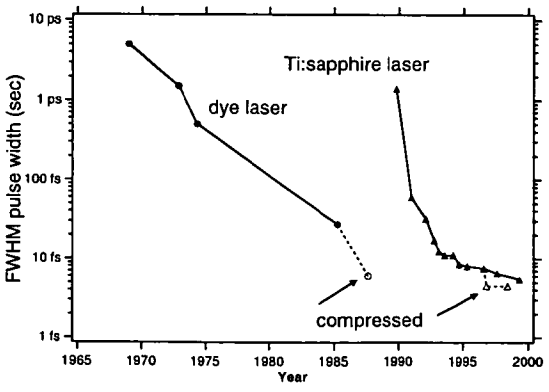

Fig. 1. Development of shortest reported pulse duration over the last three decades. Circles refer to dye-laser technology, triangles refer to Ti:sapphire laser systems. Filled symbols indicate results directly achieved from an oscillator, open symbols indicate results achieved with additional external pulse compression.

Institute of Quantum Electronics, Swiss Federal Institute of Technology, ETH Hönggerberg, HPT, CH-8093 Zürich, Switzerland.

*To whom correspondence should be addressed. E-mail: sguenter@iqe.phys.ethz.ch

spectrally broadened pulse is called dispersion, which is a linear optical effect independent of intensity. For a given optical element with length ℓ, dispersion manifests itself as a spectrally dependent propagation time. Spectral components at (angular) frequency ω are delayed by a group delay

$$T_g(\omega) = \frac{\ell}{c}\frac{\partial}{\partial\omega}(\omega n)$$

$$= \sum_{i=0}^{\infty} \frac{1}{i!}\frac{\partial^i T_g}{\partial\omega^i}\bigg|_{\omega_0} (\omega - \omega_0)^i \quad (2)$$

where c is the speed of light in vacuum, and ω_0 is a reference frequency for series expansion. The first coefficient ($i = 1$ in Eq. 2) in this dispersion series $\partial T_g(\omega_0)/\partial\omega$ is also called group delay dispersion (GDD), which is a function of reference frequency. A careful balance between frequency dependence given by dispersion and time dependence given by nonlinearity of the refractive index n is needed for efficient compression of a pulse. In most compression schemes, nonlinearity and dispersion are supplied in two successive steps, but optical fibers in the infrared provide these two effects simultaneously. This gives rise to solitons, optical pulses that are able to propagate for long distances in a nonlinear medium with either a constant or a periodically changing pulse shape (*11*, *12*).

Ultimately, compression schemes are limited by higher-order dispersion (terms with $i > 1$ in Eq. 2) and parasitic nonlinearities. For pulses shorter than 100 fs, compression is typically limited to factors of less than 10: Dye laser pulses with 50 fs duration have been compressed down to 6 fs (*5*). Similar concepts have been used for external pulse compression of 13-fs pulses from a Ti:sapphire laser (*9*) and of 20-fs pulses from a Ti:sapphire laser amplifier (*10*), resulting in both cases in approximately 4.5-fs pulses (Fig. 2). The use of a hollow fiber filled with a noble gas resulted in unsurpassed pulse energies of about 0.5 mJ with 5.2-fs pulses and a peak power of 0.1 TW (*13*).

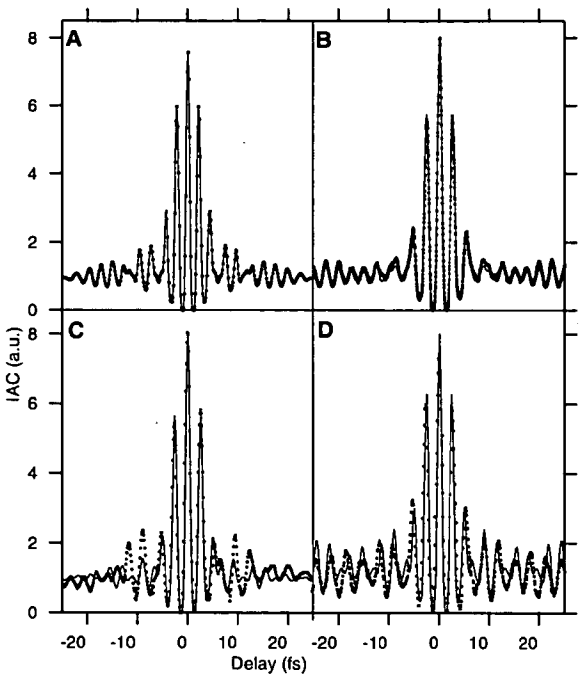

Fig. 2. Comparison of interferometric autocorrelation traces of different pulse sources in the 5-fs range. (**A**) Optical parametric amplification (*8*), (**B**) compression of cavity-dumped pulses in a silica fiber (*9*), (**C**) compression of microjoule pulses in a hollow fiber filled with krypton (*10*), and (**D**) pulses from a Ti:sapphire oscillator (*7*). Dots in (A) through (D) and lines in (A) refer to measured data, lines in (B) through (D) indicate the fit that was used to estimate pulse duration from the autocorrelation.

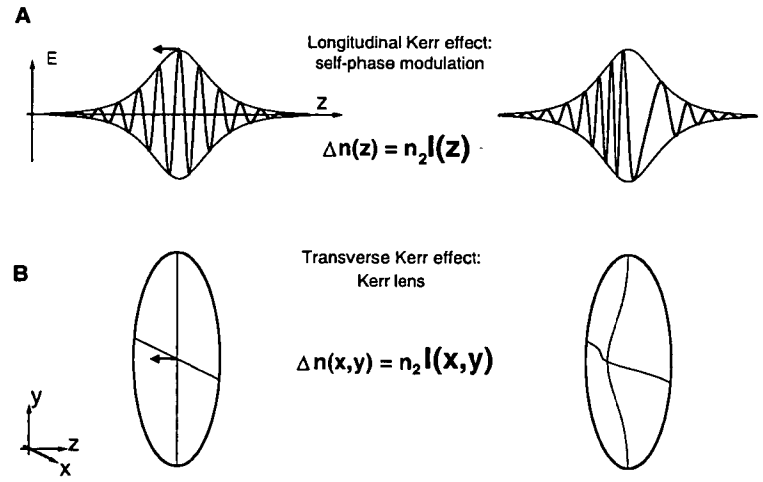

Fig. 3. The Kerr effect gives rise to an increase of the refractive index with intensity, causing a retardation of the most intense parts of a pulse. In its longitudinal form (**A**), the Kerr effect causes self-phase modulation; in its transverse form (**B**), a nonlinear lens is formed in the central part of the beam profile.

Saturable Absorbers and Passive Mode-Locking

A compression scheme can be directly integrated into a laser. In this section, we describe how to place a suitable nonlinear optical device in the feedback loop of the laser oscillator to directly support short-pulse operation (Fig. 4A). Traditionally, this type of operation of a laser has often been considered in the frequency domain (*14*). In this picture, the eigenfrequencies (or longitudinal modes) of the cavity have to be phase-locked to generate a short pulse. An amplitude modulator inside the cavity phase-locks these longitudinal modes when the modulation frequency is equal to the frequency spacing of the modes. This type of operation has been named mode-locking. In the time-domain picture, mode-locking means that the amplitude modulator opens and closes synchronously with the light propagating through the cavity. The modulator can either be driven by an external signal source (active mode-locking) or directly by the optical pulses inside the laser cavity (passive mode-locking). Here, we restrict ourselves to the latter method because it delivers the shortest pulses. The goal is to phase-lock as many longitudinal modes as possible because the broader the phase-locked spectrum the shorter the pulse that can be generated.

The passive amplitude modulator is a saturable absorber which has an increased transmission or reflection for high peak powers and produces a self-amplitude modulation (SAM). This SAM reduces the losses for short-pulse operation of a laser. An optical pulse traveling through a saturable absorber in a solid-state laser is shortened by the SAM, provided the response time of the absorber is sufficiently fast. In a mode-locked laser, pulse formation should start from normal noise fluctuations in the laser to initiate mode-locking. In the steady-state femtosec-

ond regime, dispersion and bandwidth limitation of the gain medium, mirrors, and so forth mainly cause temporal stretching of the pulse. Therefore, the pulse shortening effect must be dominant for pulse durations ranging from nanoseconds at start-up to femtoseconds at steady-state operation.

Traditionally, dyes have been used as saturable absorbers for passive mode-locking. Today in solid-state lasers, dyes have either been replaced by saturable absorbers obtained by Kerr or semiconductor nonlinearities. The precise control of optical nonlinearities, combined with the availability of a variety of bandgaps ranging from the visible to the infrared, makes semiconductor materials very attractive for use as saturable absorbers in solid-state lasers (*15*). Semiconductor materials typically provide an optical nonlinearity with two pronounced time constants. Intraband processes give rise to a very rapid relaxation in the 100-fs regime, while electron-hole recombination generates a slow response time in the picosecond regime. The slow response time can be reduced by several orders of magnitude with low-temperature epitaxy (*16*). Such semiconductors grown at low temperatures are markedly different from normally grown materials, exhibiting an increase in trap densities and decrease in carrier lifetimes of four orders of magnitude. The ability to artificially vary such parameters allowed a systematic study of pulse generation. Typically, a semiconductor saturable absorber is integrated directly into a mirror structure, resulting in a device whose reflectivity increases as the incident optical intensity increases. This general class of devices is called semiconductor saturable absorber mirrors (SESAMs) (*15*). With SESAMs, all important saturable absorber parameters, such as response time, saturation fluence, and modulation depth, can be adapted over several orders of magnitude. This allowed for the first demonstration of self-starting and stable passive mode-locking of diode-pumped solid-state lasers with intracavity saturable absorbers (*17*). The mirror structure can be manufactured using semiconductor materials (for example, AlAs/AlGaAs), standard dielectric coating materials, or a metal coating. So far, metal mirror–based SESAMs demonstrate the largest bandwidth but also limit the average output power (*18*). Schemes using broadband AlGaAs/CaF_2 Bragg mirrors are being considered as well (*19*).

The extremely rapid response and the broad bandwidth of the Kerr nonlinearity are very attractive for a mode-locking process. One way of using the phase nonlinearity of the Kerr effect for mode-locking is to convert SPM into an effective amplitude nonlinearity, that is, a SAM. The earliest mode-locking schemes based on SPM exclusively used a coupled cavity for this purpose. In the soliton laser (*20*), pulses compressed by the soliton effects in the coupled cavity are directly coupled back into the main laser cavity. This provides more gain for the center of the pulse. At 1.5 μm, pulses as short as four optical cycles or 19 fs have been demonstrated with color center lasers (*21*). Later, the SPM-to-SAM conversion with a coupled cavity was demonstrated for a case where no soliton effects were present (*22*). In this case, an uncompressed pulse was fed back into the main cavity. An effective SAM was obtained because SPM inside the coupled cavity generates a phase modulation on the pulse (Fig. 3) that adds constructively at the peak of the pulse in the main cavity and destructively in the temporal wings, thus shortening the pulse duration inside the main cavity. This is referred to as additive-pulse mode-locking (APM) (*23*). Although very powerful in principle, these coupled-cavity schemes have the severe disadvantage that the auxiliary cavity has to be stabilized interferometrically.

An alternative method for converting the reactive Kerr nonlinearity into an effective saturable absorber has been discovered in the Ti:sapphire laser: Kerr-lens mode-locking (KLM) (*24*). In KLM, the transverse Kerr effect produces a nonlinear lens (Fig. 3) that focuses the high-intensity part of the beam more strongly than the low-intensity part. Combined with an intracavity aperture, the Kerr lens produces less loss for high intensities and forms an effective fast saturable absorber (*25*). In this configuration, the Kerr lens is most efficiently used for pulse formation if the cavity is configured to support only pulsed operation and to prohibit continuous operation of the laser. A concise account of the SAM produced by the Kerr lens in different cavity regimes can be found in (*26*). The longitudinal Kerr effect also contributes to the pulse-shaping action inside the cavity, which is well known and has been used before in dye lasers. To a good approximation, the interplay of linear and nonlinear pulse-shaping effects has been explained theoretically using Haus' master equation (*27*). This aproximation works well for longer pulses. In the sub–10-fs regime however, pulse-shaping processes become very complex (*28*), and significant deviations from this simple theoretical picture are observed.

The Kerr effect is strong enough to sustain mode-locking but is typically unable to initiate it. To overcome this limitation, an ultrabroadband SESAM can be used to reliably start KLM (*7*). With the additional stabilization mechanism provided by the SESAM, resonator alignment constraints required for pure KLM are considerably relaxed. Therefore, use of the SESAM results in a cleaner spatial mode pattern (Fig. 5). This example shows how suitable nonlinear optical effects can be used in a combination of saturable absorbers that covers several orders of magnitude of pulse duration, decoupling start-up and steady-state pulse formation.

Continuum-Generation and Amplification-Based Schemes

Independent from the generation of ultrashort pulses directly from a laser oscillator, there are schemes that generate even shorter pulses by using pulse compression outside a cavity with either standard glass fibers (*9*) or noble-gas filled, hollow fibers (*10*), and by optical parametric amplification of white-light continuum pulses (*8*). These schemes rely on white-light continuum generation, which was first observed with orange amplified dye laser pulses (*29*). The resulting spectrally broadened pulses spanned over the entire visible range. Structurally, there is an important difference between the compression/amplification schemes (Fig. 4, B and C) and the direct generation in an oscillator (Fig. 4A). Whereas the direct approach of generating pulses inside the oscillator performs all steps inside the laser feedback loop, the other approaches put all processes into a linear sequence.

Continuum-based schemes start with pulses from a Ti:sapphire oscillator, which are typically amplified to >100 μJ pulse energy. To date, spectral filtering due to the limited bandwidth of the gain material has prohibited the direct generation of amplified pulses with less than 16 fs duration (*30*). To achieve a

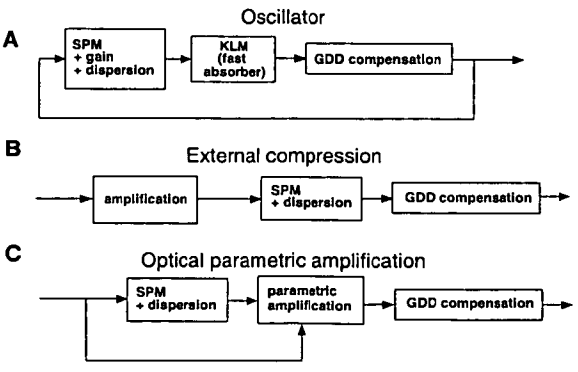

Fig. 4. Different combinations of amplification, the Kerr effect, and dispersion used for the generation of pulses in the two-cycle regime: (**A**) directly in an oscillator, (**B**) using external compression in hollow, gas-filled fibers or fused silica fibers, and (**C**) continuum generation in sapphire and subsequent parametric amplification.

bandwidth supporting two-cycle pulses, SPM is employed by focusing the amplified pulses into a nonlinear optical medium.

Noble gases such as Ar or He provide SPM with minimal dispersion. With no vibrational infrared resonance present, noble gases provide much flatter spectral dispersion than bulk materials if the same amount of SPM is desired. Additionally, they are not subject to the Raman effect, which poses another limit to the usefulness of nonlinear optical materials for SPM-based pulse compression. Because SPM is also much weaker in gases than in bulk media, higher intensities or longer interaction lengths are typically required, which is suitably provided in a strongly confined hollow-fiber geometry (*31*). Use of hollow fibers for pulse compression has produced pulses of about 4.5 fs duration. Nevertheless, similar pulse durations have been obtained in the 100-nJ pulse energy regime with standard optical fibers (*9*). The direct use with oscillators has not yet been demonstrated, and it remains to be seen how far nonlinear optical materials can be optimized and engineered for pulse compression purposes.

Frequency-conversion in nonlinear optical crystals can also be used for the generation of two-cycle pulses. Of particular interest are so-called parametric processes, which have been demonstrated with amplification bandwidths of up to 150 THz (*32*). In the parametric process, each pump photon is split into two photons, with the sum of the generated photon energies equal to the pump photon energy. If photons within the wavelength range of the parametric process are provided as a seed, they will be amplified in the nonlinear crystal. The seed pulse is derived from white-light continuum generation. Broadband parametric amplification produced pulses with a duration of <5 fs (*8*). Pumped by a frequency-doubled pulse from a Ti:sapphire amplifier system, optical parametric amplifiers (OPAs) generate sub–10-fs duration in the spectral range from 550 to 780 nm. An OPA system has been developed with microjoule pulses tunable from 1.1 to 2.6 μm and pulse durations as short as 14.5 fs (*33*).

Parametric conversion gives access to two-cycle pulses outside the spectral range of Ti:sapphire. Combination of several OPA processes seeded by the same continuum pulse allows the simultaneous generation of coherent radiation over the entire spectrum from 400 nm to 1.5 μm. This spectrum could potentially produce a single-cycle pulse (*34*), provided that dispersion compensation over such a broad range is accomplished. All continuum-based schemes require precise dispersion control, which in all cases demonstrated has been achieved using specially designed mirrors and prism sequences.

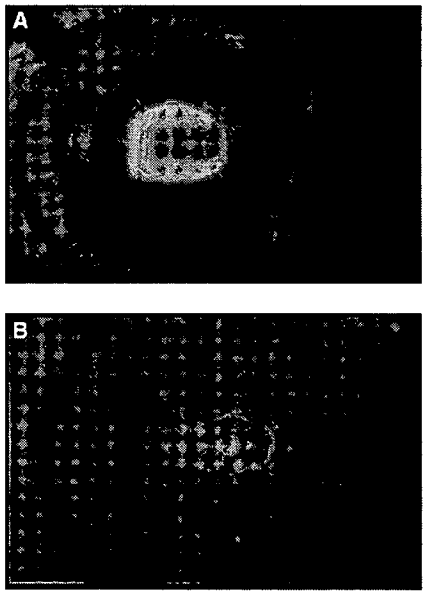

Fig. 5. Visible part of the spatial beam profiles behind one intracavity mirror of a two-cycle Ti:sapphire laser. (**A**) Cavity parameters are close to the stability limit, with pure KLM action. (**B**) Cavity is adjusted for a reduced KLM-effect with stronger stabilization action from the SESAM. Note the clearly visible yellow spectral content caused by SPM in the gain material, extending well beyond the Ti:sapphire gain bandwidth. Pictures were taken on 100ASA slide film (Kodak Elite).

Dispersion Compensation

Limited control of the intracavity dispersion is the main obstacle in the generation of extremely short pulses. For optimum pulse formation in a KLM laser, a small but constant intracavity dispersion is required over the full spectral content of the pulse (*27*). In a typical sub–10-fs Ti:sapphire laser, the uncompensated round-trip GDD caused by the laser crystal alone amounts to more than 100 fs delay between the long- and short-wavelength components covered by the gain material. To compensate for this group-delay dispersion (Eq. 2), a component with the opposite sign of dispersion has to be inserted into the cavity. Between these sections of opposite sign of GDD, the pulse width will be periodically stretched and recompressed from the sub–10-fs to the 100-fs range.

Different schemes for providing dispersion to compensate for material effects and self-phase modulation inside a laser cavity have been proposed. The prism compressor (*35*) is the most often employed scheme and introduces adjustable dispersion: However, generally it is only possible to compensate dispersion to the second order of Eq. 2 with a prism pair. For optimum performance of a laser, the prism material has to be carefully chosen and the total amount of material inside the cavity should be kept at a minimum. Pulse durations of about 8.5 fs have been demonstrated using only prism compensation (*36*). For shorter pulse operation, higher order dispersion has to be compensated for.

Specially designed mirrors can also be used for dispersion compensation. Standard dielectric mirrors are composed of identical quarter-wave layer pairs and provide high reflectance over a range of about 25% of the central wavelength, depending on the refractive index contrast of the layer materials employed. Outside this region, these simple mirror structures have considerable transmission. Special mirrors for dispersion compensation can be obtained by stacking quarter-wave layers optimized for different center wavelengths, such that long wavelengths are made to penetrate deeper into the mirror structure than short wavelengths as illustrated in Fig. 6A. Such mirrors are called chirped mirrors and the wavelength-dependent penetration depth provides the desired dispersion to compensate for material effects (*37*). In addition to dispersion compensation, chirped mirrors also give a much broader reflection bandwidth than standard mirrors.

A major problem in chirped mirror design arises due to multiple reflections between the chirped mirror structure and the top layer of the coating. The strong index discontinuity at this interface gives rise to unwanted interference, which results in oscillations of the group delay with wavelength. Double-chirped mirrors (DCMs) were developed to reduce such detrimental dispersion oscillations (*38*). Figure 6B shows the spectrally dependent penetration of the electromagnetic field into a broadband DCM coating. Reflectivity and dispersion characteristics of a DCM used in a Ti:sapphire oscillator are shown in Fig. 7, A and B, respectively. For comparison, the gain curve of Ti:sapphire is also shown in Fig. 7A.

The chirped mirror technology strongly reduces higher-order dispersion contributions inside the cavity and makes bandwidths up to 200 THz accessible for pulse generation. On a global wavelength scale, compensation is nearly perfect, yielding a small average value of the GDD. On a local scale, the mirrors introduce residual group delay oscillations with periods of several tens of nanometers (Fig. 7B). The magnitude of these residual dispersion oscillations increases with the bandwidth of the mirrors. For carefully optimized broadband DCMs, the peak-to-peak amplitude of these oscillations has been reduced to less than 1 fs per reflection, resulting in the small measured phase oscillation of the laser pulses shown in Fig. 7B. The combined action of SPM and dispersion provides a means of energy transfer within the pulse spectrum inside a mode-locked laser. Effectively, this concentrates energy at the minima of the group delay oscillations (*39*) as indicated by the strongly modulated spectra typical of sub–10-fs laser pulses; the pulse shape is strongly affected by the dispersion oscilla-

tions and significantly deviates from the simple picture predicted from the soliton-like pulse shaping (*7, 40*). Moreover, group delay oscillations can ultimately limit the intracavity bandwidth and the shortest achievable pulse width. Chirped mirrors with shifted dispersion characteristics can be combined to reduce the total intracavity group delay oscillations. Current research is directed to provide even broader bandwidth without detrimental dispersion oscillations.

Two different philosophies about the use of chirped mirrors have evolved. On the one hand, exclusive use of mirrors allows for very compact dispersion compensation schemes, which is of particular importance for oscillators (*41*). On the other hand, use of adjustable prisms in combination with chirped mirrors allows for continuous adjustment of dispersion. Using both prisms and chirped mirrors for dispersion compensation has the advantage that the chirped mirrors only have to compensate for higher-order dispersion ($i > 1$ in Eq. 2). This results in a broader bandwidth of the chirped coatings (*38*). So it is no surprise, that the shortest pulses to date have been generated with a combination of mirror and prism dispersion compensation. Combination of the chirped mirror and SESAM technology should allow for dispersion compensation in ultracompact lasers (*42*).

Measurement

Measurement of the extremely short pulses described above is as much of a challenge as the generation itself. There is one problem inherent to simple autocorrelation measurements discussed in the introduction and Fig. 2: It is generally impossible to determine the exact shape of the pulse being measured in an autocorrelation. Determination of the exact pulse width requires accurate knowledge of this shape, which is particularly difficult with the fairly complex two-cycle pulses and their strongly modulated spectra. Guessing a pulse shape for the deconvolution of the autocorrelation can give rise to inconsistent or inaccurate results. In the case of Ti:sapphire lasers, a poorly motivated choice of an autocorrelation pulse shape was shown to result in durations well below 5 fs (*6, 7*). In both cases, these pulse durations are in contradiction to independently measured spectra and their respective bandwidth limits. To detect such problems, the measurement method should also provide independent tests for the consistency of the data.

With the complex pulse shapes in the sub–10-fs regime, techniques that allow retrieving the pulse phase and amplitude are mandatory for a proper characterization of any of the sources described here. One well-established method relies on additional information from spectrally resolving the autocorrelation and is called frequency-resolved optical gating (FROG) (*43*). Another method uses the autocorrelation data together with the fundamental spectrum (*9, 44*) to provide a simultaneous fit to both measurements. Whereas the characterization techniques discussed so far require the use of an iterative fitting algorithm to retrieve the phase, SPIDER (spectral phase interferometry for direct electric-field reconstruction) allows for fast, noniterative reconstruction of the pulse from the measurement of two spectra (*45*). Phase-sensitive techniques have been used extensively to characterize femtosecond laser sources and, apart from being more accurate, give more insight into the complex pulse dynamics of sub–10-fs pulses.

Baltuska *et al.* designed their dispersion compensation after having done FROG measurements on the uncompressed continuum (*9*). The duration of the resulting pulse was measured as 4.5 fs. For oscillators, pulses with duration as short as 5.9 fs have been characterized in amplitude and phase (*7, 46*). In these measurements, the residual uncompensated dispersion mainly due to the output-coupling mirror of the laser is clearly visible (Fig. 7B). The small oscillation in the central part of the spectrum stems from dispersion oscillations of the double-chirped mirrors. The advances in measurement tools have clearly contributed to the success of generating shorter and shorter pulses.

Conclusion and Outlook

Comparison of the different techniques that currently allow for pulses in the two-cycle regime identifies three essential mechanisms: an ultrafast spectral broadening mechanism, an ultrabroadband amplification process, and a dispersion compensation scheme. Self-phase modulation is the driving force to yield a short pulse, while the other two mechanisms compensate for power losses and tem-

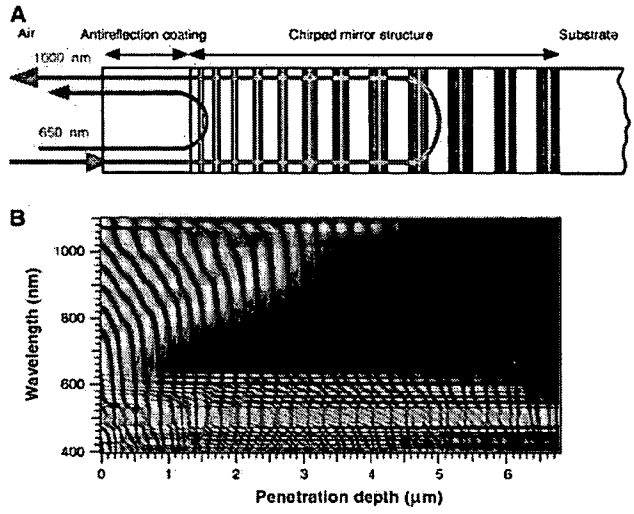

Fig. 6. Double-chirped mirror. (**A**) Structure of a typical DCM, schematically showing the path of a long-wavelength beam. (**B**) Standing-wave electric field patterns in a DCM structure versus wavelength. The dispersion of the mirrors is clearly illustrated by the dependence of penetration depth on wavelength for the range of 650 to 1050 nm. The highly transmissive region around 500 nm is used for pumping the laser.

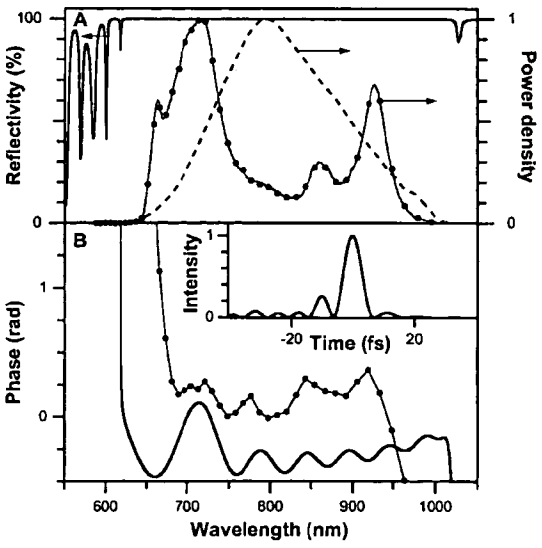

Fig. 7. (**A**) Reflectivity of a typical DCM (solid line) compared to the gain spectrum of Ti:sapphire (dashed) and the measured spectrum of a two-cycle pulse (filled circles). (**B**) Calculated phase accumulated after six reflections off a DCM and a single pass through a prism pair, as used in the external dispersion compensation (solid line) and phase of a two-cycle pulse, measured with the SPIDER technique (filled circles). The inset in (B) shows temporal intensity profile of the pulse, determined by a Fourier transform of the measured data in (A) and (B). The pulse duration is 5.9 fs.

poral pulse broadening.

The continuous improvement of femtosecond pulse sources has resulted in pulse durations of about two optical cycles, which is also close to the limit given by the bandwidth of the involved amplification and dispersion compensation processes. Compression schemes with adaptive pulse shaping (*47*) have the best prospects for further improvement in terms of pulse duration.

With the extremely short pulse durations available today, the slowly varying envelope approximation, used extensively to model nonlinear optics, is expected to break down. This approximation describes an optical pulse as a slow modulation on a high-frequency carrier wave and reduces modeling to the description of the modulation or the envelope. Experimentally, this breakdown should manifest itself in a dependence of the efficiency of nonlinear optical processes on the relative phase between the envelope and the underlying electric field of the pulse. In other words, it does matter whether the peak electric field is centered at the maximum of the intensity envelope (*48*). Recently, methods for the stabilization of the electric field structure underneath the pulse envelope with subfemtosecond accuracy were proposed (*49*).

This stabilization opens a totally new field of applications of sub–10-fs pulses. It simplifies precision optical frequency measurements that have been used for extremely accurate measurements of fundamental physical constants and could result in more precise atomic clocks (*50*). Also, there is a strong interest in phase stabilization techniques for high-harmonic generation. In this method of laser-induced coherent x-ray generation, atoms are exposed to the alternating electric field of an amplified laser source with a magnitude comparable to inner-atomic binding forces. This gives rise to the generation of a burst of x-ray pulses, potentially with attosecond (1 as = 10^{-18} s) time duration (*51*). Apart from the possible dynamic resolution, high-harmonic x-ray radiation in the 2.3 to 4.4 nm range would allow for in vivo microscopy with a good contrast between organic compounds and water (*52*). In addition, a spatial resolution of a few nanometers is possible, comparable to electron microscopy. The vision of new applications and attosecond science surely motivates today's ongoing quest for shorter laser pulses.

References and Notes

1. G. Cerullo, G. Lanzani, M. Muccini, C. Taliani, S. De Silvestri, *Phys. Rev. Lett.* **83**, 231 (1999).
2. G. J. Tearney *et al.*, *Science* **276**, 2037 (1997).
3. B. N. Chichkov, C. Momma, S. Nolte, F. v. Alvensleben, A. Tünnermann, *Appl. Phys. A* **63**, 109 (1996); J. Kruger *et al.*, *Appl. Surf. Sci.* **129**, 892 (1998).
4. J. A. Valdmanis and R. L. Fork, *IEEE J. Quantum Electron.* **22**, 112 (1986).
5. R. L. Fork, C. H. B. Cruz, P. C. Becker, C. V. Shank, *Opt. Lett.* **12**, 483 (1987).
6. U. Morgner *et al.*, *Opt. Lett.* **24**, 411 (1999); U. Morgner *et al.*, *Opt. Lett.* **24**, 920 (1999).
7. D. H. Sutter *et al.*, *Opt. Lett.* **24**, 631 (1999).
8. A. Shirakawa, I. Sakane, M. Takasaka, T. Kobayashi, *Appl. Phys. Lett.* **74**, 2268 (1999).
9. A. Baltuska, Z. Wei, M. S. Pshenichnikov, D. A. Wiersma, R. Szipöcs, *Appl. Phys. B* **65**, 175 (1997).
10. M. Nisoli *et al.*, *Appl. Phys. B* **65**, 189 (1997).
11. G. P. Agrawal, *Nonlinear Fiber Optics* (Academic Press, San Diego, CA, 1989).
12. G. I. Stegeman and M. Segev, *Science* **286**, 1518 (1999).
13. S. Sartania *et al.*, *Opt. Lett.* **22**, 1562 (1997).
14. A. E. Siegman, *Lasers* (University Science Books, Mill Valley, CA, 1986).
15. U. Keller *et al.*, *IEEE J. Sel. Top. Quantum Electron.* **2**, 435 (1996); U. Keller, in *Nonlinear Optics in Semiconductors*, E. Garmire and A. Kost, Eds. (Academic Press, Boston, 1999), vol. 59, pp. 211–286.
16. S. Gupta, J. F. Whitaker, G. A. Mourou, *IEEE J. Quantum Electron.* **28**, 2464 (1992).
17. U. Keller *et al.*, *Opt. Lett.* **17**, 505 (1992); K. J. Weingarten, U. Keller, T. H. Chiu, J. F. Ferguson, *Opt. Lett.* **18**, 640 (1993).
18. I. D. Jung *et al.*, *Appl. Phys. B* **65**, 137 (1997).
19. S. Schön, H. Zogg, U. Keller, *J. Crystal Growth* **201/202**, 1020 (1999).
20. L. F. Mollenauer and R. H. Stolen, *Opt. Lett.* **9**, 13 (1984).
21. F. M. Mitschke and L. F. Mollenauer, *Opt. Lett.* **12**, 407 (1987).
22. P. N. Kean *et al.*, *Opt. Lett.* **14**, 39 (1989).
23. E. P. Ippen, H. A. Haus, L. Y. Liu, *J. Opt. Soc. Am. B* **6**, 1736 (1989).
24. D. E. Spence, P. N. Kean, W. Sibbett, *Opt. Lett.* **16**, 42 (1991).
25. F. Salin, J. Squier, M. Piché, *Opt. Lett.* **16**, 1674 (1991); D. K. Negus, L. Spinelli, N. Goldblatt, G. Feugnet, in *Advanced Solid-State Lasers*, G. Dubé and L. Chase, Eds. (Optical Society of America, Washington, DC, 1991), vol. 10, pp. 120–124; U. Keller, G. W. 't Hooft, W. H. Knox, J. E. Cunningham, *Opt. Lett.* **16**, 1022 (1991).
26. V. Magni, G. Cerullo, S. De Silvestri, A. Monguzzi, *J. Opt. Soc. Am. B* **12**, 476 (1995).
27. H. A. Haus, J. G. Fujimoto, E. P. Ippen, *IEEE J. Quantum Electron.* **28**, 2086 (1992).
28. F. Krausz *et al.*, *IEEE J. Quantum Electron.* **28**, 2097 (1992).
29. R. L. Fork, C. V. Shank, C. Hirlimann, R. Yen, W. J. Tomlinson, *Opt. Lett.* **8**, 1 (1983).
30. K. Yamakawa *et al.*, *Opt. Lett.* **23**, 525 (1998); S. Backus, C. G. Durfee III, M. M. Murnane, H. C. Kapteyn, *Rev. Sci. Instrum.* **69**, 1207 (1998).
31. M. Nisoli *et al.*, *Opt. Lett.* **22**, 522 (1997).
32. G. M. Gale, M. Cavallari, T. J. Driscoll, F. Hache, *Opt. Lett.* **20**, 1562 (1995).
33. M. Nisoli, S. Stagira, S. De Silvestri, O. Svelto, *Opt. Lett.* **23**, 630 (1998).
34. O. Albert and G. Mourou, *Appl. Phys. B* **69**, 207 (1999).
35. R. L. Fork, O. E. Martinez, J. P. Gordon, *Opt. Lett.* **9**, 150 (1984); R. E. Sherriff, *J. Opt. Soc. Am. B* **15**, 1224 (1998).
36. J. Zhou *et al.*, *Opt. Lett.* **19**, 1149 (1994).
37. R. Szipöcs, K. Ferencz, C. Spielmann, F. Krausz, *Opt. Lett.* **19**, 201 (1994).
38. F. X. Kärtner *et al.*, *Opt. Lett.* **22**, 831 (1997); N. Matuschek, F. X. Kärtner, U. Keller, *IEEE J. Quantum Electron.* **35**, 129 (1999).
39. A. Rundquist *et al.*, *Appl. Phys. B* **65**, 161 (1997).
40. D. H. Sutter *et al.*, *IEEE J. Sel. Top. Quantum Electron.* **4**, 169 (1998).
41. L. Xu, G. Tempea, C. Spielmann, F. Krausz, *Opt. Lett.* **23**, 789 (1998).
42. R. Paschotta *et al.*, *Appl. Phys. Lett.* **75**, 2166 (1999).
43. R. Trebino and D. J. Kane, *J. Opt. Soc. Am. A* **10**, 1101 (1993).
44. J. Peatross and A. Rundquist, *J. Opt. Soc. Am. B* **15**, 216 (1998).
45. C. Iaconis and I. A. Walmsley, *IEEE J. Quantum Electron.* **35**, 501 (1999).
46. L. Gallmann *et al.*, *Opt. Lett.* **24**, 1314 (1999).
47. D. Yelin, D. Meshulach, Y. Silberberg, *Opt. Lett.* **22**, 1793 (1997).
48. I. P. Christov, *Opt. Lett.* **24**, 1425 (1999).
49. L. Xu *et al.*, *Opt. Lett.* **21**, 2008 (1996); H. R. Telle *et al.*, *Appl. Phys. B* **69**, 327 (1999).
50. T. Udem *et al.*, *Phys. Rev. Lett.* **79**, 2646 (1997); T. Udem, J. Reichert, R. Holzwarth, T. W. Hänsch, *Phys. Rev. Lett.* **82**, 3568 (1999).
51. G. Farkas and C. Toth, *Phys. Lett. A* **168**, 447 (1992).
52. P. Gibbon, *Phys. Rev. Lett.* **76**, 50 (1996).

53. We thank T. Kobayashi (University of Tokyo), A. Baltuska (University of Groningen), and M. Nisoli (Politecnico Milano) for providing the data in Fig. 2, A, B, and C, respectively. We gratefully acknowledge financial support by the Swiss National Science Foundation.

Self–Mode-Locking of Quantum Cascade Lasers with Giant Ultrafast Optical Nonlinearities

Roberto Paiella,[1]* Federico Capasso,[1] Claire Gmachl,[1] Deborah L. Sivco,[1] James N. Baillargeon,[1] Albert L. Hutchinson,[1] Alfred Y. Cho,[1] H. C. Liu[2]

We report on the generation of picosecond self–mode-locked pulses from midinfrared quantum cascade lasers, at wavelengths within the important molecular fingerprint region. These devices are based on intersubband electron transitions in semiconductor nanostructures, which are characterized by some of the largest optical nonlinearities observed in nature and by picosecond relaxation lifetimes. Our results are interpreted with a model in which one of these nonlinearities, the intensity-dependent refractive index of the lasing transition, creates a nonlinear waveguide where the optical losses decrease with increasing intensity. This favors the generation of ultrashort pulses, because of their larger instantaneous intensity relative to continuous-wave emission.

Ever since the invention of the laser in 1960, an extensive research effort has focused on the development of ultrafast laser sources. Optical pulses with duration in the picosecond and femtosecond range have been generated in several gas and solid-state laser media, particularly at wavelengths ranging from the ultraviolet to the near infrared (*1–3*). The most common technique for ultrashort pulse generation is mode-locking, in which the longitudinal modes of the laser cavity are locked in phase, by some external or internal mechanism, to produce a train of pulses with repetition rate equal to the cavity roundtrip frequency. These sources have allowed for a marked improvement in the temporal resolution of a myriad of measurements in physics, chemistry, and biology. Commercial applications are also emerging in several fields (*2*), including medical diagnostics, material processing, and optical communications. On the other hand, the technologically important midinfrared spectrum (3 to 15 μm) still lacks compact and convenient laser sources of ultrashort pulses (*4*). This spectral region is known as the molecular fingerprint region, because many chemical and biological species have their telltale absorption features associated with molecular vibrations in this wavelength range. As a result, several applications exist for ultrafast midinfrared lasers, ranging from time-resolved spectroscopy to coherent control (*2*).

We report on the generation of picosecond self–mode-locked pulses of midinfrared radiation in quantum cascade (QC) lasers (*5*, *6*). These devices are based on intersubband electron transitions, i.e., transitions between quantized conduction-band states in semiconductor quantum wells. These transitions are characterized by some of the largest optical nonlinearities ever observed (*7–10*). Furthermore, intersubband carrier relaxation is controlled by an extremely fast (picosecond) mechanism, namely scattering by optical phonons. We emphasize that although large resonant nonlinearities are found in several other laser systems, their response is always much slower. Because of this unique combination of giant magnitude and ultrafast dynamics, intersubband optical nonlinearities have attracted considerable attention, and several applications to high-speed optoelectronic devices have been proposed (*7–11*). Here, we interpret our results in terms of self–mode-locking (SML) from one of these nonlinearities, the intensity-dependent refractive index [often referred to as the optical Kerr effect (*12*)] of the intersubband laser transition. Specifically, this nonlinearity consists of a refractive index n that varies with optical intensity I according to the approximate expression $n = n_0 + n_2 I$, where n_2 is the nonlinear refractive index.

Several QC lasers were used in this work, emitting at either 5- or 8-μm wavelength and similar to the devices described in (*13*) and (*14*), except for their unusually long waveguides (≳3.5 mm). The laser material was grown by molecular beam epitaxy in the InGaAs/AlInAs material system lattice matched to InP substrates. The individual devices were mounted inside a helium flow cryostat (*15*) and biased with a dc current. Over a wide range of dc bias, these lasers were found to emit an extremely broad (up to 1.5 THz, about 50% of the gain bandwidth) multimode spectrum, characterized by a smooth multipeaked envelope. A series of these spectra, measured with a Nicolet Fourier transform infrared spectrometer (FTIR), is shown (Fig. 1), for a 3.5-mm-long 8-μm QC laser at 80 K. At the same time, these devices were found to self-pulsate at their cavity roundtrip frequency. This was ascertained by detecting their output with a fast quantum-well infrared photodetector (QWIP) (*16*, *17*) and displaying the resulting photocurrent in a spectrum analyzer. A sharp feature centered at the laser roundtrip frequency (≃13 GHz in the device of Fig. 1) was observed, whose peak power corresponds to a modulation amplitude of the laser beam of the order (at least 20%) of the measured average optical power. This feature results from the mutual beating of adjacent modes in the optical spectrum. Its large magnitude, strong stability, and narrow width (typically less than 100 kHz) indicate negligible random drift of the modes' relative phases, as expected in a mode-locked laser. An example is shown in the inset of Fig. 1.

As a result of this phase locking, the amplitudes of the lasing modes add coherently to produce a periodic time-varying optical waveform. Information about the temporal characteristics of such mode-locked wave-

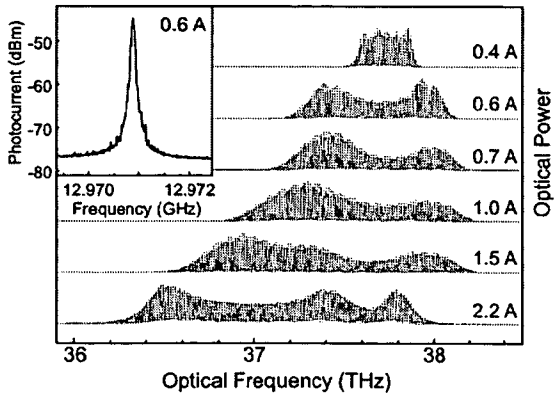

Fig. 1. Optical spectra of a 3.5-mm-long, 8-μm wavelength QC laser (from wafer D2396F) at a temperature of 80 K, under conditions of self–mode-locking, for different values of the laser dc bias current. (Inset) Microwave spectrum of the photocurrent generated by the same laser (at a bias of 0.6 A) in a high-speed quantum-well infrared photodetector (measured with a 1-kHz resolution bandwidth). As explained in the text, this peak indicates a large-signal modulation of the laser beam. A similar peak was also observed in the microwave spectrum of the QC laser current, measured through a high-speed bias "tee."

[1]Bell Laboratories, Lucent Technologies, 600 Mountain Avenue, Murray Hill, NJ 07974, USA. [2]Institute for Microstructural Sciences, National Research Council, Ottawa, Ontario, K1A 0R6, Canada.

*To whom correspondence should be addressed. E-mail: robertop@lucent.com

forms is traditionally obtained with second-order autocorrelation measurements. At present, however, these are not well developed in the midinfrared, especially at the relatively low power levels of these lasers. In any case, an indicative test of pulsed emission is provided by the linear autocorrelation traces generated by the FTIR. An example is shown for both an 8-μm (Fig. 2A) and a 5-μm (Fig. 2B) device. An FTIR is a Michelson interferometer (*18*) (Fig. 2C), and these autocorrelation traces consist of the interference fringes from the beams in the two interferometer arms. In the presence of ultrashort pulses, such fringes can only occur when pulses from the two arms temporally overlap on the detector. The result is an autocorrelation trace consisting of narrow spikes at delay times equal to multiples of the pulse separation time (*19*), which is exactly what is observed (Fig. 2). In particular, the negligible amplitude of the fringes between the spikes suggests that these lasers are indeed emitting a train of ultrashort pulses (*20*) with good modulation depth.

The multipeaked envelopes observed in the optical spectra of Fig. 1 are also consistent with pulsed emission and cannot otherwise be explained in terms of unlocked multimode emission, given the primarily homogeneously broadened narrow gain curves of these QC lasers (*14*). In particular, these structures are typical of short laser pulses undergoing strong self-phase modulation (*21*). Namely, in the presence of an intensity-dependent refractive index, the optical field develops a time-varying phase proportional to the pulse intensity profile (*12*). Correspondingly, the optical spectrum develops an oscillatory envelope and broadens to (*21*)

$$\Delta\omega_{rms} = \frac{\sqrt{2\log 2}}{\tau_p}\sqrt{1+\frac{4}{3\sqrt{3}}\phi_{max}^2} \qquad (1)$$

where $\Delta\omega_{rms}$ is the root-mean-square (rms) spectral width, τ_p is the pulse full-width-at-half-maximum (FWHM), and a Gaussian pulse shape is assumed. Finally, ϕ_{max} is the maximum nonlinear phase shift, given by

$$\phi_{max} = \frac{4\pi L}{\lambda}\Gamma n_2 I_{max} \qquad (2)$$

where L is the laser length, λ is the wavelength, Γ is the confinement factor (the fractional mode overlap with the QC active layers), n_2 is the nonlinear index, and I_{max} is the pulse peak intensity. Theoretical studies (*21*) also indicate that a first dip appears in the optical spectrum when ϕ_{max} reaches the value $3/2\pi$, and further dips are predicted to occur at higher values of ϕ_{max}.

These considerations can be used to estimate the width of these pulses (*21*, *22*). Referring to the spectra in Fig. 1, a pronounced dip is observed starting approximately at the bias of 0.6 A. We can then use Eq. 1 with $\phi_{max} = 3/2\pi$ and with $\Delta\omega_{rms}$ equal to the measured rms width of the spectrum at 0.6 A (250 GHz) to obtain an estimate for the pulse duration under these conditions: The result is $\tau_p = 3.2$ ps. We emphasize that this is an approximate result, primarily because it does not account for group-velocity dispersion. Finally, a pyroelectric detector was used to measure the emitted average power. The peak power of the pulses can then be estimated, given knowledge of their width and repetition rate: Values ranging from several hundreds of milliwatts to well over a watt were obtained.

Next we discuss our model and examine its supporting evidence. The proposed SML mechanism is illustrated in Fig. 3, together with a schematic cross section of the QC waveguide structure (Fig. 3A). If the nonlinear index n_2 of the laser active material is positive, the center part of the beam transverse profile, where the intensity is higher, experiences a larger refractive index relative to the edges. The resulting nonlinear dielectric waveguide increases the beam confinement near its center and hence narrows the beam diameter to an extent proportional to the optical power (*12*). This effect, which is essentially the spatial analog of self-phase modulation, is known as self-focusing or Kerr-lensing and is illustrated schematically in Fig. 3B, which refers to the waveguide lateral direction (the x direction in Fig. 3A). As shown, a smaller beam diameter in turn leads to a decreased mode interaction with the external gold contacts. In particular, it reduces the beam coupling to the high-loss surface plasmon mode at the metal-dielectric interface (*23*), which is a major source of waveguide losses in QC lasers (*6*). The net result is a decrease in the optical losses with increasing intensity, a so-called saturable loss mechanism, which is the fundamental ingredient for SML (*24*). In the presence of such a mechanism, it becomes favorable for the laser to emit ultrashort pulses because of their higher instantaneous intensity, and hence lower losses, relative to continuous-wave

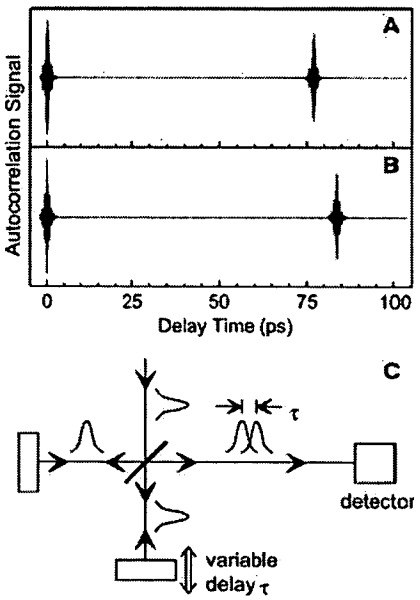

Fig. 2. Linear autocorrelation traces of two QC lasers under conditions of self–mode-locking: (**A**) a 3.5-mm-long, 8-μm wavelength device (same as in Fig. 1) at 80 K, at a bias of 1 A, and (**B**) a 3.75-mm-long, 5-μm wavelength device (from wafer D2564A) at 25 K, also at a bias of 1 A. The horizontal axis gives the delay time between the two arms of the interferometer. The time interval between consecutive spikes is the roundtrip time in the laser cavity. The side lobes observed in these spikes are due to the frequency chirp induced by self-phase modulation. (**C**) Illustration of the FTIR used to measure these traces. The constant background detected when the pulses do not overlap is automatically subtracted off the data by the FTIR.

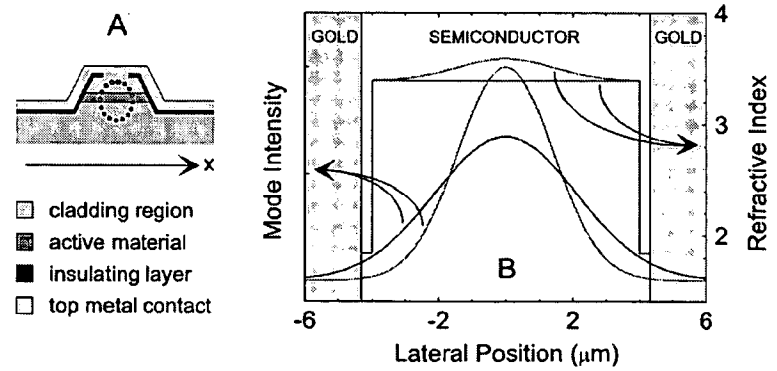

Fig. 3. (**A**) Schematic cross section of the laser waveguide structure used in this work. Typical dimensions in the lateral direction (along the x axis) range from 10 to 12 μm. (**B**) Refractive index profile and resulting intensity distribution of the fundamental waveguide mode along the lateral direction. Self-focusing of light occurs with increasing intensity (as in going from the black to the red curves). The same does not appreciably occur in the transverse direction (perpendicular to the active layer) because there the mode is primarily confined by the index profile of the cladding regions, consisting of several InGaAs/AlInAs(InP) epitaxial layers (*13*, *14*), where no strong nonlinearity exists.

(cw) emission, where the output energy is spread uniformly in time.

This mechanism differs in a fundamental way from previous demonstrations of SML (*1*). In the latter, the SML nonlinearity is provided by an external medium added inside the cavity or by some nonresonant transition in the laser host medium. In principle, a large "intrinsic" nonlinear refractive index is always present in any laser medium, provided by the lasing transition itself, and related to the gain coefficient through a Kramers-Kronig transformation (*24*). This is a resonant nonlinearity, involving a real population transfer across the lasing transition, so that its dynamic response is limited by the lifetime of the upper laser state. We argue that in QC lasers, because of its ultrafast lifetime and large magnitude, this intrinsic nonlinearity itself can give rise to SML. Also, we emphasize that SML by Kerr-lensing has never been previously observed in semiconductor lasers, although a similar mechanism is used with some solid-state lasers such as Ti:sapphire lasers (*3*, *25*).

All the experimental findings presented here are consistent with this picture of Kerr-lens SML. First of all, the observation of self-phase modulation confirms the existence of a large index nonlinearity, which is the fundamental ingredient of self-focusing. Furthermore, SML was only obtained in relatively long ($\gtrsim$3.5 mm) devices with thin (0.3 μm) dielectric blocking layers between the semiconductor material and the gold contact pads. In such devices, the saturable loss contribution resulting from self-focusing accounts for a substantial fraction of the overall losses. In particular, the thin dielectric layers allow for sufficient mode coupling to the metal, and the long waveguides ensure that such propagation losses dominate over the inevitable mirror losses [which are inversely proportional to the laser length (*24*)]. We also processed a few devices using a much thicker (4 μm) dielectric layer, and we tested a few of these devices with long waveguides, which exhibited stable cw single-mode behavior. Finally, there is no evidence of any alternative SML mechanism, such as resulting from any saturable absorber or optical feedback.

For additional evidence of SML by Kerr-lensing, we measured the far-field beam profile under cw and SML operation. In this experiment, we used an 8-μm QC laser in which SML was found to be non–self-starting. This device exhibits single-mode cw emission when dc biased; mode-locking can be achieved by modulating the current at its roundtrip frequency, as in active mode-locking (*24*). However, the laser then remains in the mode-locked state even after the modulation is switched off. This laser is ideally suited to this measurement, because it allows us to compare cw and SML cases at the same bias, temperature, and so forth. Typical results are shown in Fig. 4, where we plot collected power versus emission angle in the lateral direction. The far-field beam profile under SML conditions is broader than in cw, by more than 10%, corresponding to a narrower beam inside the waveguide. Therefore, at the higher instantaneous power levels inherent to pulsed emission, the beam does undergo self-focusing. The narrowing in beam diameter between cw and SML operation was found to increase with dc bias and hence optical intensity, also consistent with Kerr-lensing.

To estimate the corresponding loss saturation, we used an effective-index approximation (*26*) to calculate the decrease in laser losses associated with this beam narrowing. The lateral waveguide was modeled as an effective active medium (represented by the complex effective index calculated in the transverse direction) surrounded, on each side, by the dielectric blocking layer and by an effective "plasmon" medium (represented by the complex index of the plasmon mode at the gold-semiconductor interface). We used the QC waveguide parameters of (*14*), with a stripe width of 11 μm. For the nonlinear refractive index change during pulsed operation, $\Delta n = \Gamma n_2 I_{max}$, we used the value required to reproduce in this calculation the experimental beam narrowing of 10%; this is $\Delta n = 0.018$, in fair agreement with a calculation of n_2 described below. Using this value of Δn, we found a substantial decrease in the overall losses, of about 25%, qualitatively large enough to justify SML operation.

Finally, we calculated the nonlinear index of the lasing intersubband transition using the following expression (*12*), based on a two-level approximation

$$n_2 = \frac{q^2 z_{32}^2 \Delta N}{8 n_0 \varepsilon_0 h} \frac{(\Delta\nu)^2(\nu_0 - \nu)}{[(\Delta\nu/2)^2 + (\nu_0 - \nu)^2]^2} \frac{1}{I_0^{sat}}, \quad (3)$$

where z_{32} is the dipole moment of the lasing transition, ΔN is the population inversion per unit volume, n_0 is the linear refractive index, ν_0 and $\Delta\nu$ are the center frequency and the FWHM of the gain curve, I_0^{sat} is the saturation intensity at $\nu = \nu_0$, and q, ε_0, and h are the unit charge, the vacuum permittivity, and Planck's constant, respectively. Typical QC-laser parameter values (*27*) were used. Notice from Eq. 2 that n_2 is zero at the gain center frequency ν_0, which is a general property of the Kramers-Kronig transform of a symmetrical function. However, at optical frequencies detuned from ν_0 by ~100 GHz, it is already as large as $\sim 10^{-9}$ cm^2/W. For comparison, this is seven orders of magnitude larger than the nonlinear index responsible for Kerr-lens SML in Ti:sapphire lasers (*3*), and it is large enough to justify the experimental findings. In fact, using Eq. 2 with $n_2 \sim 10^{-9}$ cm^2/W and I_{max} estimated from typical measured average powers (~ 10 mW) gives a nonlinear phase shift ϕ_{max} on the order of a few multiples of π, consistent with the observed spectral shapes of Fig. 1. Furthermore, this calculation gives a nonlinear index change $\Delta n = \Gamma n_2 I_{max}$ of about 0.006 for the case of Fig. 4, with I_{max} estimated from the measured average power in that case (25 mW). Considering the uncertainties in the relevant physical parameters of Eq. 3, such as the homogeneous linewidth $\Delta\nu$ of the intersubband transition, and in the effective-index approximation, this is in fair agreement with the value (0.018) previously inferred from the far-field measurements of Fig. 4.

These considerations then indicate that the SML can indeed be initiated by the nonlinear index of the lasing transition itself. Finally, notice that self-focusing requires a positive value of n_2, whereas the nonlinear index of Eq. 2 is positive for $\nu < \nu_0$, but negative for $\nu > \nu_0$. The optical bandwidths observed under conditions of SML extend over several hundreds of GHz around ν_0, so that they sample both signs of n_2. However, the experimental observation of self-focusing indicates that the centers of mass of the SML spectra must lie at frequencies lower than ν_0; this was also consistently observed in our spectral

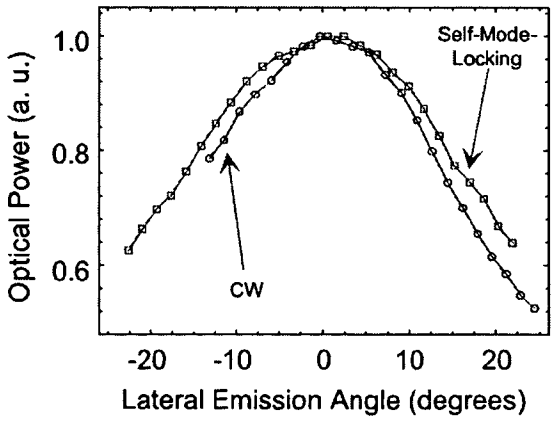

Fig. 4. Far-field beam profiles under cw and SML operation versus emission angle in the lateral direction (the *x* direction in Fig. 3A), measured from a 3.75-mm-long, 8-μm wavelength laser (from wafer D2396E) at 10 K, at a bias of 0.72 A. The two traces are superimposed to one another for ease of comparison. A relative shift of about 10° was observed between these traces.

measurements. We argue that SML is initiated by modes at these frequencies through the Kerr-lens mechanism described above; once they are locked in phase, their mutual beating produces a large enough modulation of the laser gain to bring several other modes above threshold.

References and Notes

1. W. Kaiser, Ed., *Ultrashort Laser Pulses: Generation and Applications*, vol. 60 of *Topics in Applied Physics Series* (Springer-Verlag, Berlin, 1993).
2. T. Elsaesser, J. G. Fujimoto, D. A. Wiersma, W. Zinth, Eds., *Ultrafast Phenomena XI* (Springer-Verlag, Berlin, 1998).
3. G. Steinmeyer, D. H. Sutter, L. Gallmann, N. N. Matuschek, U. Keller, *Science* **286**, 1507 (1999).
4. Present sources include mode-locked and gain-switched CO_2 lasers [see, for instance, I. V. Pogorelsky *et al.*, *IEEE J. Quantum Electron.* **31**, 556 (1995)], limited to $\lambda \simeq 10.6$ μm, and picosecond and femtosecond optical parametric oscillators [for a review, see M. H. Dunn, M. Ebrahimzadeh, *Science* **286**, 1513 (1999)], which however are still rather complex sources. Recently, we have obtained picosecond midinfrared pulses with QC lasers, including gain-switching [R. Paiella *et al.*, *Appl. Phys. Lett.* **75**, 2536 (1999)] and active mode-locking [R. Paiella *et al.*, *Appl. Phys. Lett.* **77**, 169 (2000)].
5. J. Faist *et al.*, *Science* **264**, 553 (1994).
6. F. Capasso *et al.*, *Opt. Photonics News* **10**, 31 (1999).
7. M. M. Fejer, S. J. B. Yoo, R. L. Byer, A. Harwit, J. S. Harris, *Phys. Rev. Lett.* **62**, 1041 (1989).
8. M. Segev, I. Grave', A. Yariv, *Appl. Phys. Lett.* **61**, 2403 (1992).
9. F. Capasso, C. Sirtori, A. Y. Cho, *IEEE J. Quantum Electron.* **30**, 1313 (1994).
10. E. Rosencher *et al.*, *Science* **271**, 168 (1996).
11. A. Neogi, H. Yoshida, T. Mozume, O. Wada, *J. Appl. Phys.* **85**, 3352 (1999).
12. R. W. Boyd, *Nonlinear Optics* (Academic Press, San Diego, CA, 1992).
13. J. Faist *et al.*, *IEEE J. Quantum Electron.* **34**, 336 (1998).
14. C. Gmachl *et al.*, *IEEE J. Select. Topics Quantum Electron.* **5**, 808 (1999)
15. Although room temperature operation of QC lasers is readily achieved in pulsed mode, continuous-wave operation is at present limited to temperatures below 175 K.
16. H. C. Liu, J. Li, M. Buchanan, Z. R. Wasilewski, *IEEE J. Quantum. Electron.* **32**, 1024 (1996). These detectors are also based on intersubband transitions in semiconductor quantum wells, and therefore they are very well suited for high-speed applications. The device used here has a nominal bandwidth of 12 GHz (parasitics limited).
17. For a general review of QWIPs, see B. F. Levine, *J. Appl. Phys.* **74**, R1 (1993).
18. P. R. Griffiths, J. A. de Haseth, *Fourier Transform Infrared Spectrometry* (Wiley, New York, 1986).
19. J. F. Martins-Filho, E. A. Avrutin, C. N. Ironside, J. S. Roberts, *IEEE J. Select. Topics Quantum Electron.* **1**, 539 (1995).
20. The decay in the amplitude of the spikes with increasing delay time observed in Fig. 3 is an instrumental effect, resulting from the nonperfect collimation of the beam entering the FTIR, through a mechanism known as self-apodization (*18*). This is confirmed by the fact that a decay at the same rate is observed in the interferograms for single-mode cw operation of the same lasers. On the other hand, a much faster decay would be observed if the laser modes were not phase-locked to one another (*19*).
21. G. P. Agrawal, *Nonlinear Fiber Optics* (Academic Press, San Diego, CA, 1995).
22. C. H. Lin, T. K. Gustafson, *IEEE J. Quantum Electron.* **8**, 429 (1972).
23. Surface plasmons are electromagnetic waves propagating at the interface between two materials with dielectric constants having real parts of opposite sign, such as a metal and an insulator. For more details, see, for instance, P. Yeh, *Optical Waves in Layered Media* (Wiley, New York, 1988).
24. A. Yariv, *Quantum Electronics* (Wiley, New York, 1988).
25. D. E. Spence, P. N. Kean, W. Sibbett, *Opt. Lett.* **16**, 42 (1991).
26. G. P. Agrawal, N. K. Dutta, *Long-Wavelength Semiconductor Lasers* (Van Nostrand Reinhold, New York, 1986).
27. The following parameter values, corresponding to the laser of Fig. 1, were used in the computation of $n_2 z_{32} = 1.9$ nm (theoretical); $\Delta\nu = 3$ THz (measured from electroluminescence spectra in similar devices); $n_0 = 3.3$ (measured from the mode separation frequency); $\Delta N = (I_{el}\tau_3)/(qV) = 8 \times 10^{15}$ cm^{-3}, with the carrier lifetime $\tau_3 = 1.5$ ps (theoretical), the volume of one period of active region $V = 677$ μm^3, at a current $I_{el} = 0.6$ A (corresponding to the second trace from top in Fig. 1); and $I_0^{sat} = (h^2\varepsilon_0 cn\Delta\nu)/(8\pi\Gamma q^2 z_{32}^2 \tau_3) = 1.4$ MW/cm^2, with the active-layers confinement factor $\Gamma = 23\%$. Finally, ϕ_{max} was computed with Eq. 2 with $I_{max} = 5.5$ MW/cm^2 (inferred from the measured average power at a current of 0.6 A).

28. We thank H. Y. Hwang, A. M. Sergent, and E. Chaban for technical assistance and M. C. Wanke, R. Colombelli, and A. Tredicucci for stimulating discussions. Supported in part by Defense Advanced Research Projects Agency/U.S. Army Research Office under contract DAAD19-00-C-0096.

27 July 2000; accepted 19 October 2000

Tunable Resistance of a Carbon Nanotube–Graphite Interface

S. Paulson,[1]* A. Helser,[2] M. Buongiorno Nardelli,[3] R. M. Taylor II,[2,1] M. Falvo,[1]† R. Superfine,[1] S. Washburn[1]

The transfer of electrons from one material to another is usually described in terms of energy conservation, with no attention being paid to momentum conservation. Here we present results on the junction resistance between a carbon nanotube and a graphite substrate and show that details of momentum conservation also can change the contact resistance. By changing the angular alignment of the atomic lattices, we found that contact resistance varied by more than an order of magnitude in a controlled and reproducible fashion, indicating that momentum conservation, in addition to energy conservation, can dictate the junction resistance in graphene systems such as carbon nanotube junctions and devices.

The engineering of electronic devices relies on the control and exploitation of the electronic properties of junctions. The density of states of the two materials as a function of energy is typically used to describe these properties. New opportunities arise when the momentum transfer across the junction can be controlled. Carbon nanotubes (NTs) offer a laboratory for this control because they have a highly structured Fermi surface that restricts the allowed momentum states available at the junction (*1–3*) and have atomically smooth lattices at the contact region. The molecular size and mechanical and electronic properties of NTs have made them prime targets as components of nanometer-sized electronic and actuating devices (*4–8*). Experimental studies of devices that include both metal-NT and NT-NT junctions have demonstrated that the control of contact resistance will be essential for predictable device specifications (*9*, *10*) and that it remains an elusive goal. Here we present measurements of a multiwalled NT (MWNT) in contact with a graphite [highly oriented pyrolytic graphite (HOPG)] substrate; these materials have similar energy dispersions and available momentum states. The modulation in the electrical resistance of the contact we observed demonstrates the importance of lattice registry in NT/NT devices and opportunities for sensing and actuating device designs (*11*).

We measured the resistance of a MWNT-HOPG contact as a function of the rotation angle of the atomic lattices. Measurements were made with a two-probe technique (Fig. 1A); the HOPG substrate itself served as one lead, and a conducting atomic force microscope (AFM) tip brought into contact with the top of the NT was the other. After 200 μl of a MWNT/dichloromethane suspension was dispensed onto the rapidly spinning HOPG substrate, the sample was rinsed with ethanol, cleaned by exposure to ultraviolet light, and rinsed in water. The NT was imaged in noncontact (oscillating) mode to identify its position; then in contact mode, it was pushed, causing it to rotate (and translate) on the graphite plane until the commensurate, or in-registry, position was found, as evidenced by a sharp increase in lateral force (*12*). This position is designated as $\Phi = 0°$. Schematics of NTs in registry at $\Phi = 0°$ (Fig. 1B) and out of registry at $\Phi = 10°$ (Fig. 1C)

[1]Department of Physics and Astronomy, [2]Department of Computer Science, University of North Carolina–Chapel Hill, Chapel Hill, NC 27599, USA. [3]Department of Physics, North Carolina State University, Raleigh, NC 27695–8202, USA.

*Present address: Department of Physics and Center for Nonlinear and Complex Systems, Duke University, Durham, NC 27708, USA.

†To whom correspondence should be addressed. E-mail: falvo@physics.unc.edu

FIGURES

Concept for Moving Plane 3D Display
Figure 1

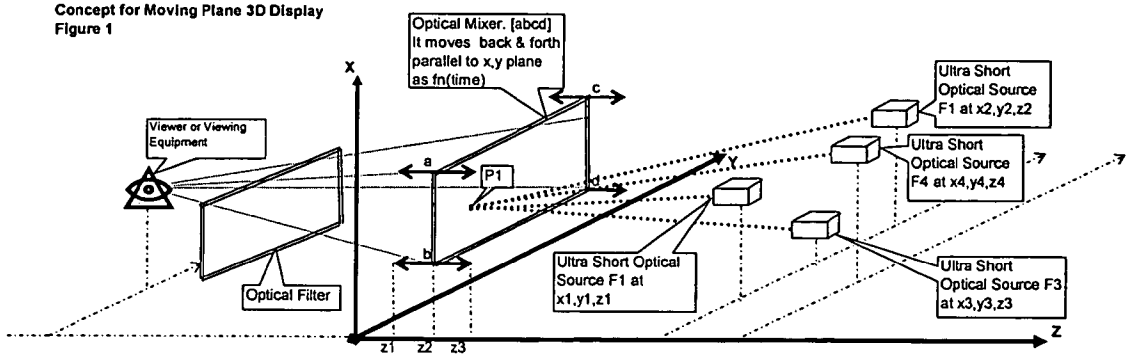

Concept for Moving Plane 3D Display
Figure 2

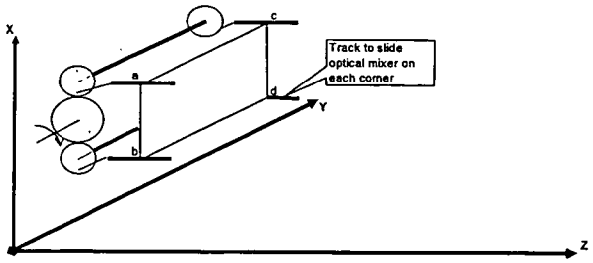

Side view of rotating 3D display
Figure 3

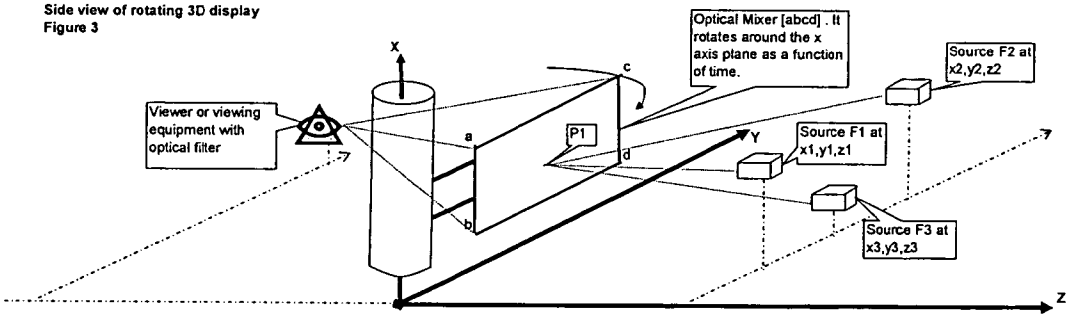

Top view of rotating 3D display
Figure 4

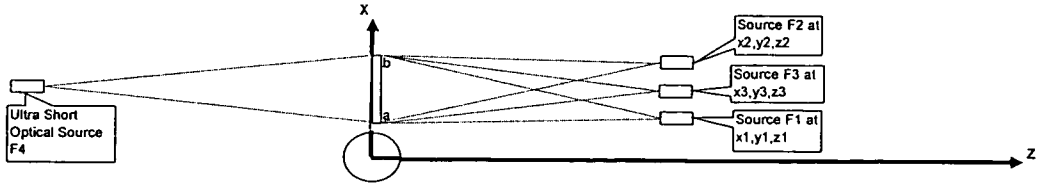

Top View 2 of Rotating 3D display
Figure 6

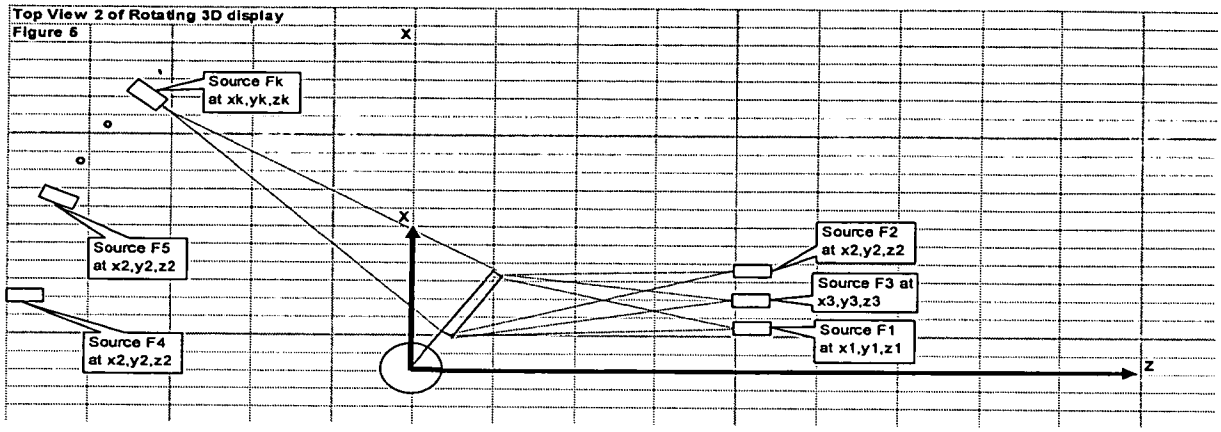

Side view of rotating 3D display
Figure 6

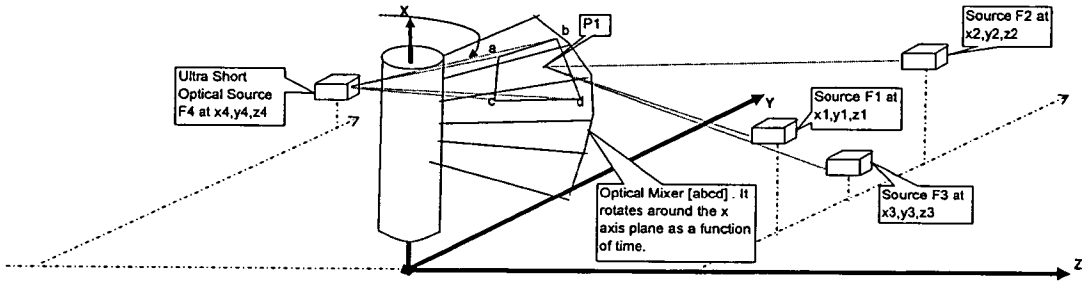

Concept for Moving Plane 3D Display
Figure 7

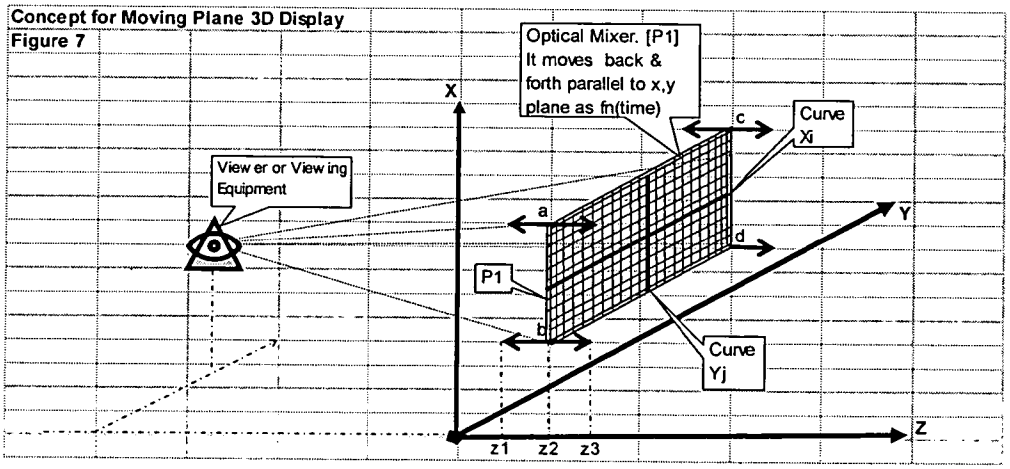

Details of Improved Optical Mixer
Figure 8

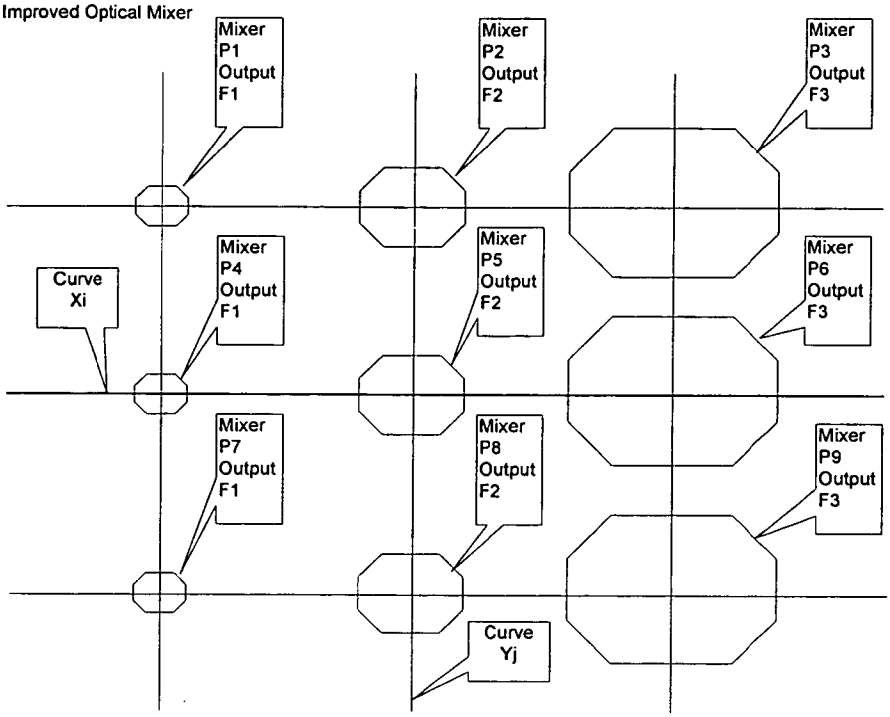

Discrete Elements Used in a Nonlinear Mixer
Figure 9

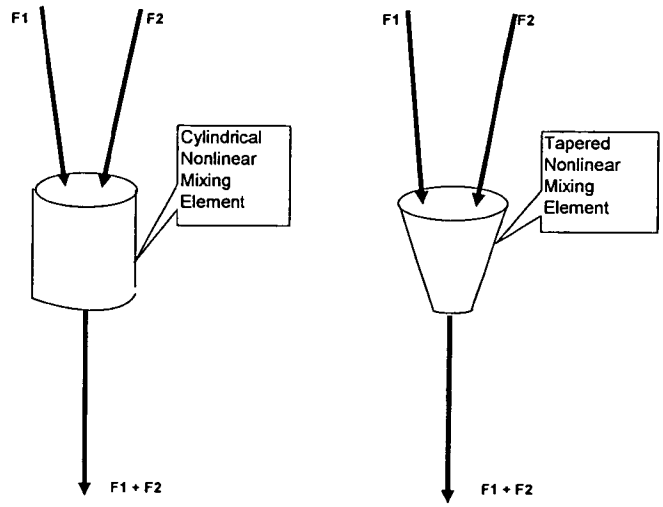

Concept for Image Scaner Using Ultrashort Pulses
Figure 1

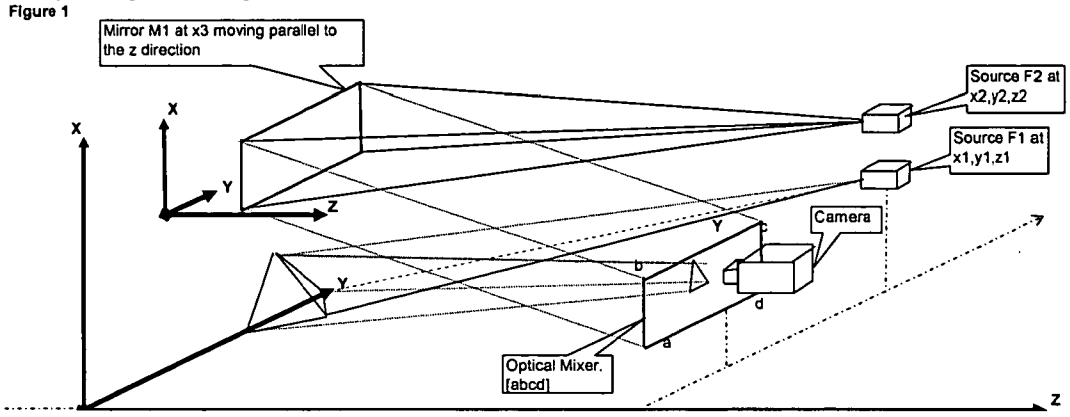

Concept for Image Scaner Using Ultrashort Pulses
Figure 2

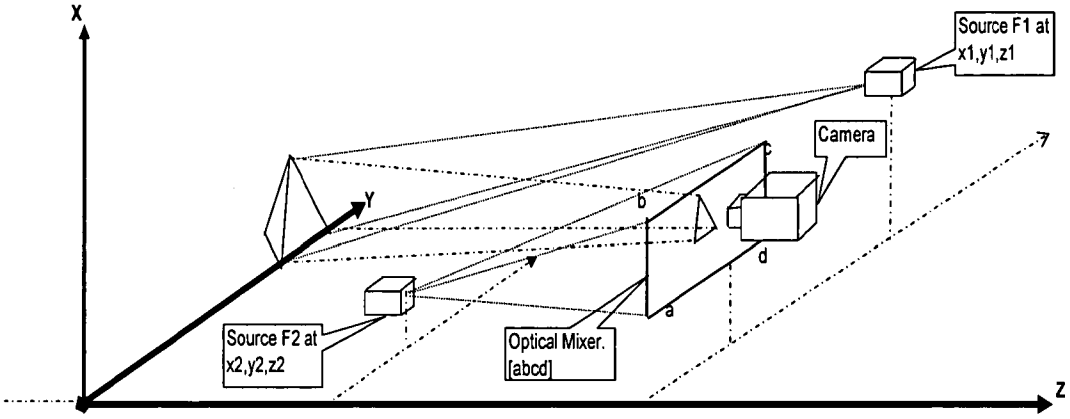

NWK2: 1114660.01
97084-00047